SSC-364

INELASTIC DEFORMATION OF PLATE PANELS

SHIP STRUCTURE COMMITTEE
1991

SSC-364

Inelastic Deformation of Plate Panels

Ship Structure Committee   1991

SHIP STRUCTURE COMMITTEE

The SHIP STRUCTURE COMMITTEE is constituted to prosecute a research program to improve the hull structures of ships and other marine structures by an extension of knowledge pertaining to design, materials, and methods of construction.

RADM J. D. Sipes, USCG, (Chairman)
Chief, Office of Marine Safety, Security
  and Environmental Protection
U. S. Coast Guard

Mr. Alexander Malakhoff
Director, Structural Integrity
  Subgroup (SEA 55Y)
Naval Sea Systems Command

Dr. Donald Liu
Senior Vice President
American Bureau of Shipping

Mr. H. T. Haller
Associate Administrator for Ship-
  building and Ship Operations
Maritime Administration

Mr. Thomas W. Allen
Engineering Officer (N7)
Military Sealift Command

CDR Michael K. Parmelee, USCG,
Secretary, Ship Structure Committee
U. S. Coast Guard

CONTRACTING OFFICER TECHNICAL REPRESENTATIVES

Mr. William J. Siekierka
SEA 55Y3
Naval Sea Systems Command

Mr. Greg D. Woods
SEA 55Y3
Naval Sea Systems Command

SHIP STRUCTURE SUBCOMMITTEE

The SHIP STRUCTURE SUBCOMMITTEE acts for the Ship Structure Committee on technical matters by providing technical coordination for determinating the goals and objectives of the program and by evaluating and interpreting the results in terms of structural design, construction, and operation.

AMERICAN BUREAU OF SHIPPING

Mr. Stephen G. Arntson (Chairman)
Mr. John F. Conlon
Dr. John S. Spencer
Mr. Glenn M. Ashe

MILITARY SEALIFT COMMAND

Mr. Albert J. Attermeyer
Mr. Michael W. Touma
Mr. Jeffery E. Beach

NAVAL SEA SYSTEMS COMMAND

Mr. Robert A. Sielski
Mr. Charles L. Null
Mr. W. Thomas Packard
Mr. Allen H. Engle

U. S. COAST GUARD

CAPT T. E. Thompson
CAPT Donald S. Jensen
CDR Mark E. Noll

MARITIME ADMINISTRATION

Mr. Frederick Seibold
Mr. Norman O. Hammer
Mr. Chao H. Lin
Dr. Walter M. Maclean

SHIP STRUCTURE SUBCOMMITTEE LIAISON MEMBERS

U. S. COAST GUARD ACADEMY

LT Bruce Mustain

U. S. MERCHANT MARINE ACADEMY

Dr. C. B. Kim

U. S. NAVAL ACADEMY

Dr. Ramswar Bhattacharyya

STATE UNIVERSITY OF NEW YORK MARITIME COLLEGE

Dr. W. R. Porter

WELDING RESEARCH COUNCIL

Dr. Martin Prager

NATIONAL ACADEMY OF SCIENCES – MARINE BOARD

Mr. Alexander B. Stavovy

NATIONAL ACADEMY OF SCIENCES – COMMITTEE ON MARINE STRUCTURES

Mr. Stanley G. Stiansen

SOCIETY OF NAVAL ARCHITECTS AND MARINE ENGINEERS – HYDRODYNAMICS COMMITTEE

Dr. William Sandberg

AMERICAN IRON AND STEEL INSTITUTE

Mr. Alexander D. Wilson

**Ship
Structure
Committee**

An Interagency Advisory Committee
Dedicated to the Improvement of Marine Structures

April 10, 1991

SSC-364
SR-1322

INELASTIC DEFORMATION OF PLATE PANELS

Inelastic deformations in plate panels are a familiar sight to those involved in ship construction and repair. These dents or set-ins are commonplace and are the result of ice pressure, green water, low energy collisions, slamming, and so forth. Criteria for assessing this type of damage and the need for repair are not clearly defined. This report proposes a methodology to determine the maximum amount of inelastic deformation that should be permitted in structural steel panels. The methodology is based on a review of existing criteria, panel deformation measurements, and finite element analyses. This report should be of interest to those involved in the construction and repair of vessels.

J. D. SIPES
Rear Admiral, U.S. Coast Guard
Chairman, Ship Structure Committee

1. Report No.	2. Government Accession No.	3. Recipient's Catalog No.

4. Title and Subtitle	5. Report Date
"Inelastic Deformation of Plate Panels"	January 1991
	6. Performing Organization Code

7. Author(s) Eric Jennings, P.E., Kim Grubbs, Charles Zanis and Louis Raymond, Ph.D.	8. Performing Organization Report No. "SR-1322"

9. Performing Organization Name and Address	10. Work Unit No. (TRAIS)
CASDE Corporation 2800 Shirlington Road, Suite 600 Arlington, Virginia 22206	11. Contract or Grant No. DTCG23-88-C-20030
	13. Type of Report and Period Covered

12. Sponsoring Agency Name and Address	
Ship Structure Committee U.S. Coast Guard 2100 Second Street Washington, D.C. 20593	Final Report
	14. Sponsoring Agency Code

15. Supplementary Notes

Sponsored by the Ship Structure Committee and its member agencies.

16. Abstract

Ship plate panels often experience inelastic deformation due to loads normal to their surface such as ice pressure, green water, slamming, docking, wheel loads and low energy collision. However, criteria for assessing the need to repair panels deformed in-service are not readily available. Design guidelines are available that restrict the allowable levels of inelastic deformation in new construction. This report presents the results of an experimental and analytical investigation related to establishing criteria for assessing the amount of plastic deformation that may be permitted on existing ship structures without compromising structural integrity. The work included the review of existing criteria for panel deformation, measurement of plate panel deformation on existing ships, finite element analyses to establish strain vs. deflection relationships for ship plate panels, and an assessment of the effects of prior plastic strain on flaw tolerance of ship steels. Based on these efforts, a methodology is proposed for determining the maximum inelastic deformation that should be permitted for ship steel structural panels.

17. Key Words	18. Distribution Statement
Plate Panels, Inelastic Deformation, Hull and Deck Structure, Fracture Mechanics, Strain, Membrane Strain. Bending Strain	Available from: National Technical Information Service Springfield, Virginia 22161

19. Security Classif. (of this report)	20. Security Classif. (of this page)	21. No. of Pages	22. Price
Unclassified	Unclassified		

Form DOT F 1700.7 (8-72)   Reproduction of completed page authorized

METRIC CONVERSION FACTORS

Approximate Conversions to Metric Measures

Symbol	When You Know	Multiply by	To Find	Symbol
		LENGTH		
in	inches	*2.5	centimeters	cm
ft	feet	30	centimeters	cm
yd	yards	0.9	meters	m
mi	miles	1.6	kilometers	km
		AREA		
in^2	square inches	6.5	square centimeters	cm^2
ft^2	square feet	0.09	square meters	m^2
yd^2	square yards	0.8	square meters	m^2
mi^2	square miles	2.6	square kilometers	km^2
	acres	0.4	hectares	ha
		MASS (weight)		
oz	ounces	28	grams	g
lb	pounds	0.45	kilograms	kg
	short tons (2000 lb)	0.9	tonnes	t
		VOLUME		
tsp	teaspoons	5	milliliters	ml
Tbsp	tablespoons	15	milliliters	ml
fl oz	fluid ounces	30	milliliters	ml
c	cups	0.24	liters	l
pt	pints	0.47	liters	l
qt	quarts	0.95	liters	l
gal	gallons	3.8	liters	l
ft^3	cubic feet	0.03	cubic meters	m^3
yd^3	cubic yards	0.76	cubic meters	m^3
		TEMPERATURE (exact)		
°F	Fahrenheit temperature	5/9 (after subtracting 32)	Celsius temperature	°C

*1 in = 2.54 (exactly). For other exact conversions and more detailed tables, see NBS Misc. Publ. 286, Units of Weights and Measures, Price $2.25, SD Catalog No. C13 10.286.

iv
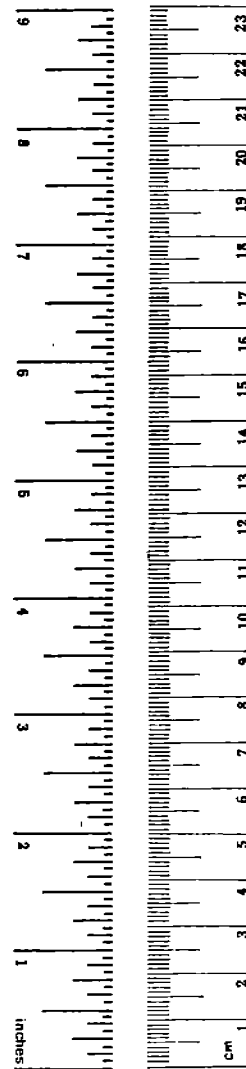
Approximate Conversions from Metric Measures

Symbol	When You Know	Multiply by	To Find	Symbol
		LENGTH		
mm	millimeters	0.04	inches	in
cm	centimeters	0.4	inches	in
m	meters	3.3	feet	ft
m	meters	1.1	yards	yd
km	kilometers	0.6	miles	mi
		AREA		
cm^2	square centimeters	0.16	square inches	in^2
m^2	square meters	1.2	square yards	yd^2
km^2	square kilometers	0.4	square miles	mi^2
ha	hectares (10,000 m^2)	2.5	acres	
		MASS (weight)		
g	grams	0.035	ounces	oz
kg	kilograms	2.2	pounds	lb
t	tonnes (1000 kg)	1.1	short tons	
		VOLUME		
ml	milliliters	0.03	fluid ounces	fl oz
l	liters	2.1	pints	pt
l	liters	1.06	quarts	qt
l	liters	0.26	gallons	gal
m^3	cubic meters	35	cubic feet	ft^3
m^3	cubic meters	1.3	cubic yards	yd^3
		TEMPERATURE (exact)		
°C	Celsius temperature	9/5 (then add 32)	Fahrenheit temperature	°F

°F -40 0 32 40 80 98.6 120 160 200 212
°C -40 -20 0 20 37 40 60 80 100

TABLE OF CONTENTS

TABLE OF CONTENTS (Continued)

LIST OF TABLES

LIST OF FIGURES

LIST OF FIGURES (Continued)

LIST OF ABBREVIATIONS AND SYMBOLS

a -   Length of long edge of plate

a' -   "Effective" defect size

a'_m -   Allowable defect size

a_o -   Initial crack length

Δa -   Crack extension

a/b -   Plate aspect ratio

ABS   -   American Bureau of Shipping

ASTM	-	American Society for Testing and Materials
b	-	Stiffener spacing, or length of short side of plate
B	-	Plate thickness
B_{Ic}	-	Critical plate thickness for plane strain, $2.5\ (K_{Ic}/YS)^2$
BMT	-	British Maritime Technology
c	-	Half crack length
c_o	-	Maximum crack size to be encountered in service
2c	-	Critical crack length
CCP	-	Center Cracked Panel
CTOD	-	Crack Tip Opening Displacement
CVN	-	Charpy V-Notch
DnV	-	Det norske Veritas
DTI	-	Damage Tolerance Index
DTRC	-	David Taylor Research Center
DZ	-	Damage Zone
E	-	Elastic modulus
EBT	-	Explosion Bulge Test
FEC	-	Fracture Strain Curve
FMDC	-	Fracture Mechanics Design Criteria
FS	-	Fracture Strength
FSC	-	Fracture Strength Curve
HAZ	-	Heat Affected Zone
J_{Ic}	-	Critical elastic-plastic energy release rate
J_R	-	J-resistance
K_I	-	Stress intensity factor
K_{Ic}	-	Critical stress intensity factor for fracture under plane strain conditions, or "fracture toughness"

K_c	-	Critical stress intensity under inelastic conditions
K_R	-	Stress intensity or resistance curve
L	-	Overall ship length
L_e	-	Elongated length of plating
L_u	-	Undeformed length of plating
LLD	-	Load-Line Displacement
MVC	-	Micro-Void Coalescence
NDE	-	Nondestructive Examination
NKK	-	Nippon Kaiji Kyokai
NRL	-	Naval Research Laboratory
r	-	Crack extension
r_0	-	Length of original crack extension
R	-	Radius of curvature
RA	-	Reduction in area
S	-	Strain energy density factor
S_{cr}	-	Critical strain energy density factor
SED	-	Strain Energy Density
SED_c	-	Strain Energy Density factor based on "locally" attaining a critical strain energy density to initiate fracture, or critical strain energy density
SED_{cr}	-	Residual toughness
SED_{FM}	-	Strain Energy Density factor based upon fracture mechanics approach
SNAJ	-	Society of Naval Architects of Japan
t	-	Plate thickness
T_R	-	Tearing modulus
U_e	-	Elastic energy released during crack growth
U_f	-	Plastic energy absorbed in the damage zone
U_u	-	Plastic energy absorbed in the uniform zone

UTS	-	Ultimate tensile strength
UWDH	-	Underwater dry habitat
V_p	-	Plastic component of clip gage opening displacement
w	-	CTOD specimen width
W	-	Strain energy per weight mass
W_v	-	Strain Energy Density
YC	-	Yield criteria
YS	-	Yield strength
z	-	Clip gage abutment height
Δ	-	Maximum center plate out-of-plane displacement
ε	-	Amount of prestrain
ε_b	-	bending strain
ε_c	-	Critical strain limit
ε_f	-	ε_c, or critical strain limits
ε_m	-	Membrane strain
ε_o	-	Maximum operating service strain
ε_p	-	Prior plastic strain
ε_{uts}	-	Strain at ultimate tensile strength
σ_o	-	Maximum operating service stress
ρ	-	Material density
δ_c	-	Critical Crack tip opening displacement, or critical CTOD
δ_e	-	Elastic component of CTOD
δ_p	-	Plastic component of CTOD

SECTION 1.0
INTRODUCTION

1.1 BACKGROUND

The basic hull and deck structure of a ship consists of steel plating reinforced with longitudinal stiffeners and transverse frames. The steel plating often experiences permanent plastic deformation from in-service loads, as well as from construction induced loading caused by welding or forming. The plate deformation is greatest between stiffeners and frames and can result in the ship hull exhibiting a "hungry horse" appearance. Such plate deformations may be caused by various loads such as ice pressure, green water, wave slamming, docking, and wheel loading on decks. Design guidelines are available that permit a level of permanent set or inelastic deformation in certain locations on the ship and under specified conditions. These design guidelines are often expressed in terms of maximum plate deflection based on location in the hull. However, the basis for these guidelines is not readily apparent.

The types of loading experienced by ship plates, and the magnitude of these loads, is in large part a function of the location of the plating on the ship. For example, hull structure in the bow is more likely to experience loads due to slamming action of the ship in a seaway, and the design and analysis of the bow structure must be performed accordingly. Design of hull and deck structure must take into account the effect of many factors, including the effect of green seas on the weather deck plating, hydrodynamic loading on the hull plating, cargo and equipment loading on the ship decks, and cyclic loading in the hull structure due to the motion of the ship in a seaway. For seaway induced loads, the ship structure located farthest from the neutral axis of the ship hull girder (i.e., deck and bottom shell structure), will experience greater loading levels. The effects of prior plastic deformation on the structural integrity of ship hull plating must therefore be examined considering the load intensity and types of loading that the panel is expected to see during service. A given plate deflection may be acceptable for a plate panel which is expected to be lightly loaded, but the same deflection may be unacceptable for a panel which is expected to be heavily loaded during service.

There are many failure modes which must be considered in the analysis of ship structure and in assessing the influence of prior plastic deformation on structural integrity. These failure modes can range from large scale whole ship failure, including buckling of the ship hull girder, to localized failure of individual plate panels. In this study, it was assumed that major ship structure, such as frames and stiffeners, remained undeformed. Therefore, the major failure mode for the panel was assumed to be rupture of the plating. Emphasis was placed on the effects of prior plastic deformation on failure of an individual plate panel under additional loading. In this report, plate and panel are used interchangeably to refer to the plating bounded by frames and stiffeners. It was assumed that major ship structure such as frames and stiffeners remained undeformed, therefore the major failure mode for the panel would involve rupture of the plate. The effects of prior plastic strain on fracture toughness and flaw tolerance was investigated. In addition, the influence of plate panel deformation on maximum strains in the plating was determined. These analyses were used to develop a methodology for establishing maximum allowable plate deformation criteria.

1.2 OBJECTIVES

The overall objective of this investigation was to develop a methodology for evaluating the structural integrity of permanently deformed ship hull and deck plating. The methodology was to be applicable to establishing criteria for repair or replacement of ship plating. Specific goals of this investigation were as follows:

1

- Compile and compare current criteria for replacement of deformed ship plate, considering both initial construction and in-service inspections.

- Identify and document typical ship plate deformations and strains by means of ship checks.

- Develop the strain/deformation relationships for representative ship plates using finite element analysis methods.

- Investigate the effects of deformation and strain on the flaw tolerance of ship hull steels.

- Propose a methodology for developing ship plate repair criteria.

1.3 APPROACH

1.3.1 Plate Deformation Criteria

Various classification societies and agencies were contacted in order to identify the levels of permanent deformation considered acceptable in ship hull and deck plating. The goal of this effort was to determine the guidelines used by the surveyors of several societies to judge whether a deformed plate was suitable for continued use, or required replacement. The guidelines received from the classification societies were compared to actual deformations measured during the ship surveys conducted in this investigation.

1.3.2 Ship Surveys

A number of commercial and U.S. Navy ships, and Military Sealift Command ships built to commercial specifications, were surveyed to quantify the various types of hull and deck plating deformation encountered in service. During these surveys, deformed areas of unstiffened plating were selected for measurement of the magnitude and distribution of plate deflection. In addition to the plate deflection, the size, thickness and location of the plate was established. Where possible, photographs were also taken of the deformed areas surveyed. Results of deflection measurements were used to estimate the local bending and membrane strains present in the plate.

1.3.3 Finite Element Analysis

A parametric study was performed using nonlinear finite element analysis methods to determine the deflection/strain characteristics of steel plates rigidly supported along four edges. The thickness and aspect ratio of the plates were varied and were intended to represent the dimensions of those encountered during the ship surveys. The plates were subjected to increasing normal pressure loadings that resulted in significant deflection. Both local bending and membrane surface strains were determined through the finite element analyses. Relationships between maximum plate deflection and maximum bending strain and membrane strain were developed for comparison to the ship survey estimates and for use in the fracture mechanics analysis.

1.3.4 Fracture Mechanics Analysis

Various fracture mechanics approaches to estimate the effect of prior plastic deformation on the flaw tolerance of ship steels were critically reviewed. These approaches included the J-Integral, the Crack Tip Opening Displacement (CTOD), the Tearing Modulus and Strain Energy Density methods. Based on this review, a fracture mechanics approach was selected and used to estimate the effects of prior plate deformation on flaw tolerance or resistance of the plate to unstable fracture.

1.3.5 Methodology for Establishing Deflection Criteria

The results of the above measurements and analyses were used to propose a methodology for establishing criteria for repair of deformed ship plating. The methodology employs a knowledge of the maximum likely flaw size, the maximum operating stress or strain, and fracture toughness properties to determine whether the deflection measured in ship hull or deck plating is acceptable or must be repaired. Recommendations are provided for the development of acceptance criteria.

SECTION 2.0
SHIP PLATE DEFORMATION CRITERIA

2.1 INTRODUCTION

Ship plating often experiences permanent deformation when subjected to in-service loads. Ship weight and material cost considerations dictate that some amount of permanent plate deformation be allowed. This permanent deformation can not be so great, however, that the strength and watertight integrity of the ship structure are compromised. In order to identify current criteria for allowable permanent plate deformation, various classification societies were contacted and documentation concerning tolerance requirements was reviewed.

The classification societies and agencies contacted in this study included Nippon Kaiji Kyokai (NKK) [1], American Bureau of Shipping (ABS) [2], British Maritime Technology International (BMT), Bureau Veritas, Lloyds Register of Shipping [3], and Det norske Veritas (DnV) [4]. Additional criteria were obtained from publications and design requirement manuals of the Ship Structure Committee and the U.S. Navy. The deformation criteria included those used by Ishikawajima-Harima Heavy Industries, The Society of Naval Architects of Japan (SNAJ), Noggrannhet vid Skrovbyggnad, and the production standard of the German Shipbuilding Industry [5]. The information obtained during this search yielded ship plate deformation criteria that falls into two categories. The first category, and the category for which the majority of the information was obtained, concerns new construction deformation limits. These are included here for completeness, though new construction tolerances are not the main concern of this study. The second category of criteria concerns deformation limits for ships that have been in service and are subject to periodic surveys. Though this information is directly pertinent to the goals of this study, few of the societies contacted quantify the in-service deformation criteria used during their surveys.

2.2 NEW CONSTRUCTION ALLOWANCES

Plate deformation during ship construction is caused by factors such as weld stresses and fit-up tolerances allowed during fabrication. Typically, these deformation allowances are small, since they must result in a fair ship. The new construction deformation allowances imposed by the classification societies contacted during this investigation are summarized in Table 2.1.

2.3 IN-SERVICE ALLOWANCES

While data on new construction plate deformation allowances was easily obtained, similar data for in-service allowances was more difficult to obtain. Out of 11 classification societies and ship design agencies surveyed, only one provided specific in-service plate deformation criteria. For the most part, the interviews with surveyors and authorities in the various societies indicated that there are no written guidelines for maximum in-service allowable plate deformation. It appears that surveyors are trained by other experienced surveyors to accept or reject a deformed plate based upon "rule-of-thumb" guidelines, and not upon a comparison of measured deflections versus established deflection criteria.

The most useful in-service plate deformation criteria was provided by the Survey Department of the Teaneck, New Jersey office of Det norske Veritas. These criteria, used in buckling analyses, are as follows:

• For shell plating located in the 0 to 0.25L (where L = overall ship length) and in the 0.75L to 1.0L portion of the hull, the maximum permissible indent is 0.05 times the minimum span length between stiffeners (or b/20, where b equals the stiffener span).

4

- For midbody plating (0.25L to 0.75L) the following guidelines are observed. If the observed deformation is 10mm to 30mm in depth, the ship owner is notified and the damage is recorded. If the observed deformation is greater than 30mm (about 1-3/16 inches) the surveyor will recommend repair or replacement of the plating.

Table 2.1 New Construction Plate Deformation Limits

SHIP COMPONENT	AGENCY					
	Ishikawajima-Harima Heavy Industries (JAPAN)		Japanese Shipbuilding Quality Standard - SNAJ (JAPAN)		German Shipbuilding Industry (GERMANY)	
	Location	Allowable Limit	Location	Allowable Limit	Location	Allowable Limit
Side shell and bottom shell	1. Parts within 0.6L* midbody 2. Fore and Aft	6 mm 7 mm	1. Parallel part, side and bottom 2. Fore and aft	6 mm 7 mm	1. Above waterline 2. Below waterline	15 mm 18 mm
Double bottom	1. Tank top 2. Floor	6 mm 8 mm	1. Tank Top 2. Floor	6 mm 8 mm	Inner bottom	18 mm
Bulkheads	1. Longitudinal 2. Transverse 3. Swash	8 mm 8 mm 8 mm	1. Longitudinal 2. Transverse 3. Swash	8 mm 8 mm 8 mm	-	18 mm
Main structural decks	1. Exposed part within 0.6L* midbody 2. Exposed part fore and aft 3. Enclosed part	6 mm 9 mm 9 mm	1. Exposed part within 0.6L* midbody 2. Exposed part fore and aft 3. Enclosed part	6 mm 9 mm 9 mm	Topside decks	15 mm
Second Deck	1. Exposed part 2. Enclosed part	8 mm 9 mm	1. Exposed part 2. Enclosed part	8 mm 9 mm	-	-
Superstructure decks and wall	1. Exposed part 2. Enclosed part	6 mm 9 mm	1. Exposed part 2. Enclosed part	6 mm 9 mm	-	15 mm
Web of girder and transverse	-	7 mm	-	7 mm	-	-
Cross deck	-	-	-	7 mm	-	-
Forecastle and poop decks	-	-	1. Bare part 2. Covered part	6 mm 9 mm	-	-
House wall	-	-	1. Outside 2. Inside 3. Covered part	6 mm 6 mm 9 mm	-	15 mm
Sheer strake	-	-	-	-	-	15 mm

* L = Overall length of ship.

SECTION 3.0
SHIP SURVEYS

3.1 INTRODUCTION

Surveys of ship hull and deck plating were performed in order to obtain information on deformation patterns in ships currently in service. This data was obtained in order to accomplish the following:

- establish a database for hull and deck plate deformations on ships currently in service, and

- determine realistic deformation values for use as input parameters to analyze the stress, strain, and fracture characteristics of ship plates.

All ship surveys were performed over a period of seven months on both commercial and naval ships, including some Military Sealift Command ships built to commercial specifications. The ships were surveyed both in dry dock and in the water, depending upon availability. The surveys were performed during the period of March 1989 through September 1989 at Bethlehem Steel Corporation Sparrows Point, Philadelphia Naval Shipyard, Norfolk Naval Shipyard, Norfolk Shipbuilding and Dry Dock Corporation, and the Military Sealift Command Docks at Lambert's Point in Norfolk, VA. The ships surveyed included three aircraft carriers, five destroyers, a naval auxiliary ship (an oiler), a Military Sealift Command FBM support ship, a Military Sealift Command vehicle cargo ship (SL-7), and two commercial cruise ships.

Table 3.1 identifies principal characteristics of the ships surveyed [6,7], and Table 3.2 describes the specific location of the plates measured during the surveys. In addition to the ships listed in Table 3.1, a preliminary survey of a commercial container ship was performed at Bethlehem Steel Corporation's Sparrows Point Yard on February 28, 1989 to evaluate and finalize measurement procedures. Also, the vehicle deck of the Military Sealift Command vehicle cargo ship Sgt. Matej Kocak USNS T-AK 3005 was surveyed; however, no significant deformations were observed in the deck plating.

Although the ship survey attempted to include as wide a range of ship types as possible, the survey of the thirteen ships listed on Table 3.1 was based primarily on ship availability, and ship owner and shipyard willingness to allow the surveys to be conducted. These factors prevented the surveying of large numbers of commercial ships since most shipping companies did not respond favorably to requests to perform surveys of their vessels. Also, additional survey opportunities were lost due to the requirement stipulated by some private shipyards that the surveyors be covered by longshoreman and dock worker insurance. These factors resulted in a larger number of surveys being performed on U.S. Navy combatant ships than on commercial or Military Sealift Command ships built to commercial specifications. The survey also attempted to include as wide a range of plating types and deformations as possible. Deck, side shell, and bottom shell plating were surveyed and included bow, amidships, and stern locations. The deformations were grouped as sea slap/slamming or impact types. The specific locations measured were limited to those with relatively large deflections, and with no associated stiffener deformation. This was in accordance with direction given by the Ship Structure Committee.

3.2 SURVEY METHODS

The initial step in each ship survey consisted of a walk-around inspection of the ship hull and deck areas to determine plate deformations suitable for measurement. For ships located in dry dock, a bottom survey was also performed. The criteria used to select survey locations was based on size of plating deformation between stiffeners, accessibility, and type and location of panels.

7

Table 3.1 Principal Characteristics of Ships Surveyed

Ship	U.S. Navy Designation	Ship Type	Length Overall (feet)	Full Load Displacement (Long Tons)
USS Kitty Hawk	CV-63	Aircraft Carrier	1,046	81,773
USS Detroit	AOE-4	Fast Combat Support Ship	793	53,600
USS Kidd	DDG-993	Guided Missile Destroyer	563	9,574
USS Kennedy	CV-67	Aircraft Carrier	1,046	80,941
USS Dahlgren	DDG-43	Guided Missile Destroyer	512.5	6,150
USNS Denebola	T-AKR 289	Vehicle Cargo Ship	946.2	55,355
USNS Vega	T-AK 286	Cargo Ship	483.3	15,404
Commercial Ship	-	Passenger Ship	619.1	30,325
Commercial Ship	-	Passenger Ship	-	-
USS King	DDG-41	Guided Missile Destroyer	512.5	6,150
USS Conyngham	DDG-17	Guided Missile Destroyer	437	4,825
USS Hayler	DD-997	Destroyer	563.2	8,040
USS Roosevelt	CVN-71	Aircraft Carrier	1,092	96,400

When a survey ship was in dry dock, a basket-type lift was used to position the survey team at the location of the deformed panel. In some cases, a closer examination of a deformed panel revealed that the deformation was not nearly as extensive as it appeared to be from a distance. In these cases, a nearby panel which appeared to be relatively undeformed when viewed from a distance was often found to have more extensive deformation, and was therefore measured.

When the ship to be surveyed was located in the water, a launch was obtained and used to allow the surveyors to make the initial inspection of the ship's hull. Panels were selected for measurement using the same criteria as for the ship in dry dock, and the launch was used to position the surveyors within reach of the hull panels. The use of a launch to position the surveyors limited the area of the hull considered for survey to an area from the waterline up to a height of about twenty feet above the waterline. In general, the majority of hull panel deformations observed on ships surveyed in this study occurred within this region of the hull.

3.3 DATA COLLECTION

Once a deformed panel was selected for survey and the surveyors reached the area, the size of the unstiffened panel was determined, and a grid pattern was drawn on the plate with chalk. When possible, the grid boundaries were selected to coincide with the stiffeners bounding the deformed plate.

Table 3.2 Ship Survey Plate Panel Locations

Measurement	Ship	Survey Date	Plate Location
1	USS Kitty Hawk, CV-63	3-22-89	Port Side Shell, Bow, About 12 ft. Above Waterline
2	USS Kitty Hawk, CV-63	3-22-89	Port Sponson Shell, Fwd Panel, About 6 ft. Below Deck
3	USS Detroit, AOE-4	3-22-89	Port Side Shell, Stern, at Waterline
4	USS Detroit, AOE-4	3-22-89	Port Side Shell, Stern, at Waterline
5	USS Kidd, DDG-993	3-22-89	Port Side, Fwd Amidships at Frame 103, 6 ft. Above Waterline
6	USS Kidd, DDG-993	3-22-89	Weather Deck Centerline, Bow, at Frame 15
7	USS Kennedy, CV-67	5-10-89	Starboard Shell, 20 ft. Fwd of Stern, 10 ft. Above Waterline
8	USS Kennedy, CV-67	5-10-89	Port Shell, Underside of Aft Elevator Fairing, 10 ft. Above Waterline
9	USS Dahlgren, DDG-43	5-10-89	Port Shell, Fwd of Frame 43, 20 ft. Above Waterline
10	USS Dahlgren, DDG-43	5-10-89	Port Shell, Stern, at Waterline
11	USNS Denebola, T-AKR 289	5-11-89	Starboard Storage Deck 2, near Frame 228
12	USNS Vega, T-AK 286	5-11-89	Port Side Shell, Amidships, Frame 149, at Waterline
13	USNS Vega, T-AK 286	5-11-89	Port Side Shell, Stern, Frame 176, Below Waterline
14	Commercial Passenger Ship	9-11-89	Starboard Bottom Shell, Amidships
15	Commercial Passenger Ship	9-11-89	Starboard Side Shell, Amidships, at Waterline
16	Commercial Passenger Ship	9-11-89	Port Side Shell, Bow, 6 ft. Above Waterline
17	USS King, DDG-41	9-12-89	Starboard Side Shell, Bow, at Waterline
18	USS King, DDG-41	9-12-89	Port Side Shell, Bow, at Waterline
19	USS Conyngham, DDG-17	9-12-89	Starboard Side Shell, Bow, 1 ft. Above Waterline
20	USS Hayler, DD-997	9-12-89	Port Side Shell, Amidships, 1 ft. Above Waterline
21	USS Conyngham, DDG-17	9-13-89	Starboard Side Shell, Stern, Frame 193, 5 ft. Above Waterline
22	USS Hayler, DD-997	9-13-89	Starboard Side Shell, Bow, 1 ft. Above Waterline
23	USS Roosevelt, CVN-71	9-13-89	Starboard Elevator, Underside Sponson Shell

9

In instances where the transverse stiffeners were spaced a great distance apart (as in the case of some aircraft carrier hull measurements), the boundaries of the grid were located on a transverse stiffener on one side, and on an area of undeformed plating on the other, totally encompassing the deformation in the plating. While the location of the ship's stiffeners was usually apparent when viewed from a distance (such as from the bottom of the dry dock) it was more difficult to locate the stiffeners when the surveyors were close to the hull surface. In those cases where the location of the stiffener was not readily apparent, an ultrasonic thickness gauge was used to locate the stiffener. The size and spacing of the grids were chosen to ensure both that the maximum deformation in the plate was measured, and that an accurate representation of the overall deformation pattern in the plating was recorded. Each node in the grid pattern was numbered to correspond to numbering on the data table where measurements were recorded. Figure 3.1 shows a typical grid pattern laid out over a deformed area of ship plating.

In order to determine the thickness of the plating, an ultrasonic thickness gauge was used at each grid point, as shown in Figure 3.2. In some instances, thickness measurements were not able to be obtained, since at some locations the paint on the hull was chipped and peeling, and did not allow an adequate sonic coupling. This was especially true for ships using special ablative paint, such as the USS Detroit; however, the overall success in obtaining readings was considered good.

After obtaining plate thickness data at all node locations, measurements of the depth of plating deformation were taken. Two different methods were used to determine the depth of deformation in the plating, depending on the size of the panel. The first method, for panels with stiffener spacing of 24" or less, used a specialized measuring device obtained from the David Taylor Research Center (DTRC) in Carderock, Maryland. This DTRC device, shown in Figure 3.3, consisted of a gauge guide used in conjunction with dial indicator gauges to measure the relative depth of the plate deformation. The dial indicator gauges had a precision of 0.001". This DTRC device consisted of two machined guide rails supported in a metal frame, and was attached to the ship's plating with four adjustable magnetic feet. The guide rails provided a flat, level surface on which the dial indicator gauges were mounted to obtain a deformation reading, as shown in Figure 3.4. Since the span length of the guide rails was 24", this was the largest stiffener spacing for which this method of plate deformation measurement was used. The second method used, in cases where the stiffener spacing exceeded 24", was the Machinist Scale/Straight Edge Method. In this method, a rigid drafting straight edge was held between the stiffeners to give a zero deformation baseline, and a machinist scale with a precision of 1/64" was used, as shown in Figure 3.5, to measure the amount of deformation at each grid point. Photographs were taken, when possible, of each deformed panel and grid layout pattern in order to provide a record of measurements and to aid in data reduction after the survey.

3.4 DATA REDUCTION METHODS

Deformation measurements obtained using the Machinist Scale/Straight Edge Method represented the true amount of plate deformation and did not require any data reduction. However, when the DTRC device was used, data reduction was necessary to obtain the actual values of permanent plate deformation. The displacement values read on the DTRC dial indicator at each frame were taken as reference points of zero deflection. The subsequent readings at each grid point were then reduced by an appropriate amount based on an interpolation of the reference readings at each frame. The resulting difference represents the amount of deformation. The data reduction results provided an accurate representation of the amount and location of the deformation in the plating surface.
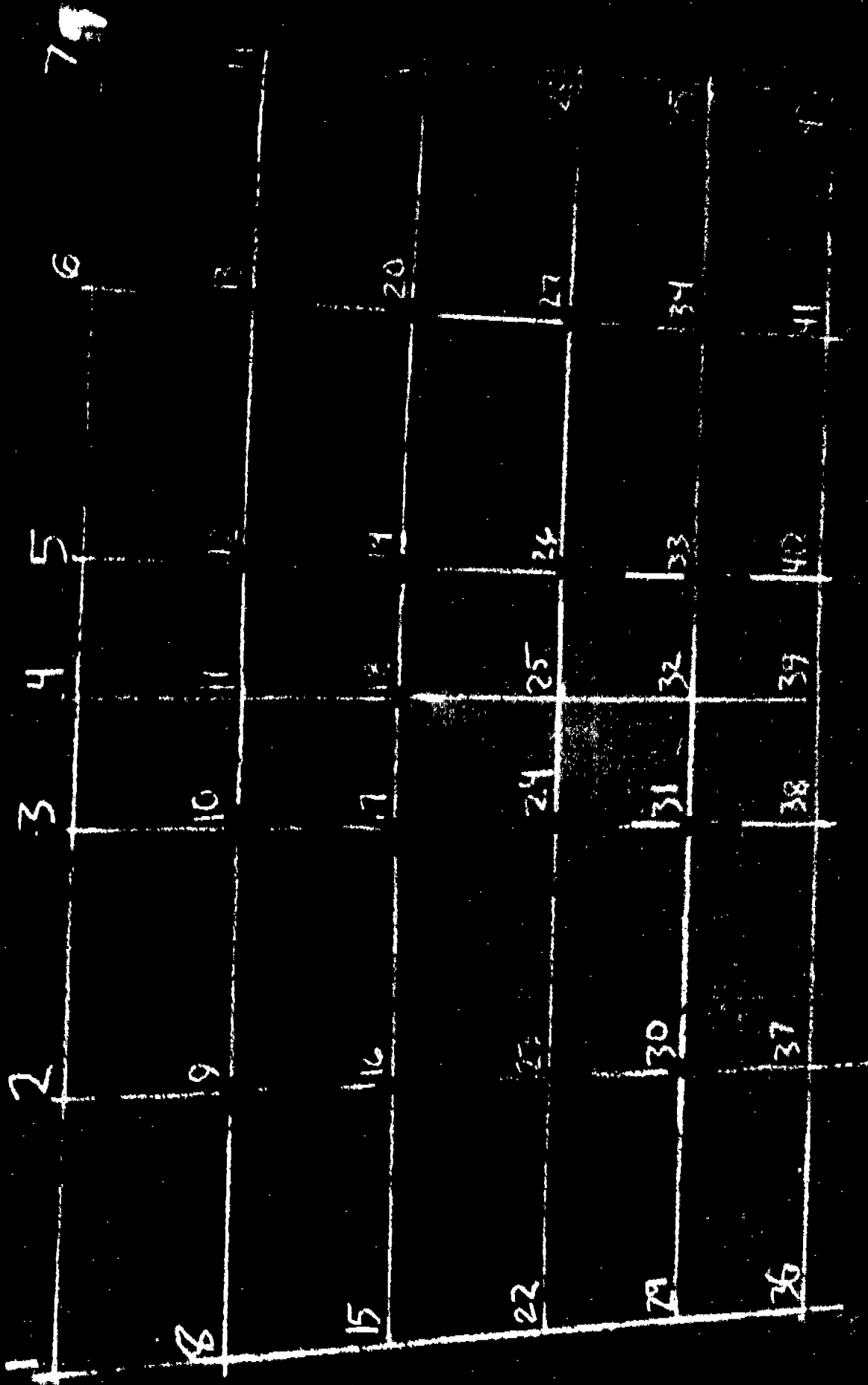
10

FIGURE 3.1 GRID PATTERN OVER DEFORMED PANEL

FIGURE 3.2
MEASURING PLATE THICKNESS USING
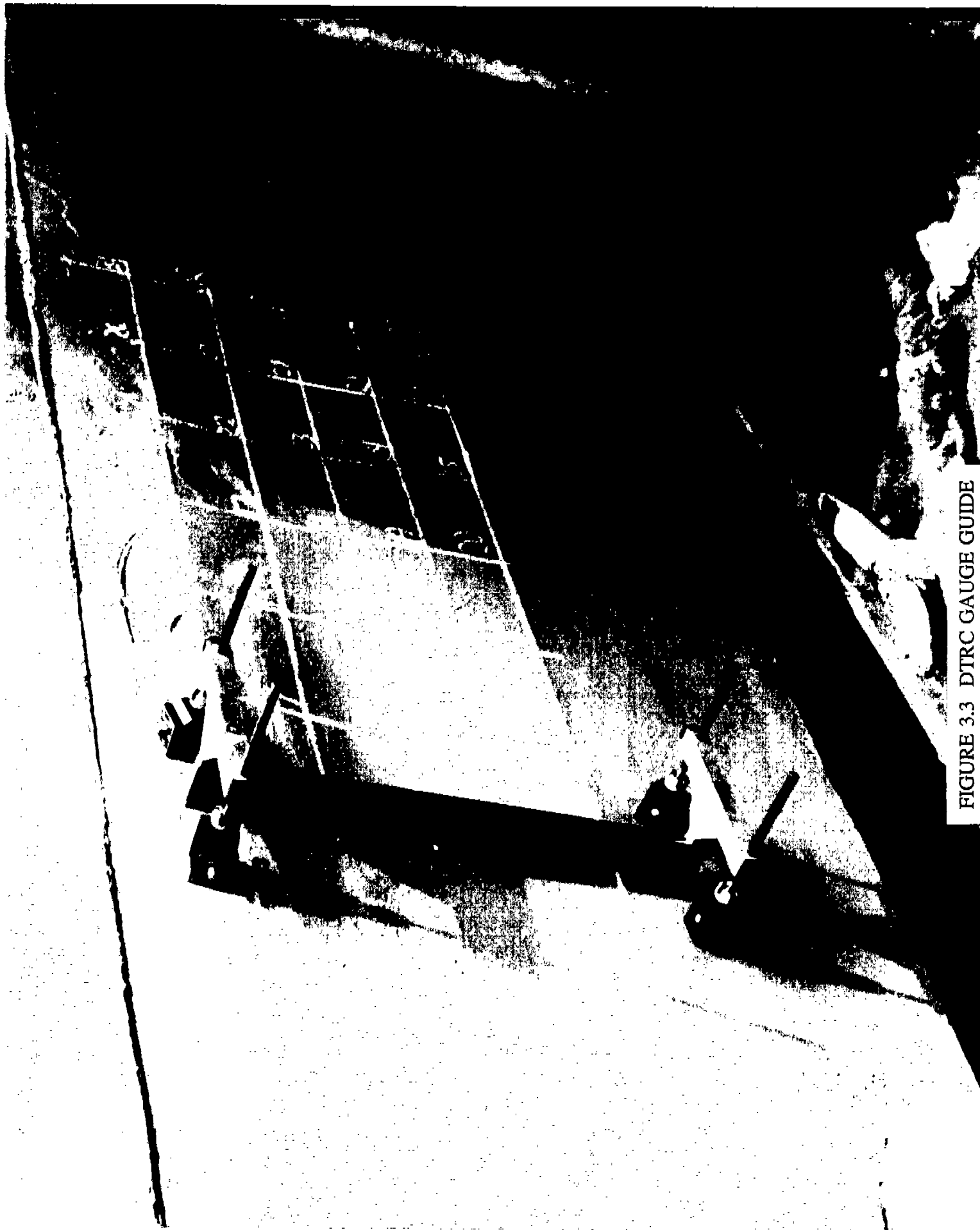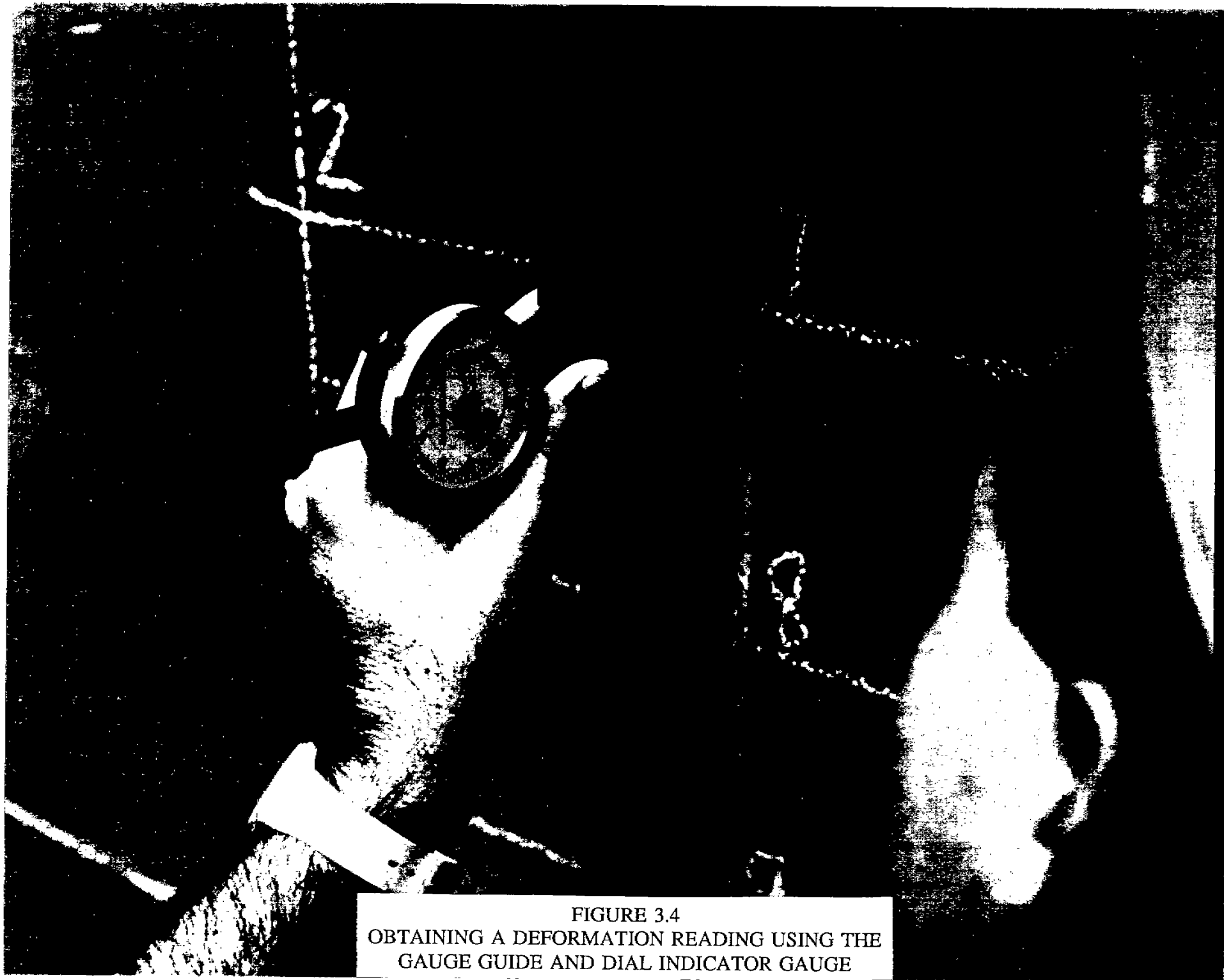THE ULTRASONIC THICKNESS GAUGE

FIGURE 3.3 DTRC GAUGE GUIDE

FIGURE 3.4
OBTAINING A DEFORMATION READING USING THE
GAUGE GUIDE AND DIAL INDICATOR GAUGE

14

FIGURE 3.5

OBTAINING A DEFORMATION READING USING THE
MACHINIST SCALE/STRAIGHT EDGE METHOD

The resulting deformation data was used to draw contour lines representing the profile of the various deformed plates. This data, along with the plate thickness and size, was used to estimate the amount of strain in the deformed plating.

3.5 RESULTS

Table 3.3 provides a summary of the deformations measured during the ship surveys. The table summarizes the plate deformation data provided in Appendix A. It was found that maximum panel deflection occurs during impact-type loading. In most cases, the impact-type deflection was highly localized and did not involve overall panel deformation. The other type of deformation was attributed to wave slap, wave slap coupled with impact loads, wheel loads, or hull grounding loads. This type of deformation was more uniform and generally was less than the localized impact-type deformation.

Table 3.4 presents estimated maximum strain measurements calculated from the deflections obtained during the ship survey. The maximum membrane strain was calculated by estimating the elongated length of the panel L_e, through the section with the greatest deformation, and comparing this with the undeformed length L_u through the same section. The membrane strain ε_m can then be approximated as:

$$\varepsilon_m = (L_e - L_u)/L_u \tag{3-1}$$

The maximum bending strain was calculated at the point on the edge of the panel where maximum bending occurs. This was located as the point inside the edge of the panel with the greatest deflection (Δ) relative to the edge. Using these two points on the panel, the radius of curvature (R) of the panel was determined at its edge. As shown by Reference [8], the bending strain ε_b can then be approximated as:

$$\varepsilon_b = \Delta/R \tag{3-2}$$

As noted in this reference, there are no material properties used in the derivation of this equation; therefore, this relation can be used for inelastic as well as elastic problems. In the case of panels deformed by impact - type loads, the maximum strains were calculated at the panel edge closest to the center of the deformation. In the case of panels deformed by wave slap, wheel loads, or hull grounding, the center of deformation and the areas of maximum strain are located in the center of the panel and at the panel edges, respectively.

16

Table 3.3 Ship Survey Plate Panel Deformations

Measurement *	a	b	a/b	t	Steel Type	Maximum Delection	Deformation Type
1	144"	64"	2.25	0.799"	HSS	2.0"	Impact
2	60"	24"	2.5	0.350"	HSS	0.444"	Wave Slap/ Impact
3	120"	30"	4.0	0.591"	**	0.812"	Impact
4	64"	30"	2.13	0.598"	**	4.25"	Impact
5	28"	27"	1.0	0.433"	MIL-S-22698	0.295"	Wave Slap
6	21"	15"	1.4	0.433"	MIL-S-22698	0.048"	Wave Slap
7	48"	48"	1.0	0.600"	**	3.469"	Impact
8	24"	16"	1.5	0.380"	**	1.245"	Impact
9	32"	28"	1.14	0.437"	HY-80	0.484"	Wave Slap/ Impact
10	42"	30"	1.4	0.45"	HSS	1.094"	Impact
11	24"	18"	1.33	0.875"	ABS Grade A	0.064"	Wheel Load
12	32"	30"	1.07	0.725"	ABS Grade A	2.594"	Impact
13	32"	26"	1.25	0.583"	ABS Grade A	1.125"	Impact
14	100"	32"	3.13	0.95"	**	1.031"	Hull Grounding
15	36"	16"	2.25	**	**	1.938"	Impact
16	26"	24"	1.08	0.638"	**	1.016"	Impact
17	30"	24"	1.25	0.438"	HY-80	1.016"	Impact
18	60"	38"	1.58	0.46"	HSS	1.188"	Impact
19	48"	18"	2.67	0.409"	HSS	0.622"	Wave Slap/ Impact
20	48"	18"	2.67	0.488"	MIL-S-22698	0.969"	Impact
21	52"	29"	1.8	0.50"	HSS	1.031"	Impact
22	30"	24"	1.25	0.438"	MIL-S-22698	2.109"	Impact
23	39"	24"	1.63	0.331"	**	0.219"	Wave Slap

* See Table 3.2 for ship and plate location
** Not Available

Table 3.4 Maximum Estimated Strains in Ship Survey Plates

Measurement	a/b	t (inches)	Maximum Membrane Strain %	Maximum Bending Strain %	Deformation Type
1	2.25	0.799	1.12	3.05	Impact
2	2.5	0.350	0.07	0.85	Wave Slap/ Impact
3	4.0	0.591	1.03	1.87	Impact
4	2.13	0.598	11.12	14.62	Impact
5	1.0	0.433	0.10	0.46	Wave Slap
6	1.4	0.433	0.00	0.11	Wave Slap
7	1.0	0.600	1.18	0.86	Impact
8	1.5	0.380	0.72	1.45	Impact
9	1.14	0.437	0.06	0.52	Wave Slap/ Impact
10	1.4	0.450	0.15	0.73	Impact
11	1.33	0.875	0.00	0.18	Wheel Load
12	1.07	0.725	1.64	2.91	Impact
13	1.25	0.583	0.25	0.60	Impact
14	3.13	0.950	0.03	1.45	Hull Grounding
15	2.25	*	1.10	*	Impact
16	1.08	0.638	0.52	1.06	Impact
17	1.25	0.438	0.31	0.88	Impact
18	1.58	0.460	0.09	0.18	Impact
19	2.67	0.409	0.06	0.94	Wave Slap/ Impact
20	2.67	0.488	0.12	0.15	Impact
21	1.8	0.500	0.05	0.36	Impact
22	1.25	0.438	1.11	1.13	Impact
23	1.63	0.331	0.02	0.27	Wave Slap

* Not Available.

SECTION 4.0
FINITE ELEMENT ANALYSIS

4.1 INTRODUCTION

Permanent plate deformations affect the residual strength characteristics of the plate. The strains induced in a plate by deformation reduce the residual load carrying capacity, modify the buckling characteristics, and reduce the flaw tolerance or fracture toughness of the plate. In order to assess the effects of plastic deformation on plates, a parametric study was conducted to determine the deformation/strain relationships of normally loaded plates of differing aspect ratios and thicknesses. The results of this study were compared to estimated strains from ship surveys and were used in developing a methodology for establishing deformation criteria. Table 4.1 summarizes the aspect ratio/plate thickness combinations analyzed in this study. Each plate analyzed was assumed to be completely fixed along all edges, and was subjected to uniform pressure loadings into the plastic range. The uniform normal pressure loadings were meant to represent the loading of a ship plate subjected to a wave slap.

Table 4.1 Plate Aspect Ratios and
Thicknesses Used in Parametric Study

Plate Size (inches)	Plate Thickness (inches)	
24 x 24 (Aspect Ratio = 1.0)	3/8	5/8
48 x 24 (Aspect Ratio = 2.0)	3/8	5/8

4.2 PARAMETRIC STUDY APPROACH

The deflection/strain relationships for the plates in Table 4.1 were determined using finite element analyses utilizing a large deformation, material nonlinear, static solution. For a given plate configuration, a quasi-static load function was used to apply normal pressure loads of increasing magnitude to the plate. Each applied pressure load created a deformation and a corresponding state of induced strain in the plate. The results of the finite element analyses of each plate were used to generate curves relating the deformation of the plate to the induced levels of strain in the plate.

4.3 FINITE ELEMENT MODEL DETAILS

The parametric study of plate panels subjected to uniform normal pressure loadings was performed using the PC-based finite element program COSMOS/M [9]. Initial attempts to perform this study using mainframe-based finite element programs such as NASTRAN [10] and ADINA [11] proved unsatisfactory, mainly due to the excessive run-time and costs associated with performing this type of nonlinear analysis. The assumptions and modeling strategies used in the COSMOS/M parametric study for each of the plates listed in Table 4.1 are discussed in detail in the following paragraphs. These details are identical for each of the four cases listed in Table 4.1. Anyone wishing to perform a similar analysis for a plate with a different aspect ratio, thickness, edge constraint, etc. may use these assumptions as a guide to modeling and performing the analysis.

In setting up a finite element model for a nonlinear analysis on COSMOS/M, the user may select from a number of options concerning the solution method to be used, the integration scheme,

19

the element representation, and the like. Before beginning this parametric study, a number of test cases were first performed on small models using various combinations of options, in order to determine the most effective combination of options for the problem at hand. The final options chosen for the analysis are summarized in Table 4.2.

Table 4.2 - COSMOS/M Options Chosen For Parametric Study

Type of Element: Nonlinear 20-node isoparametric solid, using 3x3x3 integration order
Problem Formulation: Large displacement, Updated Lagrangian formulation
Material Type: Von-Mises elasto-plastic model, utilizing a multi-linear stress-strain curve
Solution Technique: Regular Newton-Raphson Method
Integration Method: Newmark-Beta Method

From Table 4.2 it is seen that the finite element plate models were constructed using 20-node solid nonlinear elements. The geometry of a typical COSMOS/M 20-node solid element is shown in Figure 4.1. These elements are more mathematically complex than finite element plate or shell elements, and thus require greater analysis time for solution convergence. However, discussions with NASTRAN, ADINA, and COSMOS/M technical personnel indicated that for the type of analysis to be performed in this study, the use of plate or shell elements would not be appropriate, and would yield questionable results if the strain levels in the elements exceeded approximately 1 to 2 percent. It was recommended that 20-node solid elements be used. It was further suggested that each plate should be modeled using a relatively fine mesh, and the increment between applied loads be kept small. For each plate analyzed in this study, this necessitated the creation of a finite element model with a large number of elements and nodes.
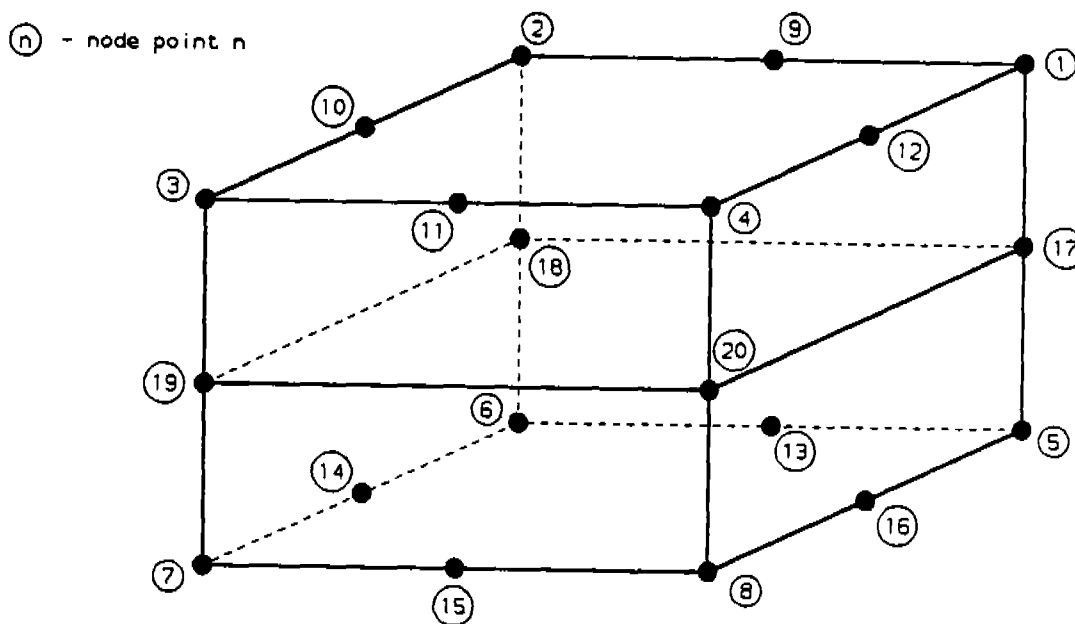
FIGURE 4.1. TYPICAL COSMOS/M 20-NODE SOLID ELEMENT

20
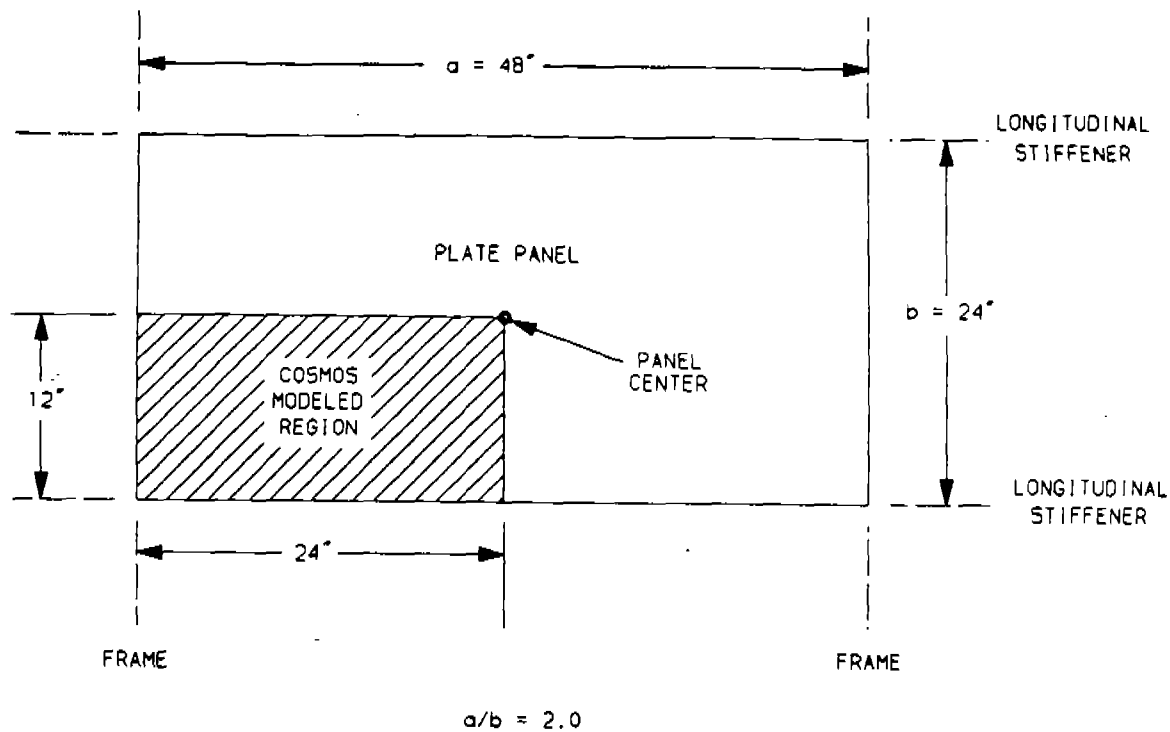
FIGURE 4.2. TYPICAL PLATE DIMENSIONS (FOR A/B = 2.0 PLATE) SHOWING REGION
MODELED FOR ANALYSIS

In order to keep the size of each plate model manageable, symmetry conditions were used to model each of the plates. Figure 4.2 shows a typical 48" x 24" ship plate bounded by frames and longitudinal stiffeners, indicating the region of the plate actually modeled in the COSMOS/M analysis. The COSMOS/M finite element model of this region is shown in Figure 4.3. This model is constructed from 256 20-node, nonlinear solid elements, generated from 1,955 node points. The corresponding stiffness matrix for this model contains 1,612,685 matrix elements, and analysis requires the simultaneous solution of 5,216 equations. Typical running time for this model using a DTK 486 computer was found to be approximately 20 hours. The costs associated with running such a model using a mainframe-based finite element program such as NASTRAN, on a time-sharing basis, are prohibitively high, and would exceed the funds allocated for this task. The mesh used to model the 24" x 24" plates, shown in Figure 4.4, was constructed in a similar manner.

In each plate finite element model (Figures 4.3 and 4.4), node number 1046 represents the center point of the plate, and is the point at which maximum out-of-plane deflection occurs when the plate is subjected to a normal pressure load. The strain levels in element #20, on the fixed boundary at the center of the long edge, are representative of the maximum bending strains in the plate. The strains in element #128, at the center of the plate where little bending occurs, are representative of the maximum membrane strains in the loaded plate.

As mentioned earlier, the finite element models of Figures 4.3 and 4.4 were constructed using 20-node, material nonlinear elements. The material nonlinearity for each element was modeled through the use of a multi-linear stress-strain curve input to COSMOS/M. For each of the plates of Table 4.1, the stress-strain curve for the ship steel of Figure 5.1, curve B was used to represent the material characteristics of the plate.

Each of the finite element models shown in Figures 4.3 and 4.4 was subjected to a uniform normal pressure load over its entire surface. In a COSMOS/M nonlinear analysis, the loads are input through the use of a load-time curve and an incremental loading scheme. In this study,
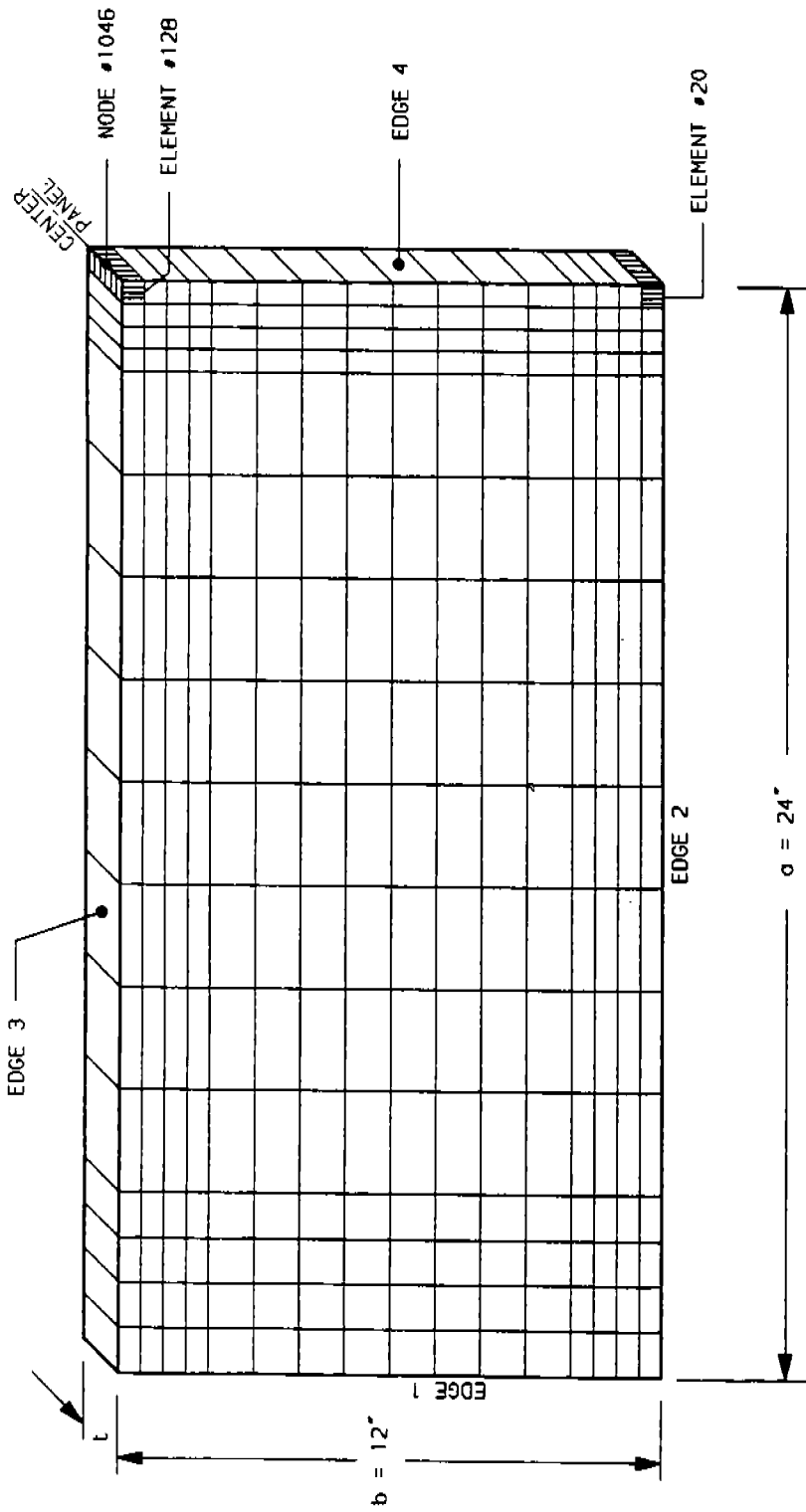
21

FIGURE 4.3. COSMOS/M MODEL FOR PLATE WITH ASPECT RATIO OF 2.0

NODE #1046
ELEMENT #128
EDGE 4
ELEMENT #20
CENTER PANEL
EDGE 3
EDGE 2
EDGE 1
a = 24"
b = 12"
t

BOUNDARY CONDITIONS:

Edge 1 – Fully restrained

Edge 2 – Fully restrained

Edge 3 – Restrained against translation in Y-direction

Restrained against rotation about X and Z axes

Edge 4 – Restrained against translation in X-direction
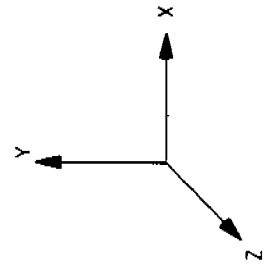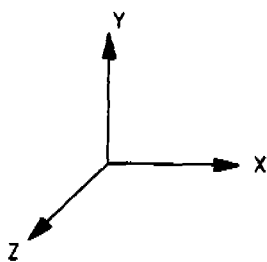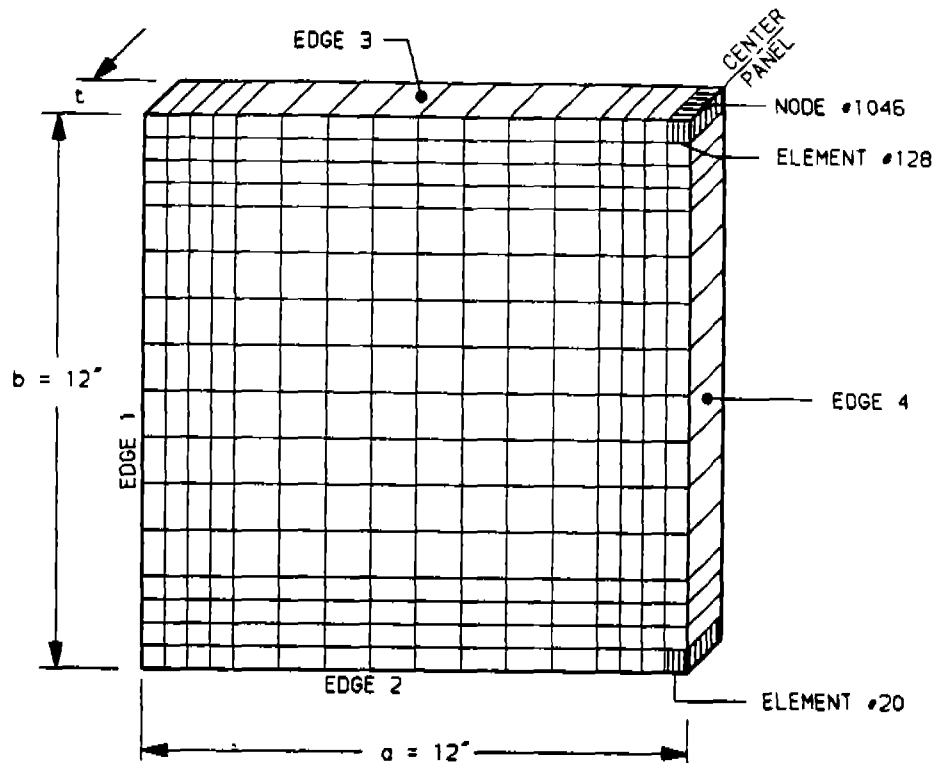
Restrained against rotation about Y and Z axes

X
Y
Z

22

BOUNDARY CONDITIONS:

Edge 1 - Fully restrained

Edge 2 - Fully restrained

Edge 3 - Restrained against translation in Y-direction

Restrained against rotation about X and Z axes

Edge 4 - Restrained against translation in X-direction

Restrained against rotation about Y and Z axes

FIGURE 4.4. COSMOS/M MODEL FOR PLATE WITH ASPECT RATIO OF 1.0

the linear load-time curve shown in Figure 4.5 was used for each plate model. Output results were requested at time increments of every 0.005 seconds, or in increments of 50 psi per step. Thus, the COSMOS/M analyses yielded stress, strain, and displacement results as each plate was subjected to pressure loads of 50 psi, 100 psi, 150 psi, etc. The analysis of each plate continued until it reached a load which produced a maximum panel bending strain of approximately 10% (10% strain in element 20). The maximum bending and membrane strains in the plates were then correlated with the maximum center plate deflections for each applied pressure load.

4.4   PARAMETRIC STUDY RESULTS

The results of the finite element parametric study for the plates listed in Table 4.1 are presented in tabular form in Tables 4.3 and 4.4, and graphically in Figures 4.6 through 4.13.

23
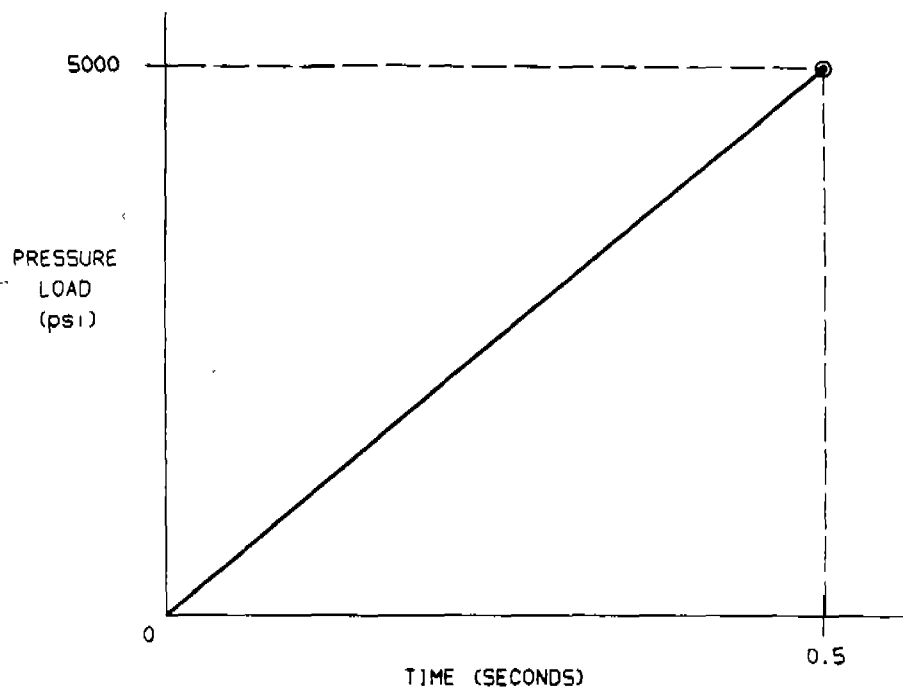
FIGURE 4.5. LOAD-TIME CURVE FOR COSMOS/M PLATE ANALYSES

In all presentations, the maximum center panel out-of-plane deflections (Δ) have been nondimensionalized by dividing by the plate short edge length (b = 24"). Table 4.3 summarizes the results of the COSMOS/M analyses for each plate, in terms of the maximum bending strains (strains in COSMOS/M element #20) determined in each plate. In this table, the maximum center plate out-of-plane deflections (deflections at COSMOS/M node #1046) are nondimensionalized by dividing by the plate short edge length (b = 24"). Table 4.4 summarizes the results of the COSMOS/M analysis for each plate in terms of the maximum membrane strains (strains in COSMOS/M element #128) determined in each plate.

In order to more clearly illustrate the effects of thickness and aspect ratio on the induced bending and membrane strains for pressure loaded steel plates, the COSMOS/M results tabulated in Tables 4.3 and 4.4 are presented graphically in Figures 4.6 through 4.13. The main features of these curves are summarized in Tables 4.5 (for bending strains) and 4.6 (for membrane strains).

Comparison of the bending strain curves (Figures 4.6 through 4.9) with the membrane strain curves (Figures 4.10 through 4.13) indicates that for the plates analyzed, the maximum induced strain levels are the bending strains at the edges of the plate, as expected for panels with fixed edges. For each particular plate configuration, a given value of Δ/b corresponds to a plate bending strain which is higher than the corresponding membrane strain.

Examination of the curves in Figures 4.6, 4.7, 4.10 and 4.11 would seem to indicate that the aspect ratio of a plate has little effect on the levels of bending or membrane strain induced by normal pressure loadings; for a given plate thickness, the resulting curves for plates with aspect ratios of 1.0 and 2.0 are practically the same. However, this should not necessarily be assumed to be true for plates with higher aspect ratios. For plates with higher aspect ratios, it is expected that the influence of the short side edge would be less, and that the maximum bending strain would be lower for a given Δ/b and plate thickness. The only way to verify this is to perform similar finite element analyses for panels with higher aspect ratios.

24

Examination of Figures 4.8, 4.9, 4.12 and 4.13 illustrate the influence of plate thickness on the induced plate strains. For a given plate aspect ratio, it is seen that for a particular value of Δ/b, the thicker plate (5/8") has lower levels of induced membrane and bending strains.

To summarize, the following strain/deformation relationships were determined from the finite element analyses:

- For a given Δ/b and plate thickness, the bending strains at plate edges are greater than the membrane strains at the point of maximum deflection.
- For a given plate thickness, changing the aspect ratio from 1.0 to 2.0 did not significantly affect the relationships between Δ/b and maximum strain.
- For a given aspect ratio and Δ/b, the maximum bending strain was greater in the 3/8-inch thick plate than in the 5/8-inch plate.
- Similarly, for a given aspect ratio and Δ/b, the maximum membrane strains were greater in the 3/8-inch thick plate than in the 5/8-inch plate.

Table 4.3 Maximum Plate Bending Strains vs. Maximum Δ/b

Maximum Bending Strain (%)	Maximum Δ/b *			
	a/b = 1.0, t = 3/8"	a/b = 2.0, t = 3/8"	a/b = 1.0, t = 5/8"	a/b = 2.0, t = 5/8"
0.00	0.0000	0.0000	0.0000	0.0000
0.25	0.0082	0.0098	0.0055	0.0066
0.50	0.0127	0.0145	0.0087	0.0100
0.75	0.0159	0.0173	0.0109	0.0119
1.00	0.0184	0.0201	0.0127	0.0139
1.25	0.0206	0.0218	0.0144	0.0159
1.50	0.0220	0.0231	0.0162	0.0178
1.75	0.0235	0.0242	0.0180	0.0198
2.00	0.0247	0.0255	0.0199	0.0216
3.00	0.0295	0.0299	0.0259	0.0265
4.00	0.0343	0.0346	0.0317	0.0313
5.00	0.0389	0.0398	0.0371	0.0364
6.00	0.0432	0.0446	0.0420	0.0416
7.00	0.0478	0.0492	0.0467	0.0465
8.00	0.0525	0.0539	0.0508	0.0511
9.00	0.0576	0.0596	0.0547	0.0554
10.00	0.0624	0.0655	0.0585	0.0595

* For b = 24 inches.

25

Table 4.4 Maximum Plate Membrane Strains vs. Maximum Δ/b

Maximum Membrane Strain (%)	Maximum Δ/b *			
	a/b =1.0, t = 3/8"	a/b =2.0, t = 3/8"	a/b = 1.0, t = 5/8"	a/b = 2.0, t = 5/8"
0.00	0.0000	0.0000	0.0000	0.0000
0.10	0.0095	0.0090	0.0064	0.0058
0.20	0.0180	0.0178	0.0127	0.0118
0.40	0.0312	0.0329	0.0225	0.0213
0.60	0.0429	0.0442	0.0291	0.0295
0.80	0.0497	0.0558	0.0356	0.0353
0.90	0.0532	0.0586	0.0394	0.0393
1.00	0.0563	0.0613	0.0440	0.0443
1.10	0.0594	-	0.0504	0.0499

* For b = 24 inches.

Table 4.5 COSMOS/M Bending Strain Curve Parameters

Figure Number	Plate Parameter Held Constant	Curves Plotted on Figure
4.6	Thickness = 3/8"	Aspect Ratio (a/b) = 1.0
		Aspect Ratio (a/b) = 2.0
4.7	Thickness = 5/8"	Aspect Ratio (a/b) = 1.0
		Aspect Ratio (a/b) = 2.0
4.8	Aspect Ratio (a/b) = 1.0	Thickness = 3/8"
		Thickness = 5/8"
4.9	Aspect Ratio (a/b) = 2.0	Thickness = 3/8"
		Thickness = 5/8"

26

Table 4.6 COSMOS/M Membrane Strain Curve Parameters

Figure Number	Plate Parameter Held Constant	Curves Plotted on Figure
4.10	Thickness = 3/8"	Aspect Ratio (a/b) = 1.0
		Aspect Ratio (a/b) = 2.0
4.11	Thickness = 5/8"	Aspect Ratio (a/b) = 1.0
		Aspect Ratio (a/b) = 2.0
4.12	Aspect Ratio (a/b) = 1.0	Thickness = 3/8"
		Thickness = 5/8"
4.13	Aspect Ratio (a/b) = 2.0	Thickness = 3/8"
		Thickness = 5/8"
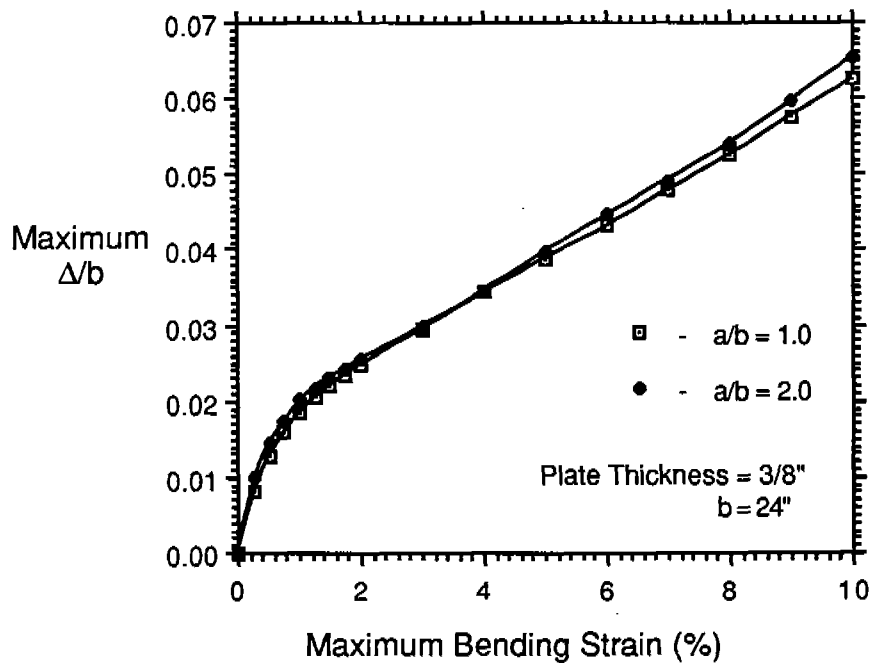
FIGURE 4.6
DEFLECTION/BENDING STRAIN CURVES
FOR PLATE THICKNESS OF 3/8"

27
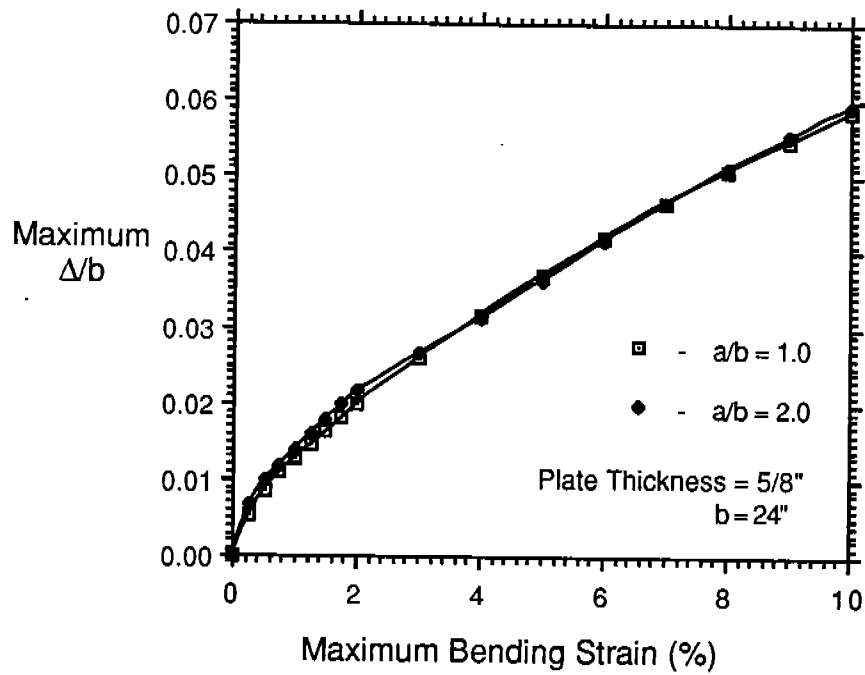
FIGURE 4.7
DEFLECTION/BENDING STRAIN CURVES
FOR PLATE THICKNESS OF 5/8"
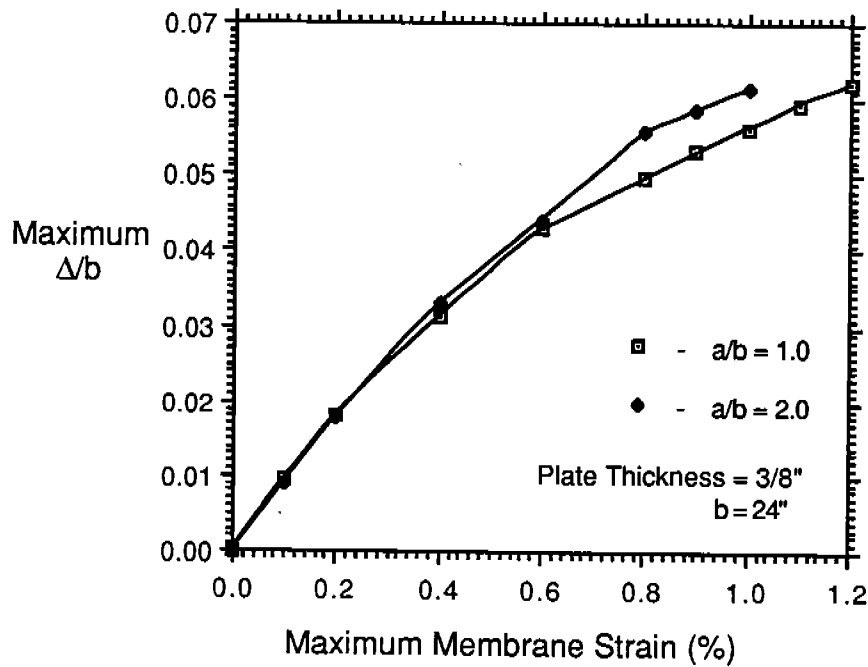
FIGURE 4.8
DEFLECTION/MEMBRANE STRAIN CURVES
FOR PLATE THICKNESS OF 3/8"

28
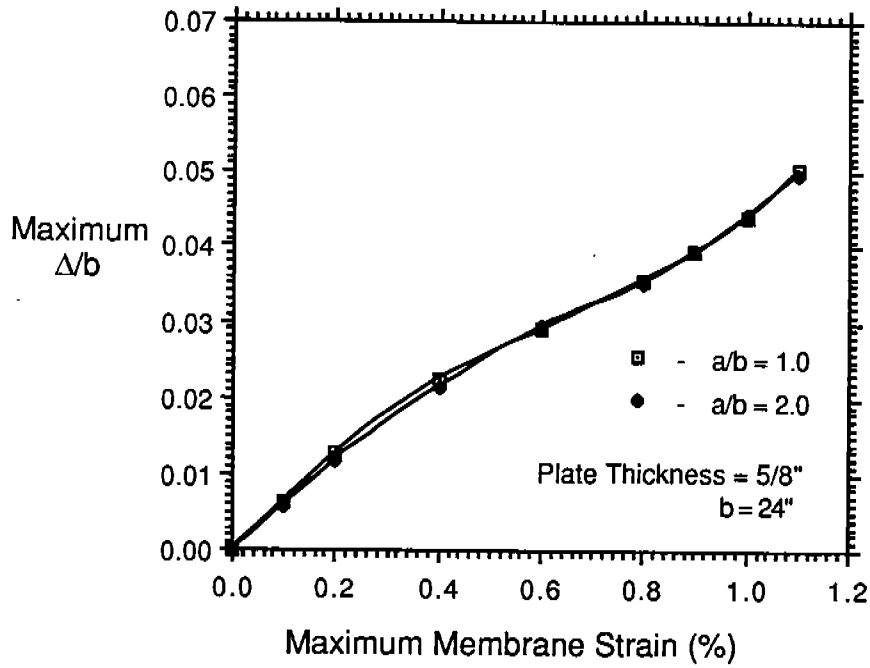
FIGURE 4.9
DEFLECTION/MEMBRANE STRAIN CURVES
FOR PLATE THICKNESS OF 5/8"
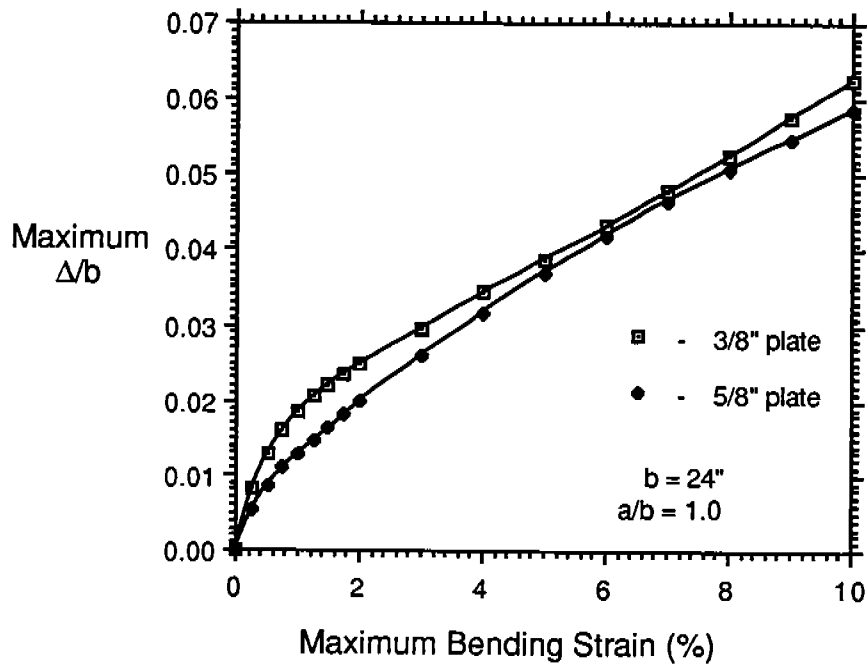
FIGURE 4.10
DEFLECTION/BENDING STRAIN CURVES
FOR ASPECT RATIO OF 1.0

29
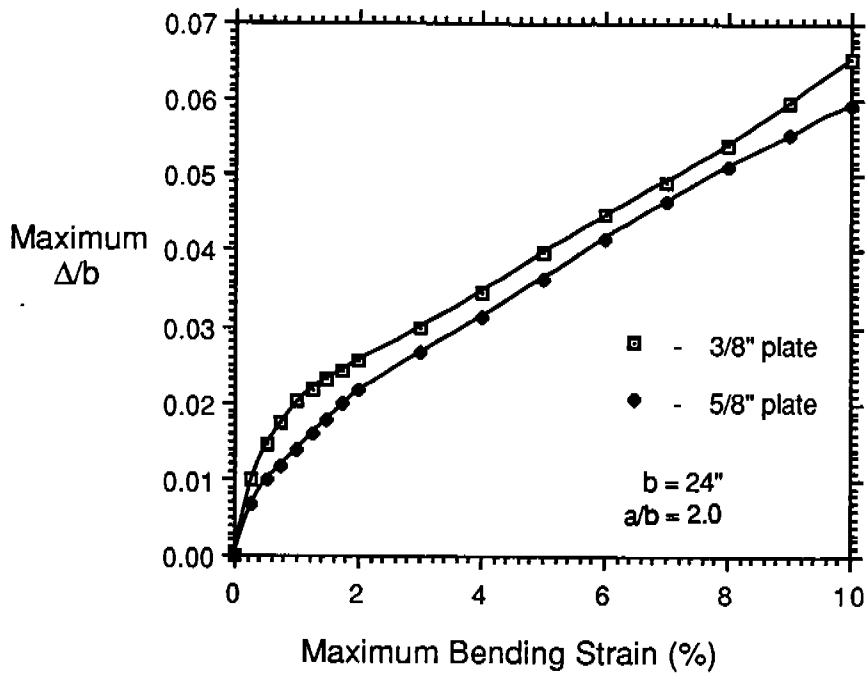
FIGURE 4.11
DEFLECTION/BENDING STRAIN CURVES
FOR ASPECT RATIO OF 2.0
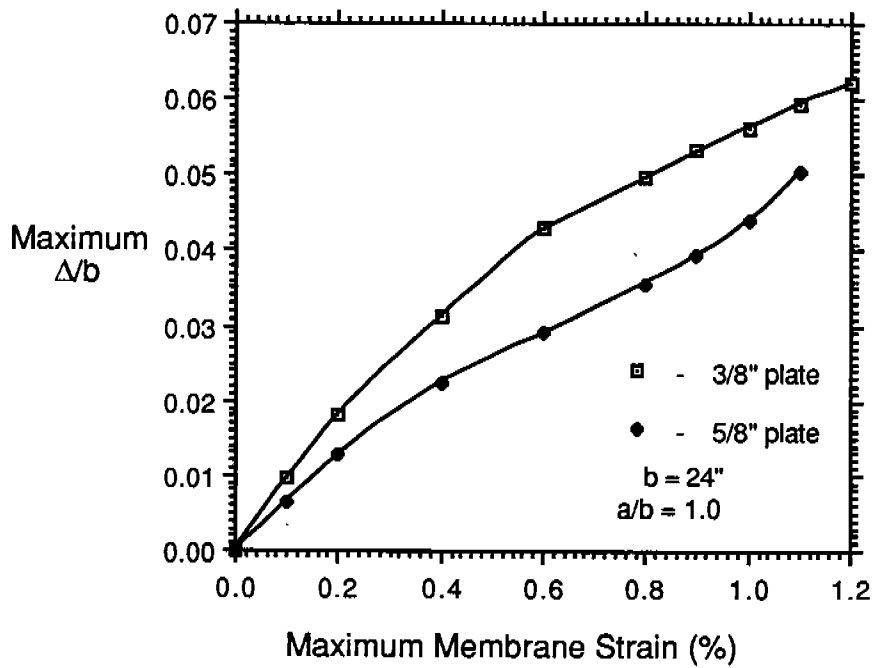
FIGURE 4.12
DEFLECTION/MEMBRANE STRAIN CURVES
FOR ASPECT RATIO OF 1.0

30
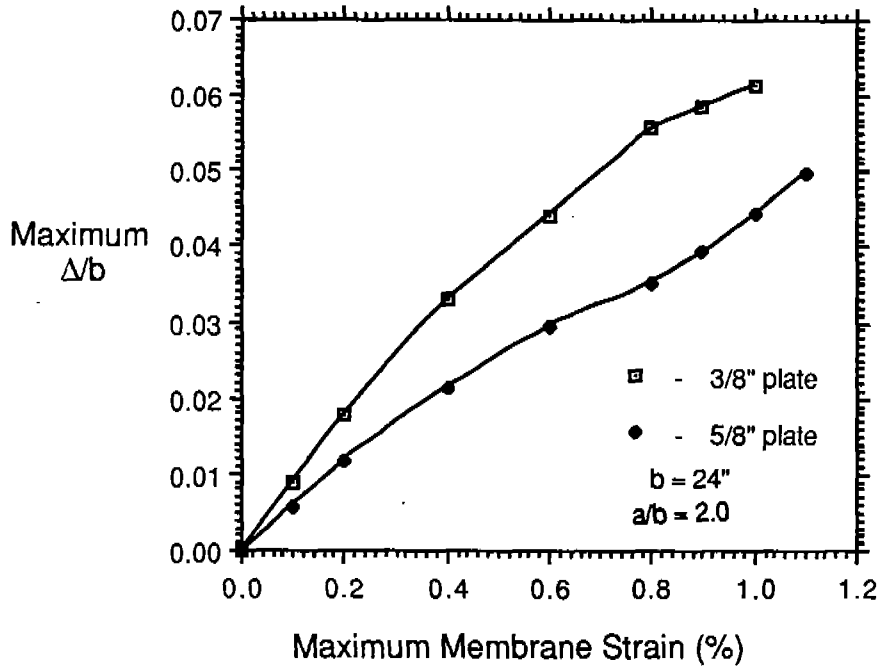
FIGURE 4.13
DEFLECTION/MEMBRANE STRAIN CURVES
FOR ASPECT RATIO OF 2.0

4.5 COMPARISON OF FINITE ELEMENT ANALYSIS RESULTS WITH SHIP SURVEY RESULTS

In order to verify the deformation/strain relationships of Figures 4.9 through 4.13, and to gain a degree of confidence in these relationships, the results of the finite element analyses were compared to the estimated strains derived from the ship survey measurements (Table 3.4).

There are three cases of plate deformation caused by wave-slap listed in Table 3.4 (Measurements 5, 6, and 23). For each of these cases, the Δ/b ratio was determined. For this value of Δ/b, using the appropriate aspect ratio and plate thickness, the strains calculated from the finite element analyses were determined. Since the plate thickness measured in each survey case did not correspond to the plate thicknesses used in the finite element analyses, interpolation between the finite element results was used. The following example illustrates this procedure.

For measurement #5 in the survey data, a 28" x 27" x 0.433" plate was found to have a maximum deflection of 0.295 inches. The Δ/b ratio for this case is thus found to be 0.295/27, or 0.0109. From Figure 4.10 (for a plate aspect ratio of 1.0), the corresponding bending strains for this Δ/b value are found to be 0.4 (for 3/8" plate) and 0.75 (for 5/8" plate). Interpolating between these two values to account for the survey plate thickness of 0.433, the maximum bending strain in the 28" x 27" x 0.433" plate, as determined by the finite element analysis results, was found to be 0.48 in/in. This compares favorably with the bending strain of 0.46 in./in. (see Table 3.4) estimated from the survey data. The membrane strain for this plate was calculated in a similar fashion.

The maximum bending and membrane strains for the three ship survey wave-slap cases, as determined from the finite element analysis results, were calculated and compared with the estimated strains tabulated in Table 3.4. The results of this comparison are summarized in Table 4.7. Examination of Table 4.7 shows excellent correlation between the finite element calculated bending strains and the ship survey estimated bending strains. For the membrane strains, the finite element analyses were found to be conservative, resulting in higher calculated membrane strains

31

than those estimated from ship survey data. Since bending strains have been shown to be much higher than membrane strains for a given deformation, this is not considered to be critical.

4.6 USE OF DEFLECTION/STRAIN CURVES

Figures 4.6 through 4.9 may be used by inspectors in the field to determine whether a permanently deformed plate should be replaced or left in place. The following example illustrates the application of these curves in the field.

An inspector measures a 0.5 inch deflection, caused by a wave slap, in the center of a 48" x 24" x 3/8" plate. The Δ/b value for the panel would be 0.5/24, or 0.0208. Referring to the curve for a/b = 2.0 in Figure 4.6, it is seen that the corresponding maximum bending strain for this case is approximately 1.07%. The inspector may then compare this value of strain to whatever criterion of strain is of interest to him. If the strain value is greater than the criterion strain, then the plate should be repaired or replaced. Otherwise, the plate may be left in place. If the thickness of the deformed plate is between 3/8" and 5/8", the inspector may interpolate between the curves of Figure 4.9 (for aspect ratio of 2.0) in order to determine the induced bending strain in the plate. This strain value may then be compared to the criterion strain in order to determine whether the plate should be replaced.

Table 4.7 Finite Element Calculated Strains Vs. Ship Survey Estimated Strains

Measurement Number (See Table 3.4)	Maximum Bending Strains (%)		Maximum Membrane Strains(%)	
	Finite Element Results	Ship Survey Results (See Table 3.4)	Finite Element Results	Ship Survey Results (See Table 3.4)
5	0.48	0.46	0.13	0.10
6	0.11	0.11	0.03	0.00
23	0.27	0.27	0.08	0.02

4.7 LIMITATIONS ON USE OF DEFLECTION/STRAIN CURVES

It is important to note that the curves of Figures 4.6 through 4.13 were developed for the plate geometries shown in Table 4.1, for a material with the stress-strain relationship characterized by curve B of Figure 5.1. These curves are applicable for cases where the plate panel material stress-strain relationships are similar to those of the material used in this study, for plates with aspect ratios between 1.0 and 2.0 and thicknesses between 3/8" and 5/8", with fixed edge conditions. These parameters effectively form the bounds for the use of these curves for the in-service evaluation of deformed plates.

It should be realized that the finite element analyses performed in the parametric study were performed for plate materials using the stress-strain relationships defined by curve B of Figure 5.1; the yield stress for this material is 58.6 ksi, characteristic of a high strength type steel. For materials with lower values of yield stress, the results given in Tables 4.3 and 4.4, and in Figures 4.6 through 4.13, are still applicable, as long as the shape of the material stress-strain curve is similar the shape of the stress-strain curve of curve B, Figure 5.1.

To verify this, a second finite element analysis of the 24" x 24" x 5/8" plate was performed. All modeling information in this second analyses was identical to the first analysis of the plate,

32

with the exception that a different stress-strain curve was input to COSMOS/M. In this second analysis, the stress-strain curve used for the first analysis (yield stress = 58.6 ksi) was essentially shifted "downward", to model a mild steel type material with a yield strength of 35 ksi. The shape of the stress-strain curve, however, was identical to the shape of the stress-strain curve used in the first analysis. Results of the second analysis verified that, for a given level of induced strain, the resulting Δ/b values of the second analysis were identical to those of the first analysis.

SECTION 5.0
FRACTURE MECHANICS

5.1 INTRODUCTION

Fracture mechanics provides the ability to quantitatively predict the structural integrity of large structures from laboratory test data obtained on small samples. Engineering applications of fracture mechanics have centered around predicting the macroscopic fracture behavior of structural components that are elastically loaded by utilizing the plane strain fracture toughness, K_{Ic}. This linear elastic analysis becomes inappropriate in attempting to predict the failure of lower strength ductile materials, such as ABS Grade B ship steels, especially at a thickness less than those required for plane strain. This section discusses the effects of inelastic deformation as it relates to reduced damage tolerance in ship steel panels.

5.2 OBJECTIVES

The objective of this section is to present the results of a comparative assessment of various fracture mechanics analysis methods potentially applicable to predicting the influence of prior plastic deformation on the flaw tolerance of ABS Grades of ship steels. A preferred fracture mechanics method will be identified and will be used to illustrate how the influence of prior plastic deformation on flaw tolerance can be estimated.

5.3 REVIEW OF FRACTURE MECHANICS METHODS

5.3.1 J-Integral (ASTM STD E813)

J-integral is the American approach to measuring the point of crack instability or point for the onset of rapid fracture. It is the forerunner to the British Crack Tip Opening Displacement (CTOD) approach. J-integral and CTOD are essentially identical in the method of analysis and the end products. The J-integral test method measures the load-line displacement (LLD) in order to calculate the work (Force x Distance) performed on a test coupon up to the point of crack instability. The plane strain fracture toughness (K_{Ic} per ASTM STD E399 [12]) can be estimated from the critical elastic-plastic energy release rate, J_{Ic}, using the following relationship:

$$K_{Ic} = \sqrt{J_{Ic} E} \qquad (5-1)$$

The plane strain fracture toughness (K_{Ic}) is considered to be an invariant property of the material, similar to the yield strength or tensile strength.

The J-integral method does not provide an analytical approach for estimating "residual toughness" under plane stress (inelastic) conditions. The J-integral is an experimental method of estimating K_{Ic} and is not analytically related to a "critical" strain limit.

Testing to establish J_{Ic} is conducted on sub-thickness (compared to thickness required for plane strain) plates in accordance with ASTM STD E813 [13]. These results can then be used to estimate K_{Ic}, critical stress levels, and critical thickness requirements for linear elastic fracture mechanics analyses. As illustrated by the following table, the fracture toughness and critical section thickness change dramatically with yield strength.

34

Material	Yield Strength (YS, ksi)	Fracture Toughness (K_{Ic}, ksi$\sqrt{in}$)	$B_{Ic} = 2.5 (K_{Ic}/YS)^2$ (B, inch)
AISI 4340	240	60	0.2
Ti-6Al-4V	120	80	1.0
A533B	70	220	25
ABS Grade B	50	250	60

From the above data, it is noted that fracture toughness generally increases with decreasing yield strength. Also, for ABS Grade B steel with a yield strength of about 50 ksi, a minimum section thickness of 60 inches, B_{Ic}, would be required to measure a valid K_{Ic} per ASTM E399. The J-integral method can be used to estimate K_{Ic} values in much thinner section of ABS Grade B steel.

5.3.2 Crack Tip Opening Displacement (CTOD) (British STD 5762 [14]; ASTM STD C1290)

The CTOD test method was developed in the United Kingdom and is used to measure the point of crack instability or the point for onset of rapid fracture. CTOD is an experimental method that utilizes a clip gage to measure the displacement at the mouth of a crack, in a notched bend specimen. The critical opening displacement, δ_c, is that measured at the onset of rapid fracture. The critical CTOD is related to K_{Ic} and can be expressed as follows:

$$CTOD = \delta = \delta_e + \delta_p = \frac{K^2}{2\ YS\ E'} + \frac{0.4(w-c)V_p}{0.4w + 0.6c + z} \qquad (5\text{-}2)$$

and

$$G = \frac{K^2}{E'} = 2\ YS\ \delta_c \qquad (5\text{-}3)$$

or

$$K_{Ic}(CTOD) = \sqrt{2\ E'\ YS\ \delta_c} \qquad (5\text{-}4)$$

where:

δ = CTOD

δ_c = critical CTOD

δ_e = elastic component of CTOD

δ_p = plastic component of CTOD

K = stress intensity factor

YS = yield strength

E' = elastic modulus in plane strain $= \dfrac{E}{1 - v^2}$

w = specimen width

c = crack length

V_p = plastic component of clip gage opening displacement

z = clip gage abutment height

Although physically more appealing in relating the microscopic concepts of crack initiation to the macroscopic toughness parameters, the CTOD is more difficult to measure and to interpret than

the J-integral. Analytically, the CTOD can provide the same information and utilizes the same testing procedures as the J-integral.

5.3.3 Tearing Modulus

The Tearing Modulus is an attempt to experimentally measure the resistance to crack extension by ductile tearing prior to crack instability under elastic-plastic (inelastic) conditions. Since J_{Ic} is measured by extrapolation of test data under inelastic conditions, the slope of the J-resistance (J_R) versus crack extension (Δa) curve would be a measure of resistance to tearing under inelastic conditions or,

$$\text{slope} = \frac{\Delta J_R}{\Delta a} \equiv T_R \qquad (5\text{-}5)$$

The tearing modulus (T_R) under plane stress conditions will depend on the crack size, plate thickness, and loading conditions. The tearing modulus does not lend itself to analytically estimating damage tolerance under plane stress (inelastic) conditions. The tearing modulus must be measured for each plate thickness and for each level of damage. Analogous procedures have been developed for using the slope of the CTOD-resistance curve.

5.3.4 R-Curve (ASTM STD E561 [15])

R-curve is an experimental method of measuring the resistance to crack extension under inelastic conditions; i.e., at thickness $B < B_{Ic}$. The analysis is conducted in terms of the following stress intensity parameters:

K_R = Stress intensity or resistance curve, which is a function of crack extension (Δa).

K_c = Critical stress intensity under inelastic conditions, which is a function of initial crack size (a_0).

The value of K_c is greater than K_{Ic}, and K_c is __NOT__ an invariant property as with K_{Ic}. The parameter K_c depends on plate thickness and starting crack size. The resistance curve $(K_R$ vs. $\Delta a)$ is considered to be the invariant property of the material. The R-curve method does not lend itself to analytically estimating "residual toughness" under plane stress (inelastic) conditions.

5.3.5 Strain Energy Density (SED)

Since it utilizes a "critical" strain limit (ε_c) and is derived from the strain as measured in a tensile test, Strain Energy Density appears to be the most promising approach to analytically predicting the influence of prior plastic deformation on the flaw tolerance of ship steels. Two basic approaches to Strain Energy Density were evaluated: (1) SED_c and (2) SED_{FM}.

5.3.5.1 SED_c

SED_c is based on "locally" attaining a critical strain energy density to initiate fracture. The critical strain energy density is calculated by integrating the area under a true stress - true strain curve. This Strain Energy Density approach does not address the existence of cracks nor does it predict critical strain without conducting a finite element analysis. The SED_c model has been used to predict failure of weld joints with irregular cross-sections and different tensile properties across the weld joint. A detailed description of the analysis is given in Appendix B.

5.3.5.2 SED$_{FM}$

SED$_{FM}$ is more directly related to a fracture mechanics analysis than the SED$_c$ method. The SED$_{FM}$ analysis lends itself to analytically estimating both K$_{Ic}$ and the R-curve. This method described in Appendix C is based on analyzing three different zones in front of the crack tip. The far field or elastic zone is analyzed on the basis of the elastic strain energy density under a tensile curve. The near field or uniform plastic (J-integral) zone is analyzed on the basis of the uniform plastic strain energy density zone under a tensile curve; i.e., the area up to the ultimate tensile strength, where necking or non-uniform plastic deformation begins. The damage zone, at the tip of the crack (generally excluded from J-integral analysis), is analyzed on the basis of the non-uniform plastic strain energy density zone under a tensile curve; i.e., the area beyond the ultimate tensile strength up to the point of fracture. SED$_{FM}$ analysis permits the calculation of critical crack size for a variety of configurations.

The result of the SED$_{FM}$ analysis is either a fracture strength curve for applied stresses less than yield, or a fracture strain curve for stresses and strains above yield. These curves relate fracture stress or strain to crack size for various thickness and amount of prior plastic deformation.

5.4 SELECTION OF MOST APPLICABLE FRACTURE MECHANICS APPROACH

Based upon the above review, Strain Energy Density appears to be the best approach to analytically assess the influence of prior plastic strain on the residual toughness of ship steels. The stress-strain curve which is the basis for calculating SED$_{FM}$ can be analyzed as noted in Appendix C to estimate the influence of prior plastic strain on residual toughness and critical crack size. As noted earlier, the SED$_c$ method requires a finite element analysis program to relate changes in strain energy density to critical fracture stress. This analysis becomes very complex in handling a three-dimensional problem with a pre-existing crack. The SED$_{FM}$ approach eliminates the need for finite element analysis and can predict a relationship between prior plastic strain and a change in critical crack size as a function of applied stress or strain. The basic requirement for the SED$_{FM}$ analysis is a full range stress-strain curve.

With regard to an alternate, empirically based method to establish allowable crack size, the British Standards Institution's Welding Standards Committee has prepared Published Document (PD) 6493 [16] to provide guidance on some methods for determining acceptance levels for defects in fusion welded joints. PD6493 outlines step-by-step procedures for assessing the criticality of a defect in either base metal or in the fusion and heat-affected zone of weldments. When the applied stress levels are below yield stress, a linear elastic analysis is performed on a given defect, to determine an effective defect size. The defect is regarded as acceptable if the stress intensity (K$_I$ value) calculated using the effective defect size is less than 0.7 x the critical value of K$_{Ic}$ for the material. When the applied stress or strain levels are above yield, or when the applied stress levels are below yield but a valid K$_{Ic}$ cannot be obtained due to inadequate section thickness, PD6493 utilizes the CTOD measurements and a series of charts to determine both an effective defect size, a', and a tolerable defect size, a'$_m$. When this effective defect , a', is less than the tolerable defect, a'$_m$, then the defect is considered acceptable. When a' is greater than a'$_m$, the defect must be repaired. The relationships between CTOD and defect size parameters are empirical. Application of CTOD and the method outlined in PD6493 to the analysis of damaged ship plates would require measurement of the K$_{Ic}$ or CTOD for the plastically deformed materials. PD6493 could then be used to assess the influence of applied stress or strain on critical flaw size and the need to repair the plate.

5.5 EFFECTS OF PRIOR STRAIN

The SEDFM approach was selected as the method for addressing the problem of estimating the effect of prior plastic strain on the damage tolerance. The material selected for evaluation was ABS Grade B ship steel at room temperature, with thicknesses ranging from 3/8- to 1-inch. For analysis purposes, a maximum prior plastic strain of 15% was selected. The minimum tensile properties for the ABS-Grade B steel are specified as 34 ksi YS, 58-71 ksi UTS, 22% (2 inch) elongation. The typical plane strain fracture toughness of this material at room temperature would probably be in the range of 250-300 ksi$\sqrt{in}$; therefore, the plane strain thickness per ASTM E399 is about 60 inches. Thus, a plate less than one-inch thick would be in a condition of plane stress, would exhibit 100% shear, and would undergo a completely ductile fracture.

Estimating the fracture toughness alone is not sufficient to evaluate the impact on damage tolerance. The yield strength is also a consideration. The damage tolerance or tolerance to a defect of a given size is a function of the ratio of K_{Ic}/YS. In a material that is cold worked or has prior plastic deformation, the yield strength increases and the toughness decreases. Both properties must be taken into account to evaluate the change in damage tolerance. For the purposes of this report, the ratio of K_{Ic}/YS will be defined as the damage tolerance index or DTI. The DTI is useful for estimating the plate thickness (B_{Ic}) necessary to encounter plane strain or plane stress fracture (YC).

Since a full range stress strain curve or true stress-true strain curve to fracture was not available for the ABS Grade B ship steel, laboratory tests were conducted to measure these properties. Two separate samples of ship steel were supplied by the Norfolk Shipbuilding and Dry Dock Company (NORSHIPCO), which were designated sample A2 (0.2-inch thick), and sample B2 (0.3-inch thick). Full range tensile tests were performed on the two samples. The resulting test data was then analytically converted to a full range true stress- true strain curve. Sample calculations for the analytical conversion of engineering stress-strain to true stress- true strain and a tabulation of the tensile properties obtained from these tests are given in Appendix C. Figures 5.1 through 5.4 represent a graphical analysis of the tensile test data in terms of engineering stress-strain as well as true stress-true strain.
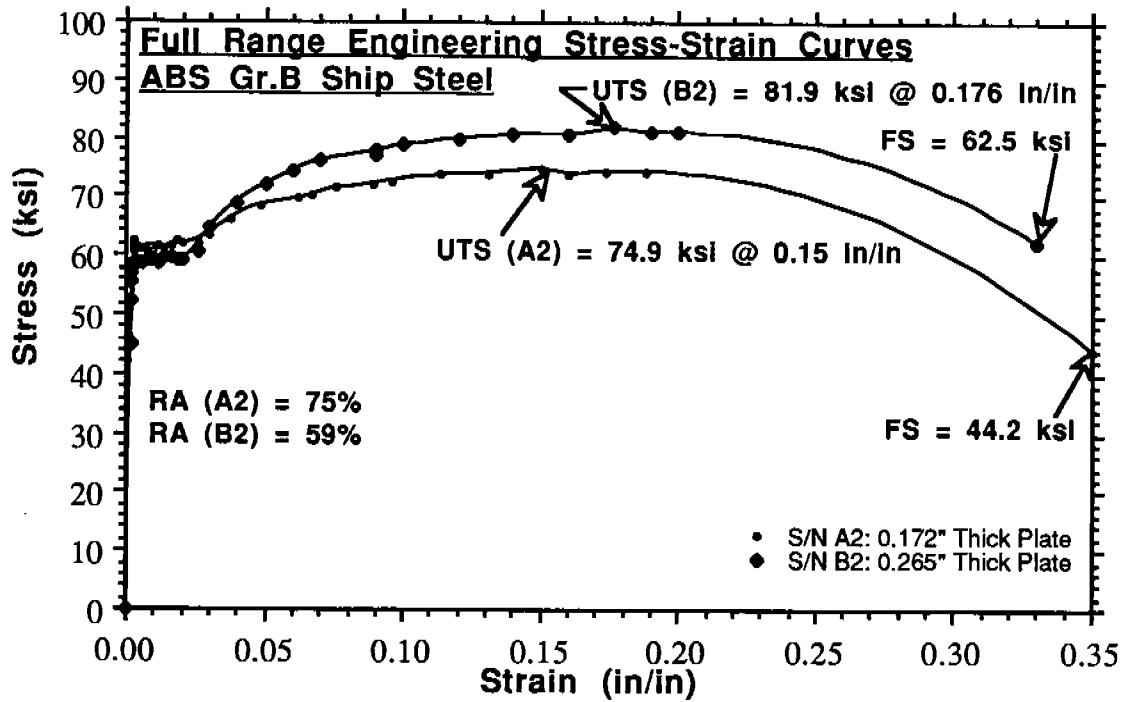
FIGURE 5.1 FULL RANGE ENGINEERING STRESS-STRAIN CURVE
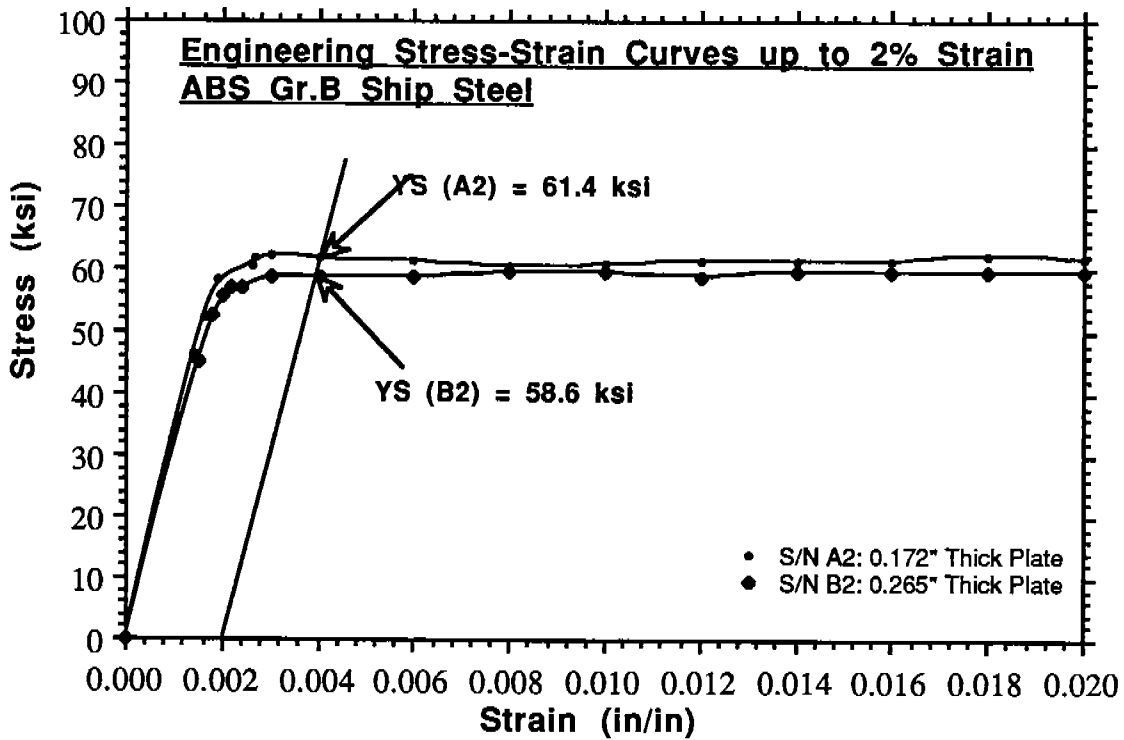
FIGURE 5.2 ENGINEERING STRESS-STRAIN CURVES UP TO 2% STRAIN
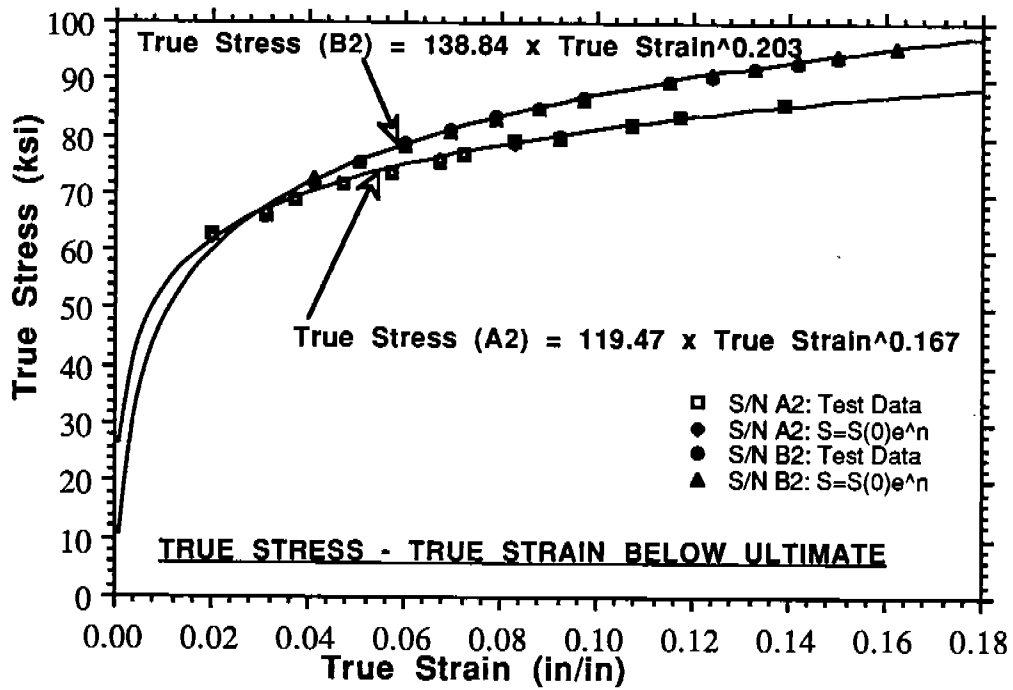
FIGURE 5.3 TRUE STRESS-STRAIN BELOW ULTIMATE TENSILE STRENGTH
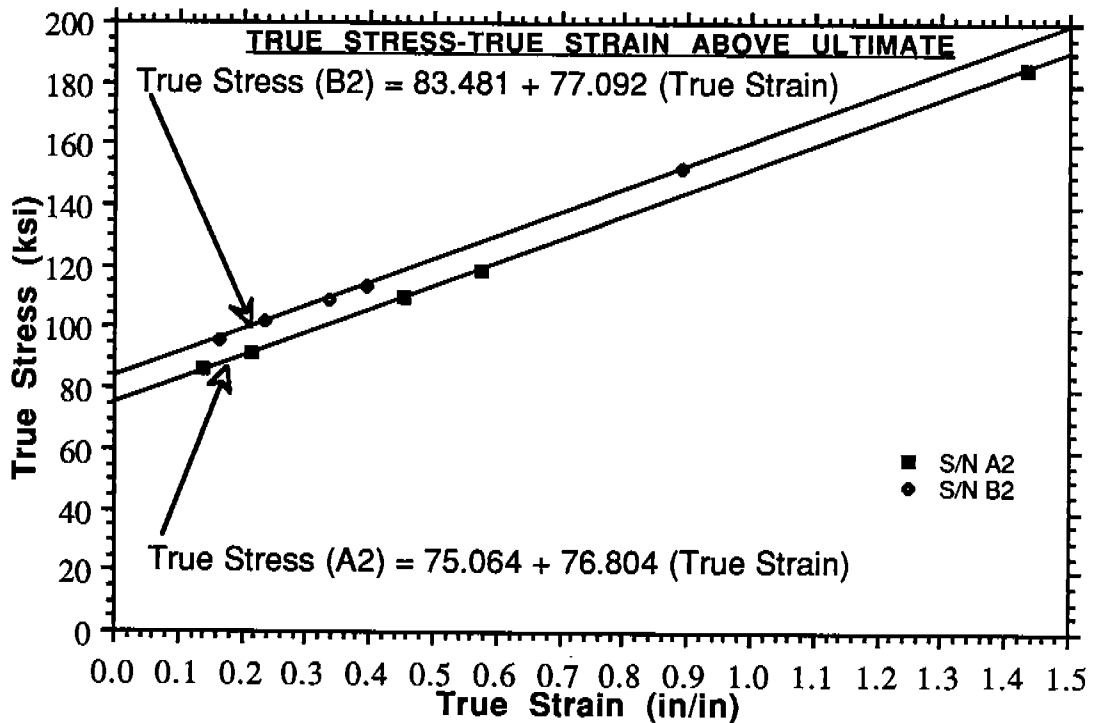
FIGURE 5.4 TRUE STRESS-STRAIN ABOVE ULTIMATE TENSILE STRENGTH

40

The measured tensile properties of the samples are summarized in Table 5.1

Table 5.1
Full Range Stress-Strain Curve Properties of Steel Samples

Material	Yield Strength	ε_{UTS}	UTS	RA	Fracture Strength
ABS Grade B MIL-S-22698	34 ksi, min "Ordinary Strength"	---	58-71 ksi	---	---
Sample A2	61.4 ksi, min	0.15	74.9 ksi	75%	44.2 ksi
MIL-S-22	"High Strength"	---	68-85 ksi	---	---
Sample B2	58.6 ksi	0.17	81.9 ksi	59%	62.5 ksi

It is noted that the yield strength and tensile strength values measured for these steels are significantly higher than the minimum values required for ABS Grade B steel. In addition, there were significant differences in the reduction of area and the fracture strength of the two samples. Chemical analyses of these materials (Table 5.2) indicated insignificant differences in the carbon content of the two steels. The higher carbon content of sample B2 most likely accounts for the higher strength and lower ductility of this material. It is not clear from the mechanical properties and chemical composition measurements in this study that the steels are actually ABS Grade B steel. However, these steels do possess comparable chemical and mechanical properties.

Table 5.2 Results of Chemical Analysis of Plates A and B

ELEMENT	SAMPLE A2 (WEIGHT %)	SAMPLE B2 (WEIGHT %)	SPECIFICATION* (WEIGHT %)
Carbon	0.08	0.16	0.21 maximum
Manganese	0.67	0.97	0.8 - 1.10 **
Phosphorus	0.010	0.013	0.04 maximum
Sulfur	<0.001	0.007	0.04 maximum
Silicon	0.07	0.22	0.35 maximum
Chromium	0.01	0.10	-
Nickel	<0.01	0.09	-
Molybdenum	<0.01	0.05	-
Copper	0.01	0.01	-
Iron	Remainder	Remainder	-

* Requirements of MIL-S-22698C(SH) specification.
** 0.06 minimum for fully killed or cold flanging steel.

5.5.1 Results of SED$_{FM}$ Analysis:

The SED$_{FM}$ model considers three zones around the crack tip and correspondingly divides the true stress - true strain curve into three different strain energy zones: (1) elastic strain energy density, (2) uniform plastic strain energy density and (3) the damage zone or strain energy density corresponding to non-uniform plastic flow. The SED$_{FM}$ analysis extends the Griffith approach of defining instability as unstable crack growth when the total plastic energy absorbed is less then the elastic energy released during crack growth. The SED$_{FM}$ analysis then sums up the three different strain energy density zones. The critical crack size can then be calculated for a variety of specimen configurations, including a single edge crack in a compact tension specimen, resulting in a calculation of K$_{Ic}$, or a through thickness center cracked panel (CCP), resulting in calculation of fracture strength or strain curves.

The results of fracture toughness K$_{Ic}$ calculations, using the SED$_{FM}$ analysis to estimate K$_{Ic}$, are presented on Tables 5.3a and 5.3b. As noted thereon, increasing levels of prestrain (plastic deformation) both increase the yield strength and dramatically reduce the plane strain fracture toughness. Plastic deformation up to 14 or 15% reduces K$_{Ic}$ by up to about 80% for both samples of steel. The increased yield strength and reduced K$_{Ic}$ result in a dramatic reduction in DTI and in the critical thickness, B$_{Ic}$ required for plane strain conditions. It is noted from the YC (ductile, plane stress fracture) thickness values listed in these tables that 14 to 15 % prior plastic deformation will result in mixed mode, elastic-plastic fracture in steel thicknesses greater than 0.4 to 0.6 inches. In sum, these analyses show significant reduction in flaw tolerance when the ABS Grade B type steels are subjected to prior plastic deformation.

Table 5.3a. Estimated Fracture Toughness and Damage Tolerance
Values for ABS-A2 Steel

Prestrain (%)	YS (ksi)	K$_{Ic}$ (ksi√in)	DTI (K$_{Ic}$/YS)	B$_{Ic}$ (Brittle) ≥ 2.5 (DTI)^2	YC (Ductile) B≤ 0.4 B$_{Ic}$
00	61.4	312	5.1	64.5	25.8
05	71.2	243	3.4	29.0	11.6
10	73.5	164	2.2	12.4	5.0
14	74.6	59	0.8	1.6	0.6

Table 5.3b. Estimated Fracture Toughness and Damage Tolerance
Values for ABS-B2 Steel

Prestrain (%)	YS (ksi)	K$_{Ic}$ (ksi√in)	DTI (K$_{Ic}$/YS)	B$_{Ic}$ (Brittle) ≥2.5 (DTI)^2	YC (Ductile) B ≤ 0.4 B$_{Ic}$
00	58.5	178	2.6	23.2	9.3
05	74.5	142	1.9	9.1	3.6
10	78.5	105	1.3	4.5	1.8
15	80.9	54	0.7	1.1	0.4

With regard to the change in damage tolerance of center cracked panels (CCP) with through the thickness cracks and loaded in tension, the SED$_{FM}$ analysis was used to calculate fracture strength curves (FSC) and fracture strain curves (FEC) for the two samples of steel.

The fracture strength curves are used to evaluate the failure conditions for center cracked panels under plane stress conditions when the applied stress is below the yield strength. The FSC is a plot of fracture stress versus the critical half crack length for fracture of a center cracked panel. FSC for samples A2 and B2 are presented in Figures 5.5a and 5.5b. The critical half crack length (c) is seen to decrease as the applied stress increases. Also, prestrain reduces the critical half crack length for a given level of applied stress. Referring to Figure 5.5a for example, a center cracked panel with a crack c = 10 inches (total crack length = 20 inches) would fracture at a stress of about 60 ksi. After 14% prestrain, the fracture stress would be reduced to about 30 ksi. For both the samples evaluated herein, A2 and B2, the FSC's were not significantly changed by prestrains of 5 to 10 percent. Beyond 10%, the flaw tolerance of the materials is significantly reduced.

The fracture strain curve is used to evaluate the effects of above yield stress loading on the critical half crack length (c) of undeformed and prestrained (plastically deformed) ship steel. Figures 5.6a and 5.6b present FEC's for the steels evaluated in this study. Examination of these curves indicate that critical half crack lengths decrease with increasing amounts of applied strain or prior prestrain. For example, referring to Figure 5.6b, the critical half crack length for a center cracked panel is about 1.0 inch for undeformed plate at an applied strain of about 7.0 percent. As the prestrain or plastic deformation of the plate is increased to about 10 percent, the critical half crack length is decreased to about 0.3 inches. This means that plating that has been subjected to about 10% prestrain (prior plastic deformation) and containing a 0.6 inch long (i.e., 0.3 x 2) through thickness crack will not fracture in a brittle manner at applied tensile strains as high as 7.0 percent.

When considering the effect of plate thickness in connection with critical fracture stress or critical fracture strain, the relationships illustrated in Figures 5.5 and 5.6 are considered appropriate for plates with thicknesses ranging from 0.4 to 1.0 inch. With regard to small surface or partial through the thickness cracks with depths equal to half the crack length, the stresses required for "pop in" to a through the thickness crack would be at or above the yield strength for cracks with depths up to 0.7 x the thickness. Based on the fracture toughness values estimated from the SED$_{FM}$ analyses, pop in of small part through cracks to through thickness cracks is not considered likely.

It must be remembered that all of the calculations included in this report are based on tensile curves at room temperature and under conventional loading rates, which in all probability corresponds to the upper shelf. Since the dynamic tear impact transition curve shows a brittle transition at 0°C, the tensile test curves used in this analysis should be at high loading rates and lower temperatures. Figure 5.7 shows impact temperature data on typical ABS Grade B steel plates.
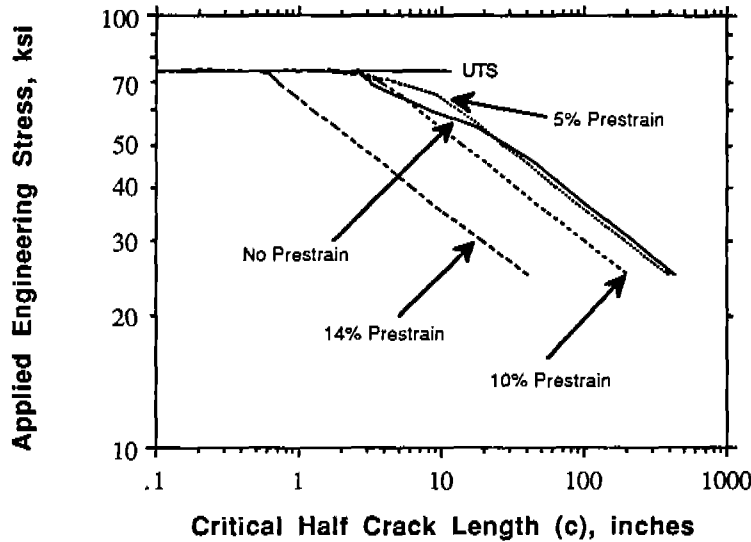
Fracture Strength Curve for estimating the critical crack size for fracture under an applied stress, below the yield strength of the material, which is 61.4 ksi for the ABS-A2 ship steel with no damage (no prestrain). The yield increases with the extent of damage (% prestrain); i.e., see Table 5.3a, 71.2 ksi (5%), 73.5 (10%), and 74.6 (14%). The critical crack size (half length, c) of a center cracked panel is seen to decrease with increasing amounts of damage. The differences become significant only after about 10% prestrain.

FIGURE 5.5A FRACTURE STRENGTH CURVE FOR
USE WITH STRESSES BELOW YIELD, ABS-A2 STEEL
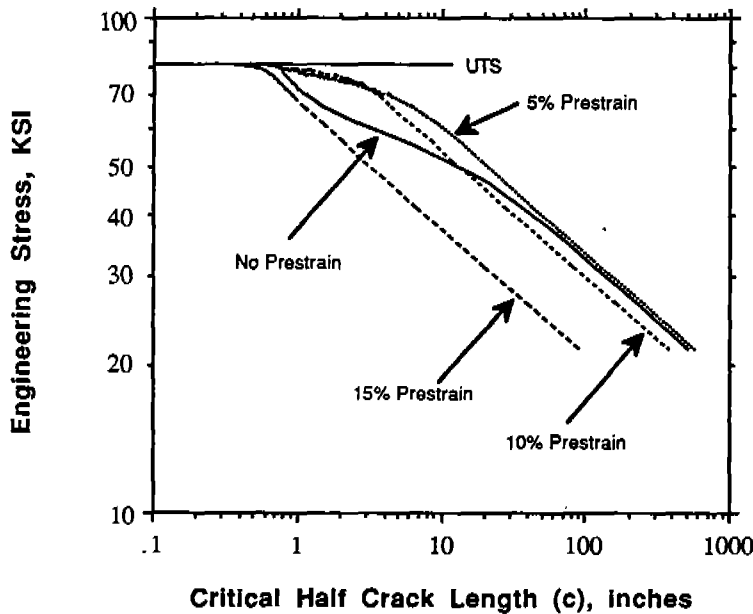
Fracture Strength Curve for estimating the critical crack size for fracture under an applied stress, below the yield strength of the material, which is 58.5 ksi for the ABS-B2 ship steel (slightly stronger than ABS-A2) with no damage (no prestrain). The yield increases with the extent of damage (% prestrain); i.e., see Table 5.3b, 74.5 ksi (5%), 78.5 (10%), and 80.9 (14%). The critical crack size (half length, c) of a center cracked panel is seen to decrease with increasing amounts of damage. The differences become significant only after about 10% prestrain.

FIGURE 5.5B FRACTURE STRENGTH CURVE FOR
USE WITH STRESSES BELOW YIELD, ABS-B2 STEEL
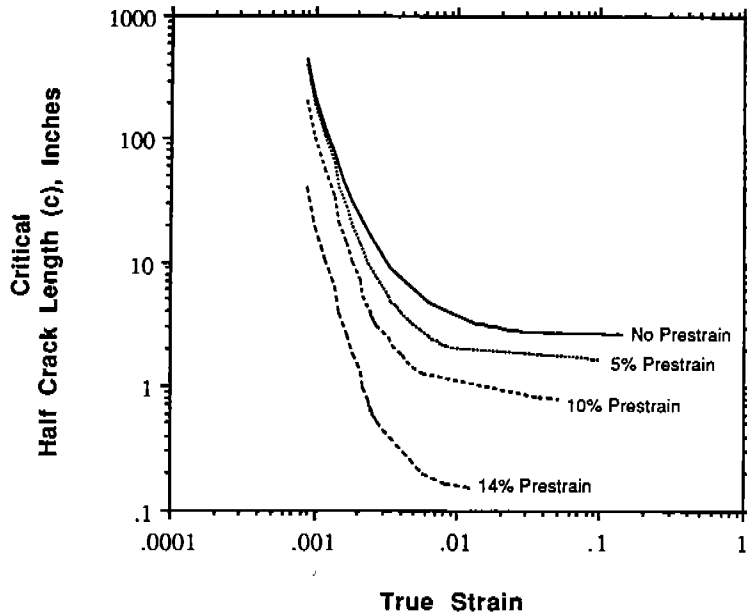
Fracture Strain Curve for estimating the critical crack size for fracture at stresses above the yield strength (0.2%). The critical crack size (half length, c) of a center cracked panel is seen to decrease with increasing amounts of deformation (applied strain). The critical crack size (2c) is estimated to be about 5 inches (2 x 2.5 inches) for the ABS-A2 ship steel with no damage.

FIGURE 5.6A FRACTURE STRAIN CURVE FOR
USE WITH STRESSES ABOVE YIELD, ABS-A2 STEEL
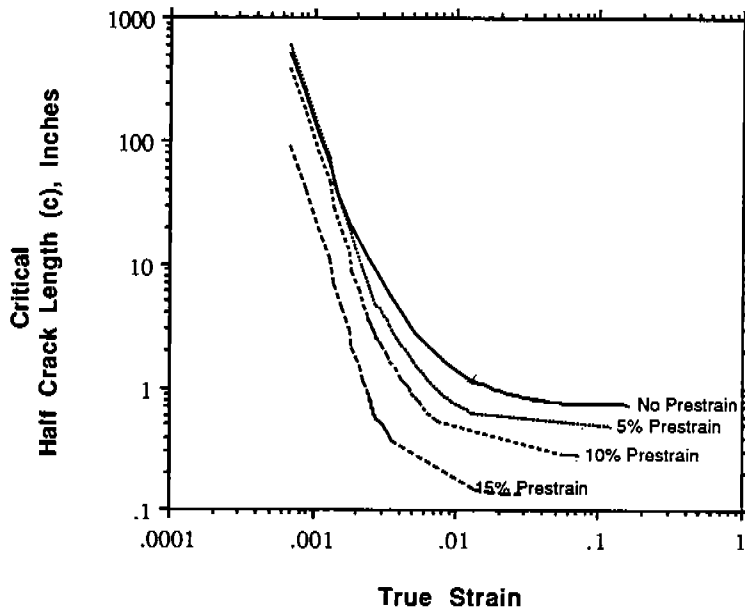
Fracture Strain Curve for estimating the critical crack size for fracture at stresses above the yield strength (0.2%). The critical crack size (half length, c) of a center cracked panel is seen to decrease with increasing amounts of deformation (applied strain). The critical crack size (2c) is estimated to be about 4 inches (2 x 2.0 inches) for the ABS-B2, Grade B ship steel with no damage.

FIGURE 5.6B FRACTURE STRAIN CURVE FOR
USE WITH STRESSES ABOVE YIELD, ABS-B2 STEEL

45
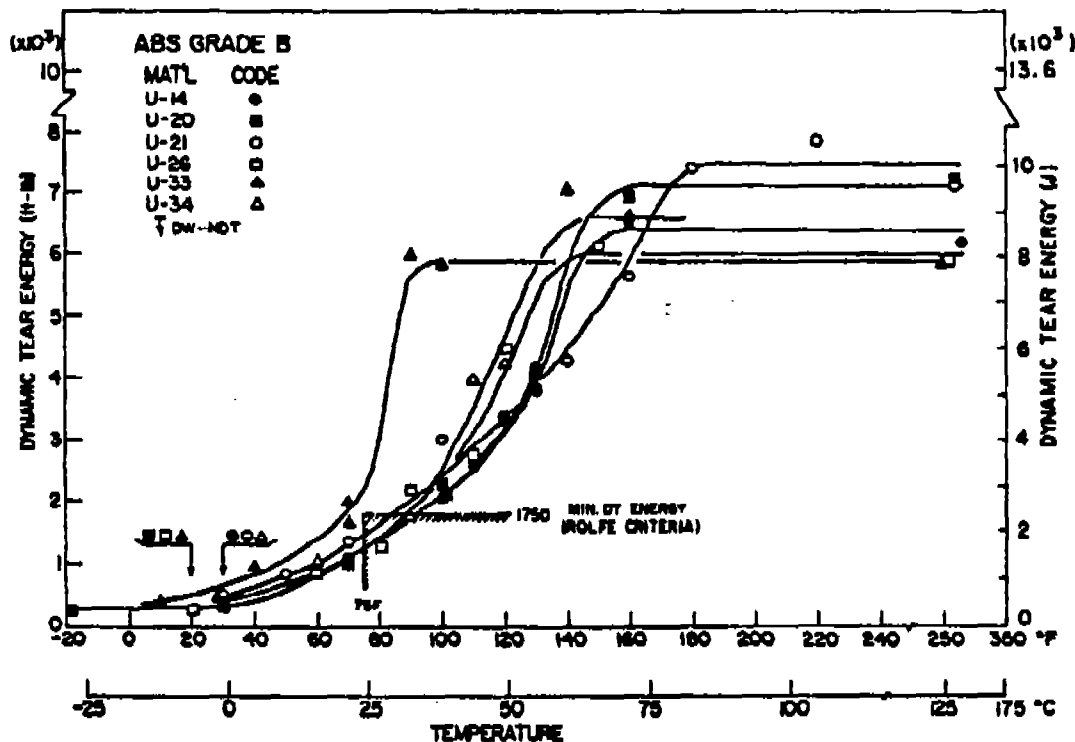
FIGURES 5.7 DUCTILE TO BRITTLE TRANSITION DT TESTS OF ABS GRADE B
PLATES

5.6 DYNAMIC FRACTURE RESISTANCE

As part of a U.S. Navy sponsored investigation [17] of the fracture characteristics of underwater, dry habitat weldments, explosion bulge crack starter tests were performed on 1-inch thick ship steel plate conforming to MIL-S-22698B, DH36 [18]. The chemical composition and mechanical properties of this steel are presented in Tables 5.4 and 5.5. It is noted that these properties are similar to those of the steels used for the SEDFM analysis.

A sketch of the explosion bulge crack starter weldments is presented in Figure 5.8. It is noted that a brittle crack starter bead about 3/8- inch wide was placed across the weld deposit and notched in the heat affected zone to evaluate the steel's ability to arrest a pre-existing crack under explosive loading. The crack starter test specimens were positioned over a 15-inch diameter female die and subjected to repeated explosive loading at +30° F. After each explosive shot, the crack length, depth of bulge (plate deflection), plate thickness, and surface strains were measured.

Table 5.6 presents a summary of the explosion bulge crack starter tests on MIL-S-22698B ship steel. It is noted that in every case, the crack starter bead cracked after the initial explosive shot but the crack did not penetrate the plate. The plastically strained plates containing surface cracks of about 1/2 inch long were able to withstand over yield stress loading without pop-in or unstable crack propagation. For the most part, all plates were able to arrest cracks after experiencing 1% reduction in thickness (1.4% surface strain). One plate arrested a 3/8-inch to 1/2-inch long crack without through thickness pop-in after more than 2% prior reduction in thickness (about 2.5% surface strain). Results of the comparison of reduction in thickness to surface strain are presented in Figure 5.9.

46

The performance of these 1-inch thick weldments generally supports the findings of the SEDFM analysis, which indicated that there was very little effect of prior strain (up to 10%) on the damage tolerance of MIL-S-22698B ship steels. It appears from the fracture analysis and tests reported herein, that ship steel plates up to 1-inch thick can resist brittle fracture at +30° F in the presence of significant cracks after more than 2% reduction in thickness (about 2.5% surface strain). Extending these results to higher levels of pre-strain will require a testing and evaluation program.

Table 5.4 Base Plate Chemical Analysis

Element	Requirement 1/	Analysis
Carbon	0.18	0.14
Sulfur	0.04	0.005
Manganese	0.90 - 1.60	1.50
Phosphorus	0.04	0.028
Silicon	0.10 - 0.50	0.257
Chromium	0.25	0.05
Molybdenum	0.08	0.009
Nickel	0.04	0.03
Copper	0.35	0.015
Vandium	0.10	0.090
Aluminum	-	0.051
Columbium	0.05	0.044
Carbon Equivalency	0.40 Minimum	0.423

1/ Values are maximum unless otherwise indicated.

Table 5.5 Base Plate Tensile Test Results

	Requirement	Test value 1/
Yield Strength (ksi)	51.0 minimum	61.8 62.0
Ultimate Tensile Strength (ksi)	71.0 to 90.0	81.0 80.7
Elongation (%)	22 minimum	27.0 27.0

1/ Manufacturer's Data
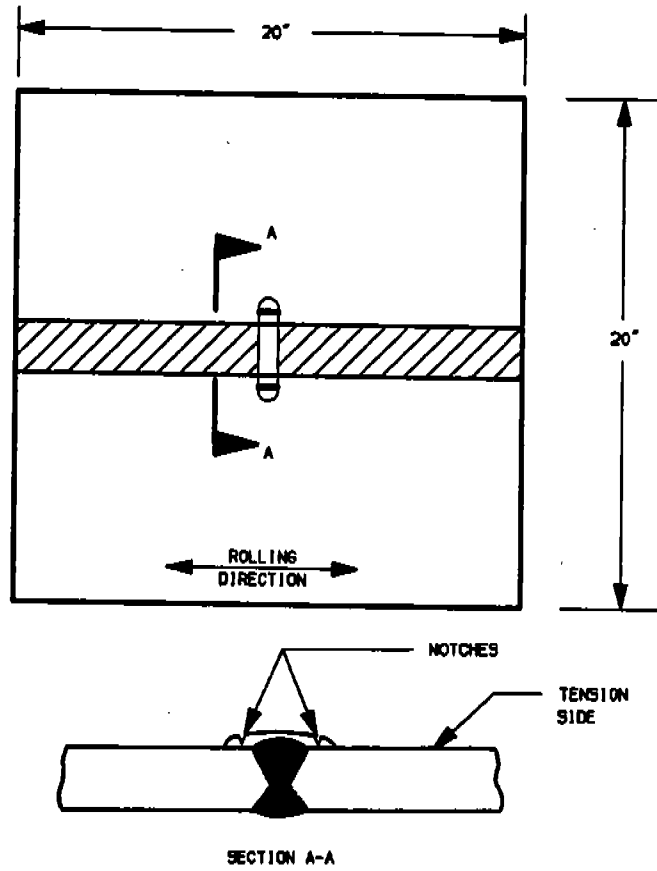
FIGURE 5.8. EXPLOSION BULGE WELDMENT CRACK STARTER
CONFIGURATION
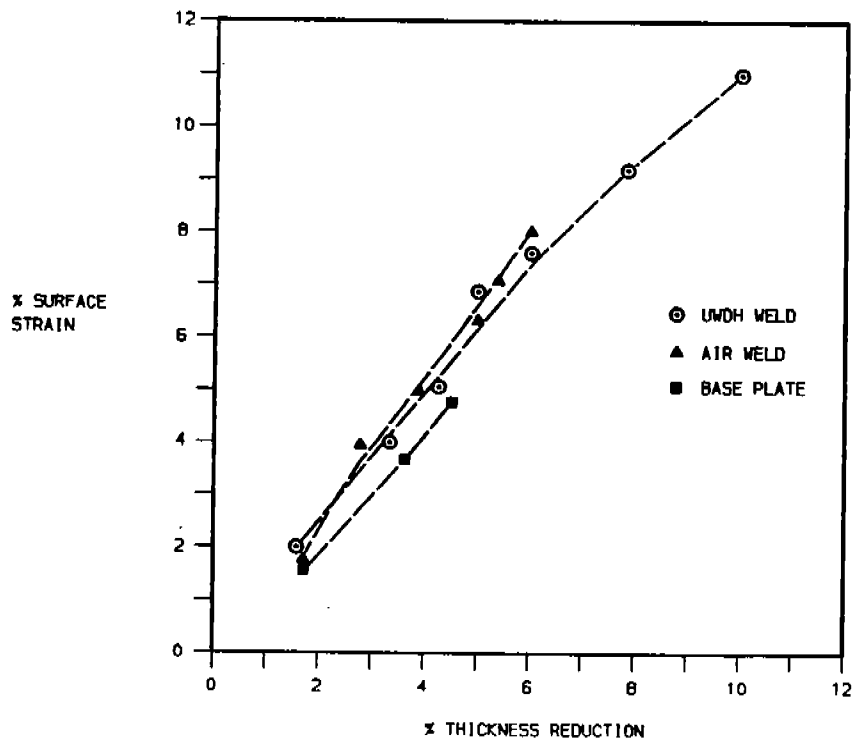
FIGURE 5.9. SURFACE STRAIN VS. THICKNESS REDUCTION
OF EXPLOSION BULGE TEST SPECIMEN

48

Table 5.6 Summary of Explosion Bulge/Crack Starter Test Results

Weld ID/Type	Total Shots	Final Bulge Depth 1/	% Thickness Reduction 1/	% Thickness Reduction Per Shot	Remarks 2/
AW-2/Air	3	1-15/16"	2.1	1.1	1st shot, CS cracked 3rd shot, thru crack
AW-3/Air	2	1-7/16"	1.6	0.78	1st shot, CS cracked 2nd shot, thru crack
AW-4/Air	3	2-1/16"	2.6	0.87	1st shot, CS cracked 3rd shot, thru crack
UW-1/UWDH 3/	3	1-15/16"	2.4	0.78	1st shot, CS cracked 3rd shot, thru crack
UW-2/UWDH	2	1-5/8"	1.8	0.88	1st shot, CS cracked 2nd shot, thru crack

1/ Average of two sides of specimen.
2/ Test temperature = 30 degrees Fahrenheit, Standoff = 21", Charge = 7 lbs. Comp. B.
3/ UWDH = Underwater Dry Habitat

5.7 METHODOLOGY FOR ASSESSING ALLOWABLE PANEL DEFLECTION

This section outlines a proposed procedure for using the plate deflection-plastic strain relationships developed in Section 4 and the plastic strain-critical crack size relationships from this section to assess the need to replace a deformed ship panel. This assessment is based on the fracture resistance of plates subjected to uniform prior plastic deformation (wave slap, etc.) and does not address other failure modes (such as fatigue or collapse), for reasons noted earlier, and does not address non-uniform, highly localized deformation (i.e. impact damage).

The following steps outline the proposed methodology illustrated on Figure 5.10 for assessing plastic deformation in ship plating.

a. Establish a maximum crack size, c_0, likely to be encountered in service. This size may be based on the largest crack likely to be missed during NDE, or another criteria (e.g., maximum leak rate).

b. Establish the maximum operating or service stress, σ_0, and strain, ε_0. The magnitude of these values may vary depending upon plate location (deck, side shell, bottom shell and forward, midship or after).

c. Utilize the fracture strain curve (FEC) or fracture stress curve (FSC) to determine the maximum allowable pre-strain or prior plastic deformation for the steel of interest. Use the FEC for above yield operations and the FSC for below yield operations. Locate the operating point representing c_0 and the σ_0 or ε_0 on the appropriate (FSC or FEC) curve. The highest prestrain curve that falls above the operating point represents the maximum prestrain that should be permitted for the particular steel. Since the maximum σ_0 or ε_0 may vary with location, one or more maximum prestrain values may be appropriate.

d. Referring to the A/b versus maximum strain curves, mark the maximum prestrain determined in the previous paragraph on the strain axis and draw a vertical line. The intersection of the vertical line with an a/b curve defines the maximum A/b that should be permitted for a plate with that aspect ratio.

It should be noted that the proposed methodology and curves presented in this report were developed only as a guide for developing acceptance criteria for plastically deformed plates in ship hulls. Significantly more testing and analysis, including consideration of other potential failure modes, e.g., fatigue, will be required to establish standardized acceptance criteria.

In order to implement the above methodology, a series of statistically based fracture strength and fracture strain curves must be developed for a full range of hull steels and thicknesses. This process would require tensile testing to establish full range true stress-true strain curves for the ship steels in the thickness range of interest. Analyses should be performed using the SEDFM model presented herein. The accuracy of these analyses in predicting critical stress or critical strain should then be confirmed by testing a series of center cracked panels. Alternatively, a series of CTOD measurements per PD6493 could be performed to establish the influence of prior plastic strain on the CTOD for a full range of ship steels. This data could be used to evaluate the influence of prior plastic strain on the maximum tolerable flaw size. The empirically based relationship between CTOD and tolerable flaw size could then be used to estimate maximum strains for use with the Δ/b versus maximum strain relationships. A library of these relationships should be developed for a full range of plate aspect ratios and plate thicknesses.

5.8   SUMMARY OF FRACTURE ANALYSIS

1. The Strain Energy Density Fracture Mechanics (SEDFM) appears to be a useful method to predict the flaw tolerance of ship steel after prior plastic deformation.
2. Based on the Strain Energy Density Analysis, ABS-Grade steel plate shows very little effect on flaw tolerance under quasi-static loading (for prior plastic strain up to about 10%), for plate thicknesses up to one inch. After 10% prior plastic strain, the change in damage tolerance becomes increasingly significant, although the absolute value of the critical crack size is still relatively large.
3. A methodology is proposed to establish maximum deflection criteria for ship plate panels based on fracture mechanics analysis of plastic strain effects on flaw tolerance.
4. Damage tolerance estimates of the SEDFM approach should be verified experimentally by measuring the tensile curves of prestrained material and conducting center cracked panel testing.
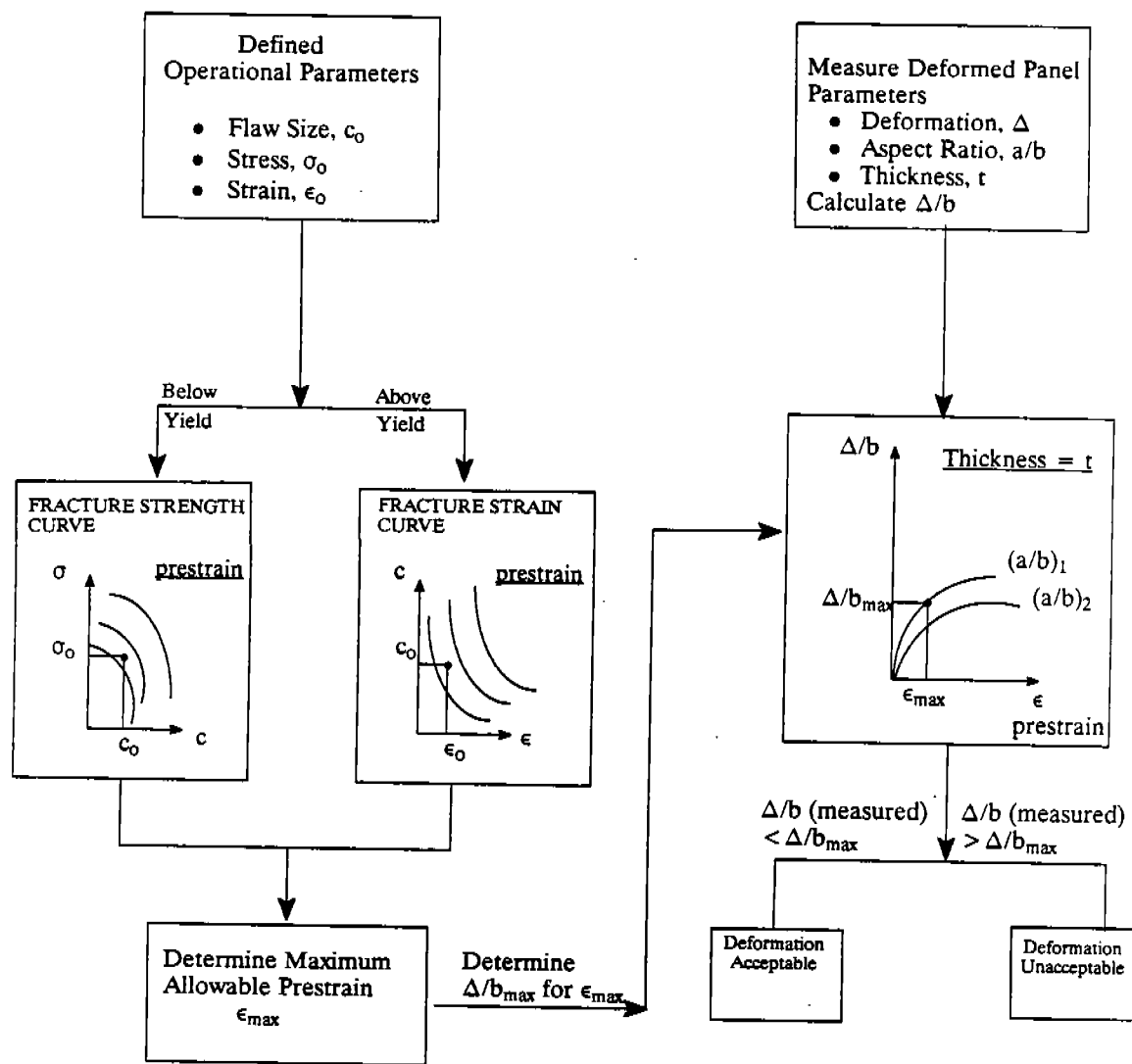
FIGURE 5.10
FLOW DIAGRAM FOR ASSESSING ALLOWABLE PANEL DEFORMATION
(BASED ON FRACTURE MECHANICS)

51

SECTION 6.0
SUMMARY AND RECOMMENDATIONS

This report presents the results of an experimental and analytical investigation related to establishing criteria for assessing the amount of plastic deformation that may be permitted on existing ship structures without compromising structural integrity. The work included review of existing criteria for panel deformation, measurement of plate panel deformation and strain on 13 ships, finite element analyses to establish deflection versus strain relationships for representative ship plate panels, and an assessment of the effects of prior plastic strain on flaw tolerance of ABS Grade B type ship steels. Based on these efforts, a methodology is proposed for determining the maximum plastic deformation that should be permitted for ship steel structural panels. The following paragraphs summarize the results of this investigation.

a. Current Deformation Criteria. Out of eleven (11) classification societies and ship design agencies surveyed, the only quantitative deformation limits were obtained from the offices of Det norske Veritas. For shell plating located in the 0 to 0.25L and the 0.75 to 1.0L portion of the hull, the maximum permissible indent is 0.05 times the minimum span length between stiffeners. For midships plating, (0.25 to 0.75L), if the observed deformation is 10mm to 30mm in depth, the ship owner is notified and the damage is recorded. If the observed deformation is greater than 30mm, the surveyor will recommend repair of the plating.

b. Ship Surveys. Measurements on 13 ships revealed that maximum panel deflection appears to be associated with impact-type loading and is typically highly localized on the panel. Measured deflections associated with localized impact damage ranged from 4.25 inches to slightly less than 1.0 inch. Panel deflections associated with wave slap, grounding, or other events were broader, more uniform, and significantly lower than the impact deflections. These deflections were usually less than 1 inch. Maximum bending strains and membrane strains were calculated for the deformed panel measurements obtained during the ship surveys. Extensive photographs and details of these measurements are presented in Appendix A of this report.

c. Finite Element Analysis. Nonlinear finite element analyses of fixed edge steel plates of varying aspect ratios and thicknesses, subjected to normal uniform pressure loadings over their entire surface, were performed using the finite element program COSMOS/M. Plates with aspect ratios of 1.0 and 2.0, with thicknesses of 3/8" and 5/8", were analyzed. The results of the finite element analyses were used to establish relationships between the plates' maximum out-of-plane deflection and the maximum induced bending and membrane strains. Once established, these relationships were presented in the form of nondimensionalized deformation/strain curves for each plate analyzed. Results of these finite element analyses were found to be in excellent agreement with the calculated strains obtained during the ship surveys. The nondimensional deformation/strain relationships were applied in the proposed methodology for determining maximum plastic deformation criteria for ship plate panels.

d. Flaw Tolerance after Prior Deformation. Based on a critical review of various fracture mechanics approaches to estimating the influence of prior strain on flaw tolerance of relatively low strength ABS Grade steel plate, the Strain Energy Density was determined to be most appropriate. Specifically, the Strain Energy Density Fracture Mechanics (SED$_{FM}$) model was used to predict the flaw tolerance of ABS Grade B type steel plate as a function of prior plastic strain.

The results indicated that there is very little effect on flaw tolerance for prior plastic strains up to about 10% plastic for plate thicknesses up to 1 inch thick. Beyond 10% plastic strain, flaw tolerance reductions become increasingly significant, but critical crack sizes are still relatively large. A methodology is proposed for establishing criteria for maximum plastic deformation in ship

panels. The methodology considers fracture toughness, flaw sizes, operating loads, panel geometry and measured deflection. Recommendations are presented regarding the testing required to implement the methodology.

e. Recommendations. It is recommended that maximum deflection criteria for ship plates be developed using the methodology proposed in this report. Specific areas that must be addressed include finite element analyses of a broad range of ship geometry/ thickness combinations and panel edge conditions; and development of statistically based fracture toughness properties for prestrained ship steels using the Strain Energy Density or the CTOD methods. In addition, analysis of different failure modes, including fatigue failure and buckling, should be investigated.

SECTION 7.0
ACKNOWLEDGMENTS

Project Technical Committee Members

Cmdr. Tom Gilmour	U.S. Coast Guard
Cmdr. Michael Parmalee	U.S. Coast Guard
Mr. David Knoll	Shell Oil Company
Mr. Mike Touma	Military Sealift Command
Mr. Rick Anderson	Military Sealift Command
Mr. Robert Vom Saal	Bethlehem Steel Corporation
Mr. Chao H. Lin	Maritime Administration
Mr. Gary J. North	Maritime Administration
Mr. Greg Woods	Naval Sea Systems Command
Mr. William Siekierka	Naval Sea Systems Command
Mr. Alexander Stavovy	National Research Council
Mr. Albert Chen	American Bureau of Shipping
Mr. David Kihl	David Taylor Research Center

APPENDIX A
Ship Survey Data
MEASUREMENT #1

DATE: 3-22-89

LOCATION: Philadelphia Naval Shipyard

SHIP: USS Kitty Hawk, CV-63

PLATE LOCATION:
- General - port side, near bow, above waterline.
- Frame Number - between Fr. 19 and Fr. 20. (based on numbers near keel)
- Location vs. Waterline - approximately 12 ft. above (+).

PLATE SIZE:
- "a" dimension = approximately 12 ft. (between transverse frames).
- "b" dimension = 64" (between longitudinals)
- "t" dimension (design) = 3/4"

Scale: 1 Grid = 2"
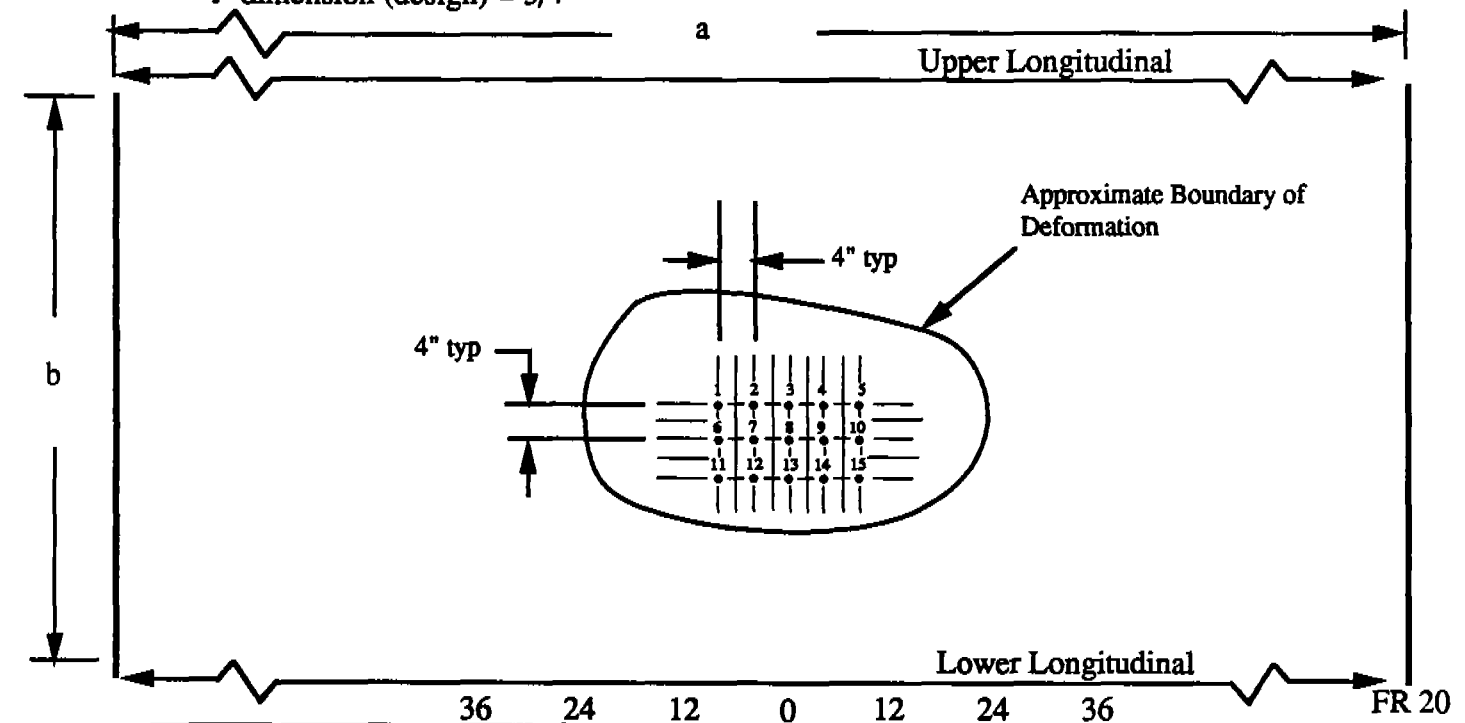
LOCATION	DEPTH READING	THICKNESS
1	5/16"	0.799"
2	13/16"	0.795"
3	1-1/16"	0.785"
4	1-1/8"	0.795"
5	11/16"	0.799"
6	11/16"	0.795"
7	1-5/16"	0.791"
8	2"	0.756"
9	1-9/16"	0.772"
10	1-5/16"	0.799"
11	9/16"	0.799"
12	1-1/8"	0.787"
13	1-11/16"	0.780"
14	1-3/8"	0.787"
15	7/8"	0.787"

NOTE: Depth Measurements were taken by placing a straightedge across the plate as a baseline and measuring in to deflected surface. Accuracy is ±1/16"

A-1

In-Plane View of Deformation (looking vertically)

NOTE: Horizontal grid scale is 1 Grid = 2 inches
      Depth grid scale is 1 Grid = 1 inch

Section through points 1-5

← FWD

1 2 3 4 5

Section through points 6-10

← FWD

6 7 8 9 10

Section through points 11-15

← FWD

11 12 13 14 15

Assumed Flat to Frame

Assumed Flat to Frame
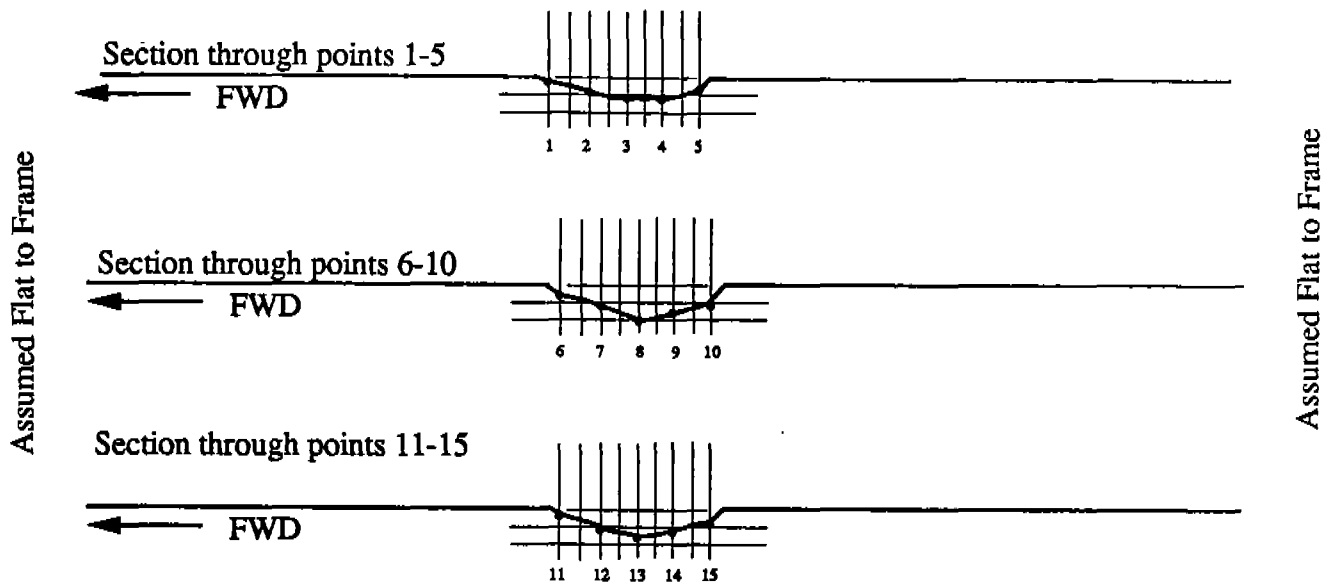
Measurement Notes: Due to the large area covered by the deformation, the 24" gauge
                   guide could not be used. The measurements were taken by placing
                   a straightedge against the hull and measuring in to the deflection.
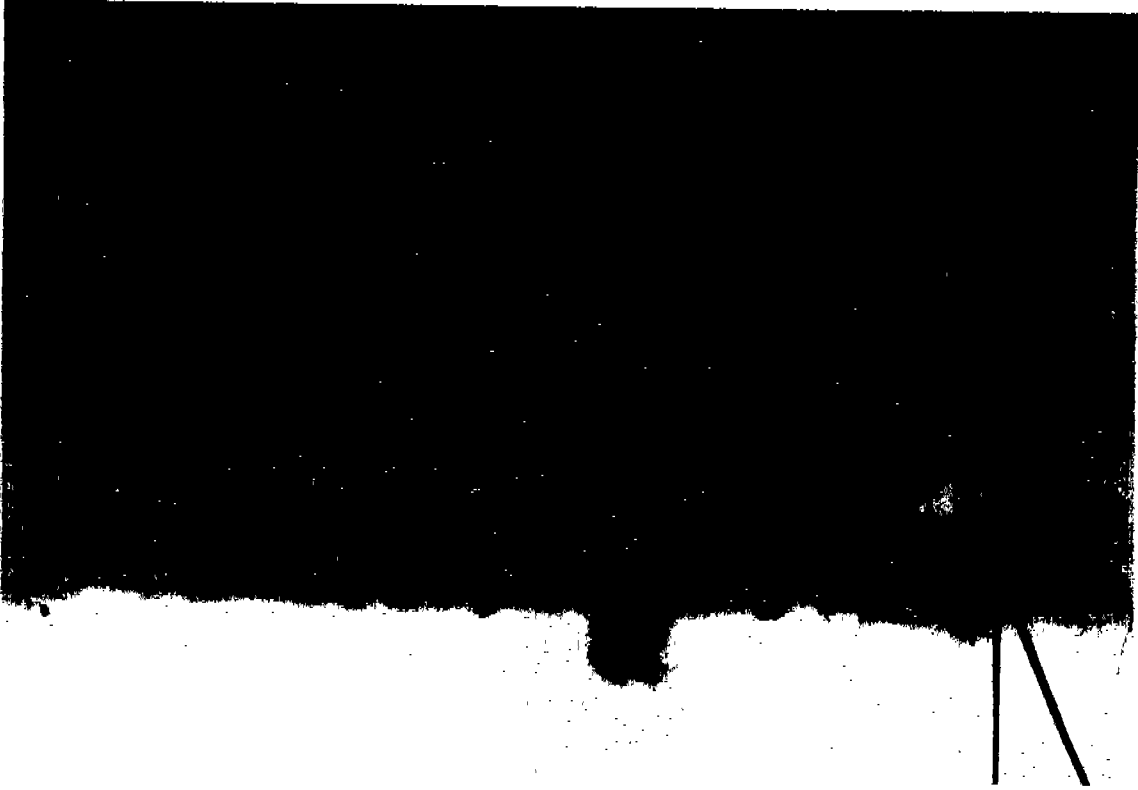
FIGURE A-1. MEASUREMENT #1 - USS KITTY HAWK

DATE: 3-22-89

LOCATION: Philadelphia Naval Shipyard

SHIP: USS Kitty Hawk, CV-63

PLATE LOCATION: Port side sponson, forwardmost athwartship panel,
approximately 6 ft. below deck.

PLATE SIZE:
- "a" dimension = 5' (minimum) 5'-8" (maximum) - between transverse frames.
- "b" dimension = 2' between longitudinal frames
- "t" dimension (design) = 1"

Scale: 1 Grid = 1"
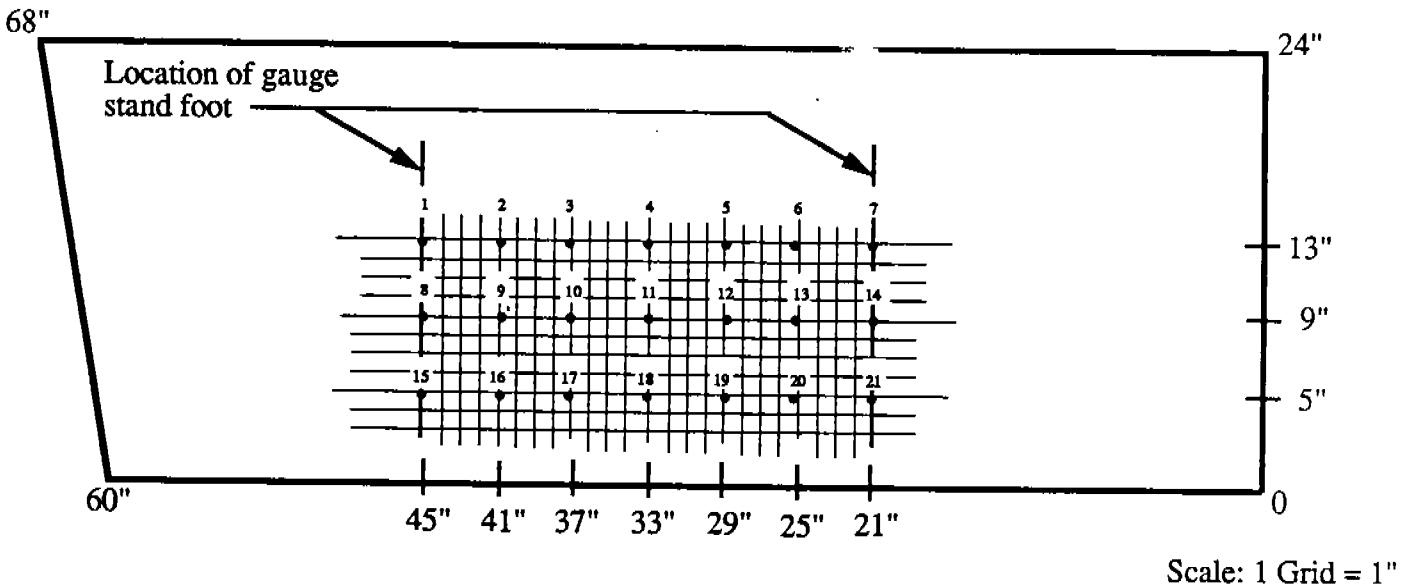
LOCATION	DEPTH READING	THICKNESS	LOCATION	DEPTH READING	THICKNESS
1	-	0.354	11	0.604	-
2	0.300	0.354	12	0.427	0.350
3	0.387	-	13	0.299	-
4	0.462	0.354	14	-	-
5	0.443	-	15	-	-
6	0.394	-	16	0.162	-
7	-	0.350	17	0.210	-
8	-	-	18	0.259	0.354
9	0.300	-	19	0.232	-
10	0.402	0.354	20	0.186	-
			21	-	0.346

A-4

Reduced Data

LOCATION	ABSOLUTE DEPTH (in)	LOCATION	ABSOLUTE DEPTH (in)	LOCATION	ABSOLUTE DEPTH (in)
1	-	8	-	15	-
2	0.140	9	0.140	16	0.002
3	0.227	10	0.242	17	0.050
4	0.302	11	0.444	18	0.099
5	0.283	12	0.267	19	0.072
6	0.234	13	0.139	20	0.026
7	-	14	-	21	-

Sectional Views of Deformation

Section 1-7
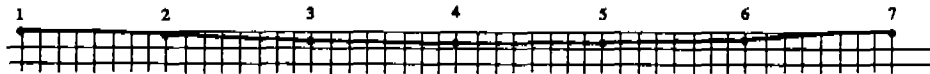
Section 8-14
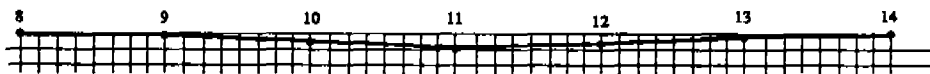
Section 15-21
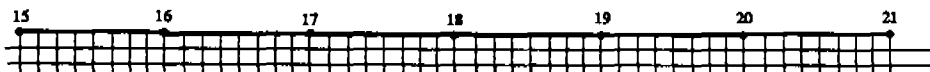
No noticeable deformation   Scale: 1 Grid = 1/2"

The feet of the stand were bottomed and the panel was considered underformed under the feet. The gauge was zeroed and the zeroed gauge indicated 0.16"; therefore, 0.16" was subtracted from the raw data to obtain the reduced data.
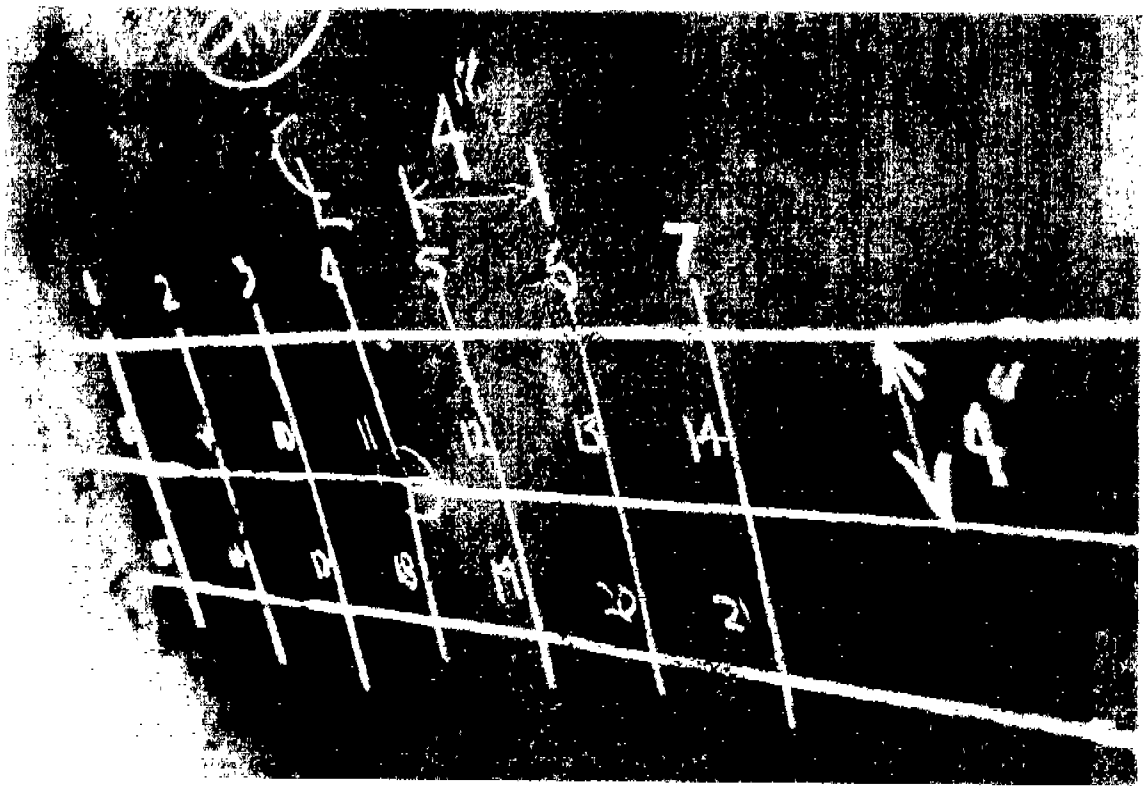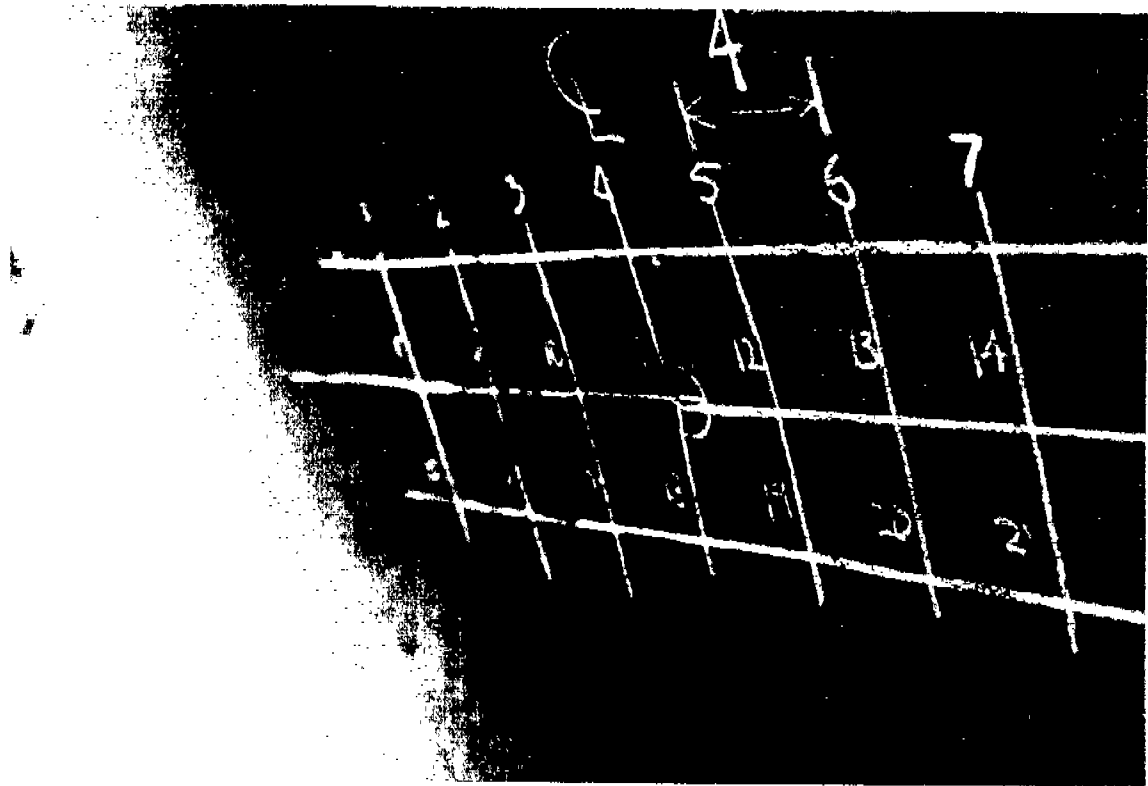
FIGURE A-2. MEASUREMENT #2 - USS KITTY HAWK
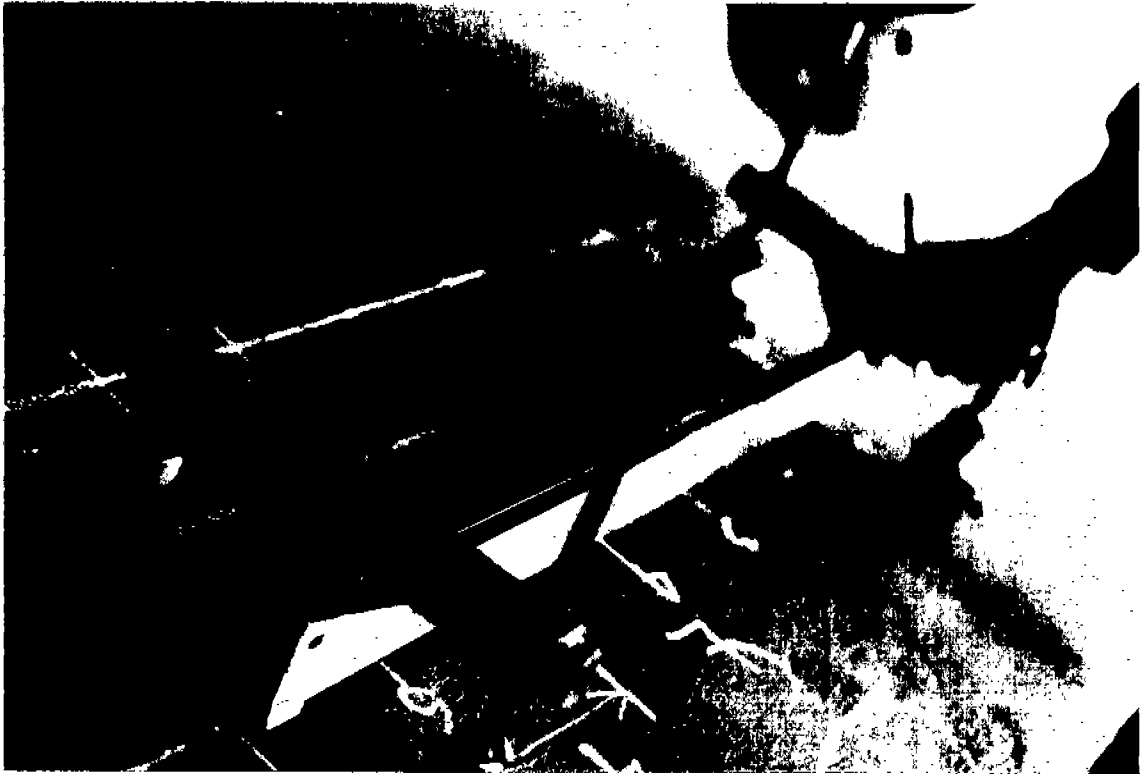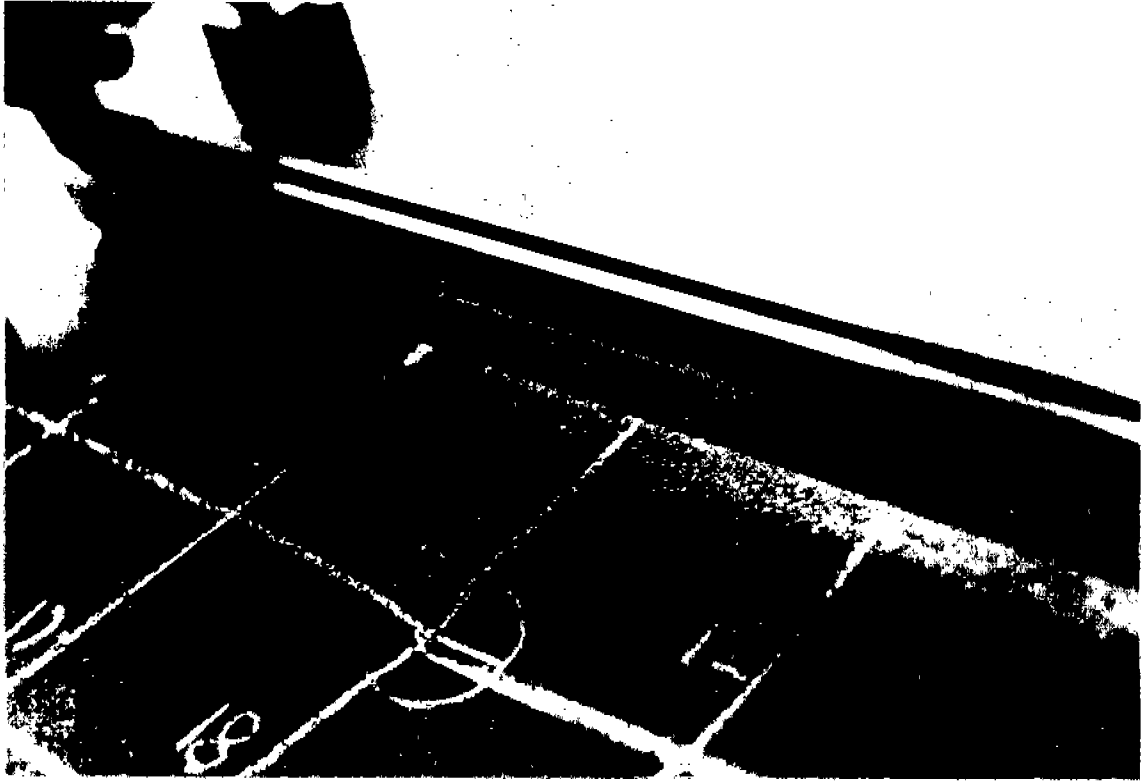
FIGURE A-3. MEASUREMENT #2 - USS KITTY HAWK
DIAL INDICATOR GAUGE GUIDE SHOWN
IMPACT LOAD INDENTATION CIRCLED AT POINT #11

DATE: 3-22-89

LOCATION: Philadelphia Naval Shipyard

SHIP: USS Detroit, AOE-4

PLATE LOCATION:
- General - Port side, above forward external shaft bearing, at waterline.
- Frame number -
- Location vs. Waterline - on waterline

PLATE SIZE:
- "a" dimension = 120" (between transverse frames)
- "b" dimension = 30" (between longitudinals)
- "t" dimension (design) = not available

Location of gauge stand foot

Scale: 1 Grid = 1"
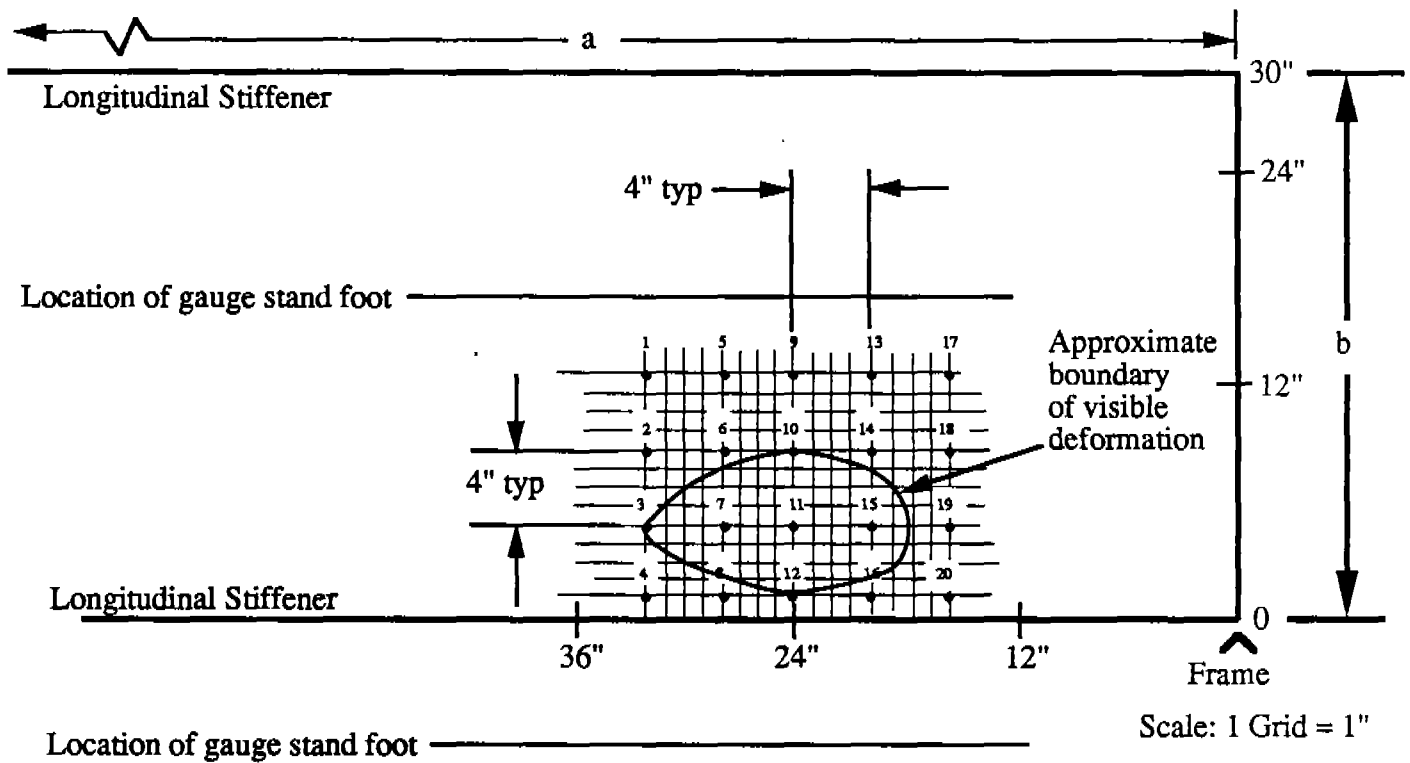
Actual Measurement Data

LOCATION	DEPTH READING	THICKNESS	LOCATION	DEPTH READING	THICKNESS
1	0.442	0.591	13	0.387	No Reading
2	0.593	0.634	14	0.503	0.606
3	0.502	No Reading	15	0.632	0.587
4	-0.027	0.579	16	-0.042	No Reading
5	0.631	0.587	17	0.360	0.587
6	0.801	0.594	18	0.369	0.604
7	0.977	0.591	19	0.385	No Reading
8	0.063	No Reading	20	-0.043	0.571
9	0.400	0.591			
10	0.592	0.579			
11	0.918	0.591			
12	-0.041	0.591			

A-8

In-Plane View of Deformation (looking aft)

NOTE: Horizontal scale is 1 grid = 1 inch
   Depth scale is 1 grid = 0.5 inch

Section through points 1-4

Section through points 5-8

Section through points 9-12

Section through points 13-16

Section through points 17-20
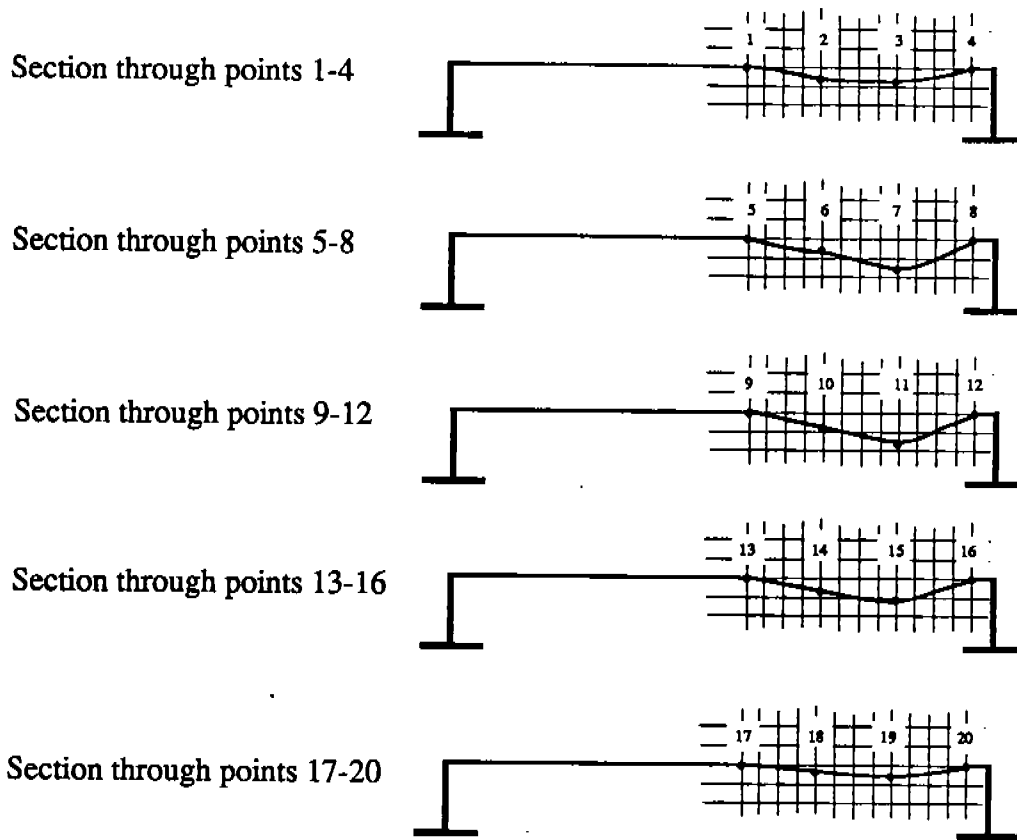
Measurement Notes: Due to the thickness of the paint on the hull, the gauge guide would not magnetically attach to the hull and had to be held in place by hand. This should not affect the results. Due to chipping of the ablative paint, the UT gauge did not always achieve a satisfactory couple with the hull. The thickness measurements in these areas are given as "no reading". The measurements were taken on a vertical line (parallel to the transverse frames) using a dial indicator gauge with an accuracy of ±.001". The maximum panel deflection was found to be 0.697" at point 11. The vertical placement of the gauge guide was the most favorable since the deflection was of the form of a crease running fore and aft above the frame and the vertical placement allowed the gauge guide to span the crease.

Reduced Data

| Location	Actual Deflection	Thickness	Location	Actual Deflection	Thickness
1	0.000	0.591	13	0.000	No Reading
2	0.307	0.634	14	0.259	0.606
3	0.373	No Reading	15	0.531	0.587
4	0.000	0.579	16	0.000	No Reading
5	0.000	0.587	17	0.000	0.587
6	0.359	0.594	18	0.143	0.604
7	0.725	0.591	19	0.294	No Reading
8	0.000	No Reading	20	0.000	0.571
9	0.000	0.591			
10	0.340	0.579			
11	0.812	0.591			
12	0.000	0.591			

A-9
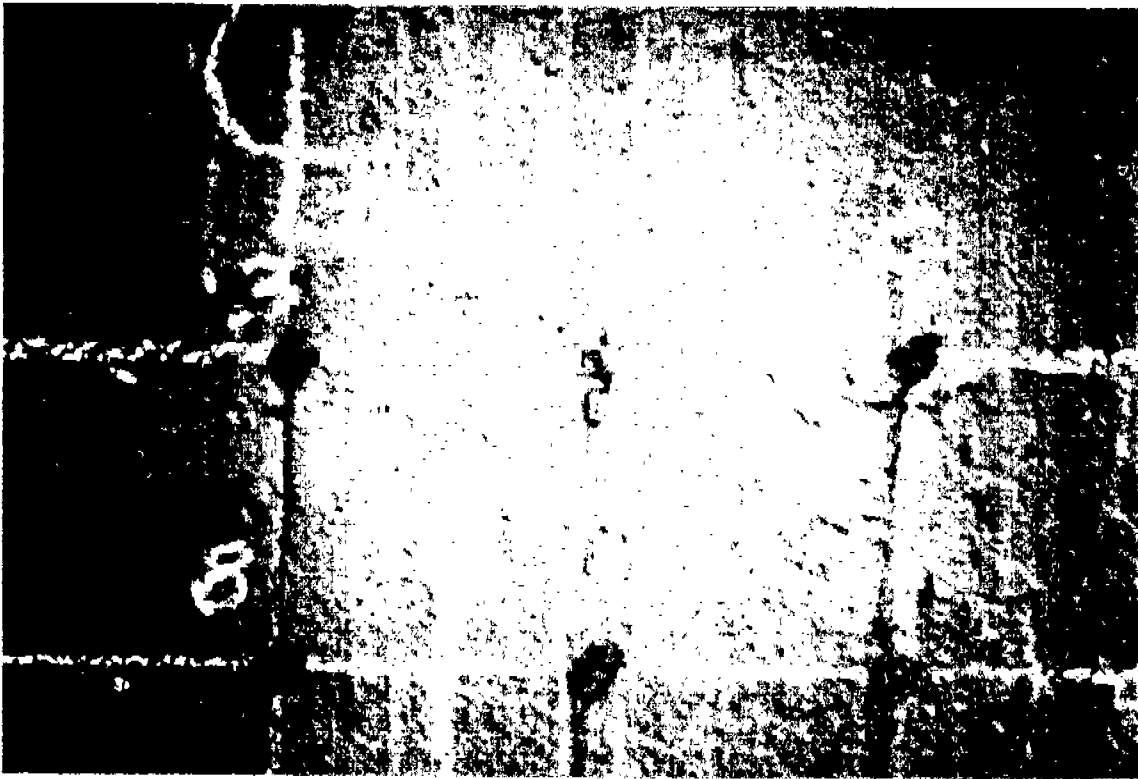
FIGURE A-4. MEASUREMENT #3 - USS DETROIT
CHIPPING OF ABLATIVE PAINT SHOWN
(PREVENTED SONIC COUPLING FOR THICKNESS MEASUREMENT)

DATE: 3-22-89

LOCATION: Philadelphia Naval Shipyard

SHIP: USS Detroit, AOE-4

PLATE LOCATION:
- General - port side, just aft of forward external shaft bearing, at waterline
- Frame Number -
- Location vs. Waterline - on waterline

PLATE SIZE:
- "a" dimension = 64" (between transverse frames)
- "b" dimension = 30" (between longitudinals)
- "t" dimension (design) = not available
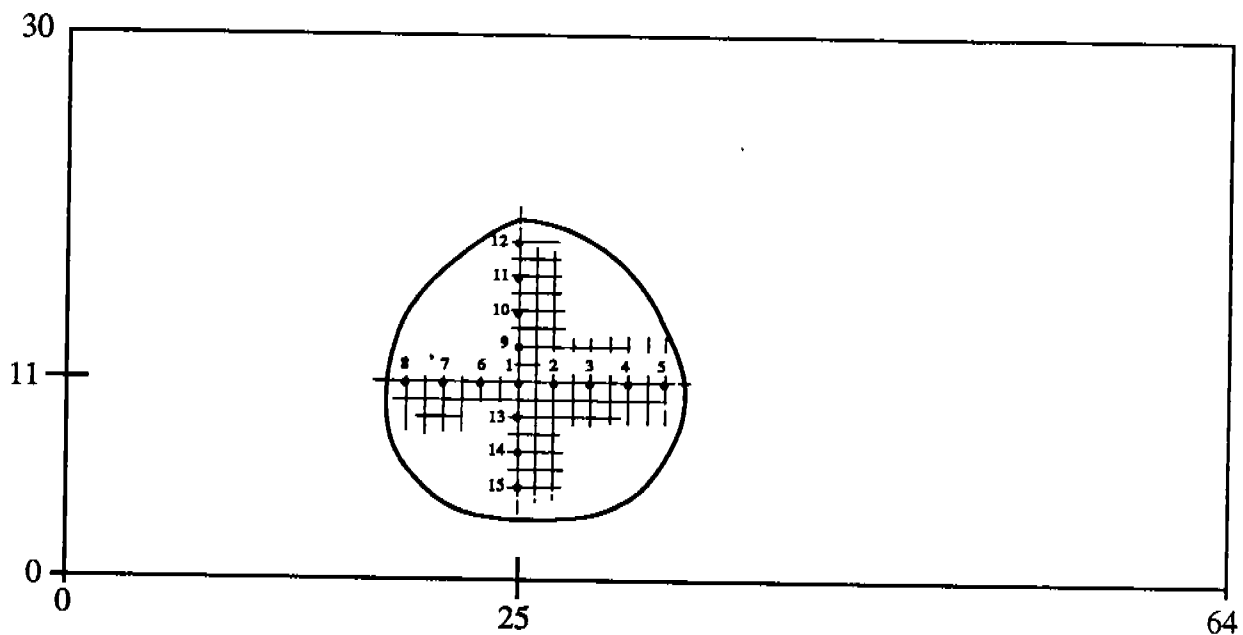
Scale: 1 Grid = 1"

LOCATION	DEPTH READING	THICKNESS
1	4-1/4"	0.563
2	3-9/16"	0.567
3	3"	0.575
4	2-7/16"	0.591
5	2-1/16"	0.598
6	3-7/8"	0.563
7	3-1/16"	0.594
8	2-5/16"	0.591
9	4-1/16"	0.528
10	3-3/16"	0.551
11	2"	0.598
12	1-9/16"	0.587
13	3-9/16"	0.575
14	2-5/8"	0.622
15	1-15/16"	0.591

NOTE: Depth Measurements were taken by placing a straightedge across the plate as a baseline and measuring in to deflected surface. Accuracy is ±1/16"

In-Plane View of Deformation

NOTE: Scale in each direction is 1 grid = 1 inch

Section looking up through points 8-5

Section looking aft through points 12-15
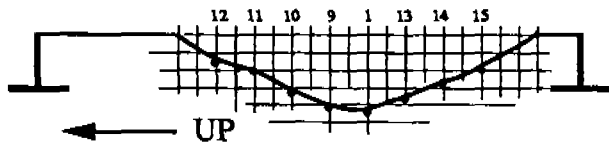
Measurement Notes: Due to the large deflection of the deformation, the dial indicator gauge with its 1.000" maximum range was not used. Instead, the straightedge was placed on the hull over the deformation in both a longitudinal and a transverse manner. Measurements were then taken from the straightedge to the deflected hull panel.

FIGURE A-5. MEASUREMENT #4 - USS DETROIT

DATE: 3-22-89

LOCATION: Philadelphia Naval Shipyard

SHIP: USS Kidd, DDG-993

PLATE LOCATION: Port side, 6 ft. above waterline, near Frame 103

PLATE SIZE:
- "a" dimension = 28" (transverse)
- "b" dimension = 27" (longitudinal)
- "t" thickness (design) = 3/8"
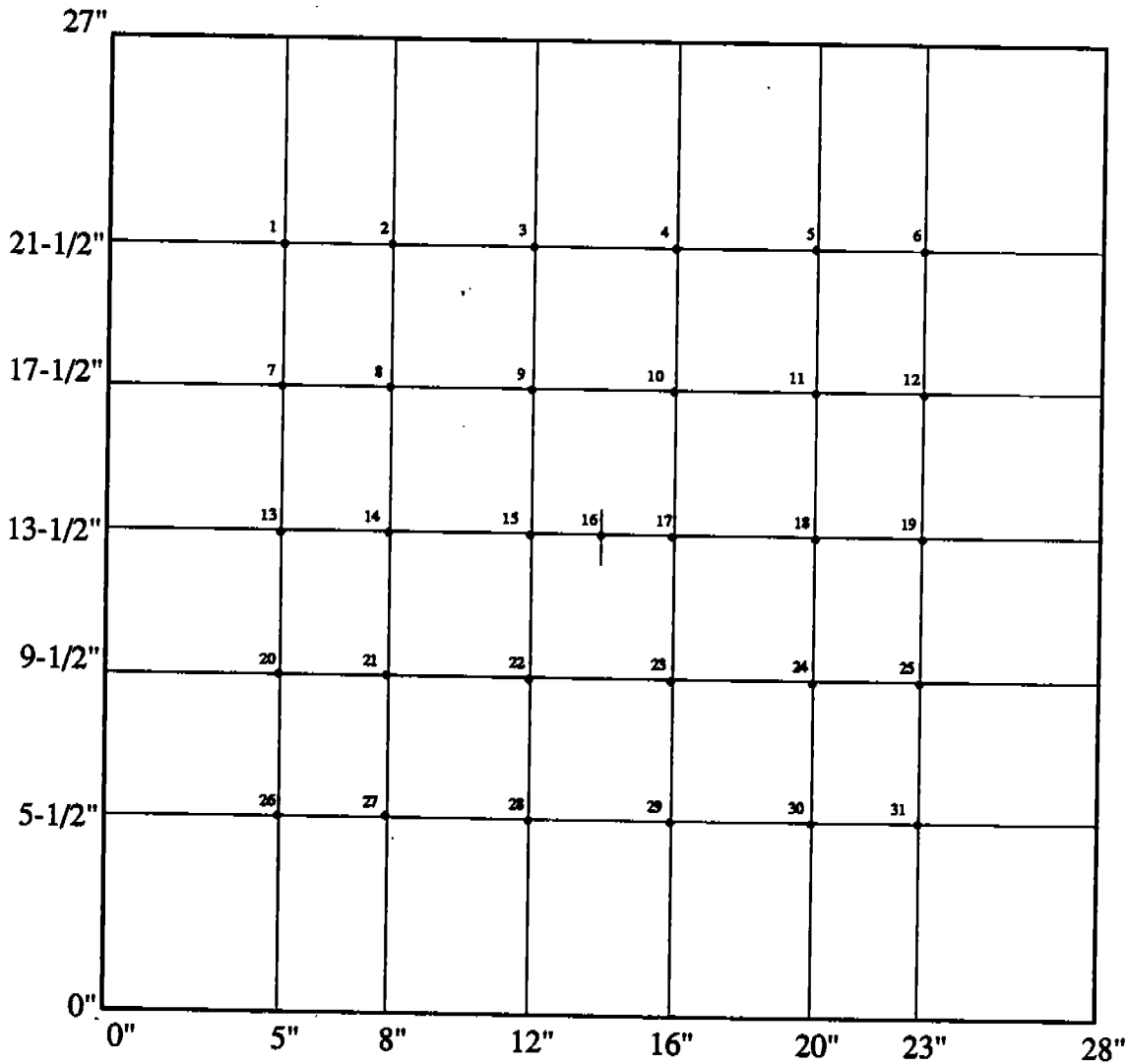
Deformation was "hungry horse" - Typical of sea
loading, not a localized deformation.

Reduced Data

| LOCATION	DEPTH READING	THICKNESS	LOCATION	DEPTH READING	THICKNESS
1	0.000	0.417	17	0.287	0.433
2	0.106	0.417	18	0.227	0.425
3	0.133	0.421	19	0.000	0.429
4	0.134	0.417	20	0.000	0.433
5	0.106	0.425	21	0.185	0.433
6	0.000	0.425	22	0.235	0.433
7	0.000	0.437	23	0.240	0.429
8	0.181	0.433	24	0.196	0.429
9	0.233	0.433	25	0.000	0.429
10	0.231	0.421	26	0.000	0.425
11	0.175	0.421	27	0.107	0.465
12	0.000	0.425	28	0.128	0.445
13	0.000	0.441	29	0.128	0.441
14	0.222	0.433	30	0.107	0.433
15	0.283	0.437	31	0.000	0.433
16	0.295	0.433			

Section through points 1-6
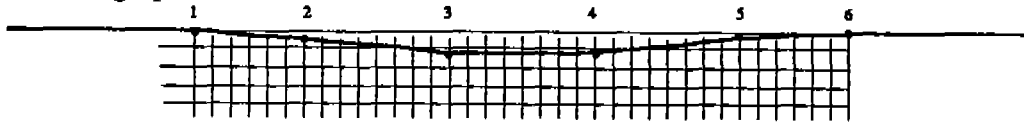
Section through points 7-12

Section through points 13-19
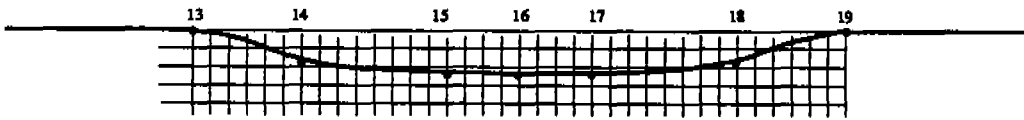
Section through points 20-25
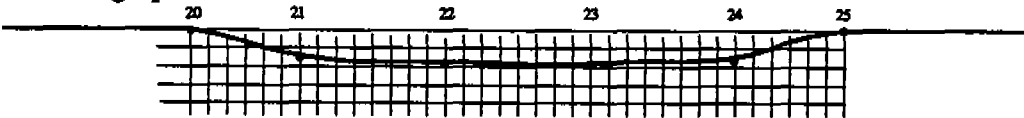
Section through points 26-31
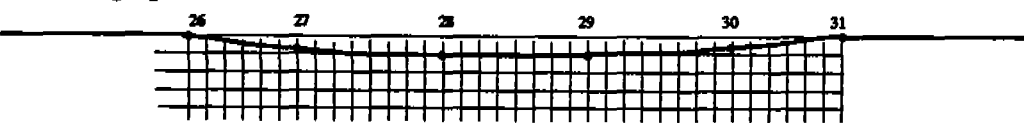
A-16

Horizontal scale: 1 grid = 1/2"
Depth scale: 1 grid = 1/8"

DATE: 3-22-89

LOCATION: Philadelphia Naval Shipyard

SHIP: USS Kidd, DDG-993

PLATE LOCATION:
  • General - Forward weather deck, centerline
  • Frame Number - 15
  • Location vs. Waterline - On deck

PLATE SIZE:
  • "a" dimension = 21"
  • "b" dimension = 15"
  • "t" thickness (design) = 3/8"
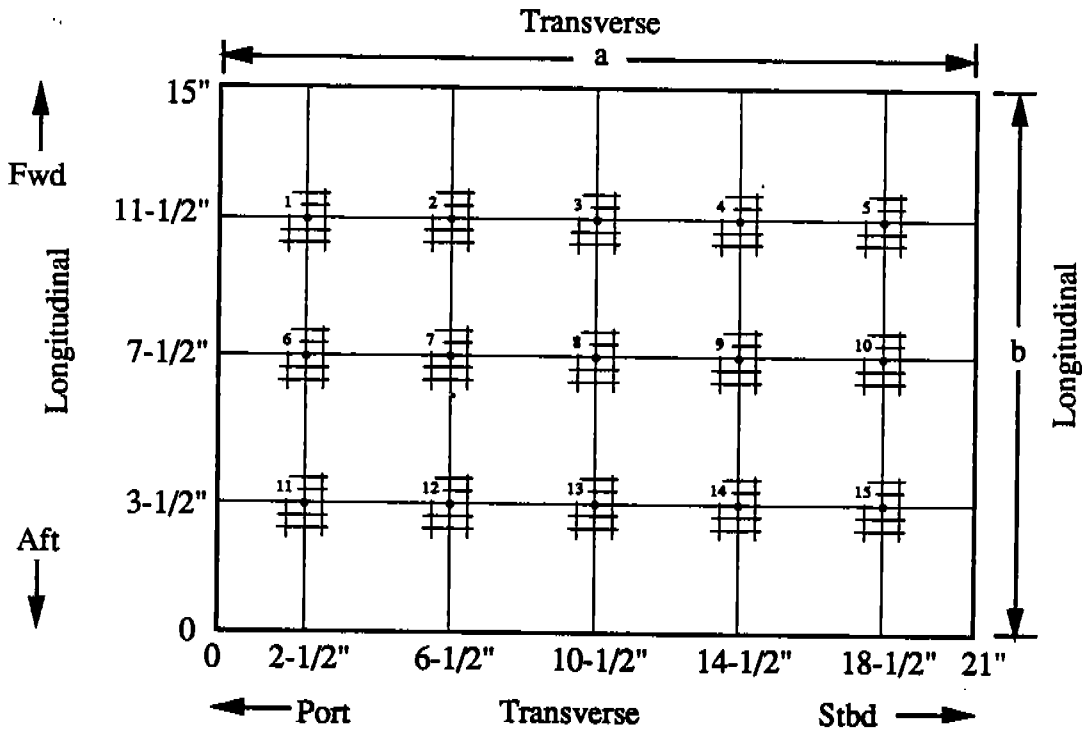
Scale: 1 Grid = 1/2"

LOCATION	DEPTH READING	THICKNESS
1	0.210	0.433
2	0.241	0.425
3	0.258	0.425
4	0.235	0.457
5	0.209	0.421
6	0.229	0.421
7	0.278	0.433
8	0.292	0.417
9	0.280	0.429
10	0.268	0.421
11	0.198	0.417
12	0.228	0.437
13	0.247	0.433
14	0.239	0.433
15	0.225	0.417

In-Plane View of Deformation (looking forward)

NOTE: Horizontal grid scale is 1 grid = 0.5 inches
Depth grid scale is 1 grid =0.02 inches

Section through points 1-5
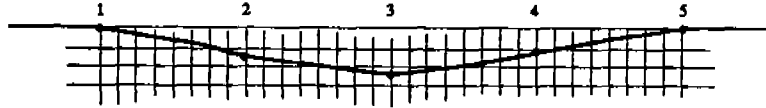
Section through points 6-10
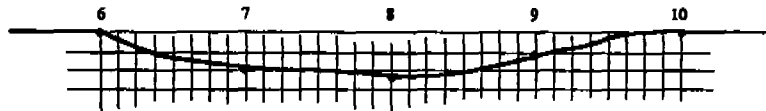
Section through points 11-15
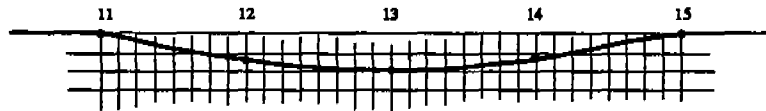
Measurement Notes: The deformation measurements were made using the dial indicator gauge and gauge guide. The feet of the gauge guide were located 1-1/2" off either longitudinal, with the zero deflection point taken 2-1/2" inside each longitudinal. The maximum deflection of 0.048" for the 21" span suggests initial weld distortion more than any sea loading.

Reduced Data

LOCATION	ACTUAL DEFLECTION	THICKNESS
1	0.000	0.433
2	0.031	0.425
3	0.048	0.425
4	0.025	0.457
5	0.000	0.421
6	0.000	0.421
7	0.039	0.433
8	0.043	0.417
9	0.022	0.429
10	0.000	0.421
11	0.000	0.417
12	0.023	0.437
13	0.035	0.433
14	0.021	0.433
15	0.000	0.417

DATE: 5-10-89

LOCATION: Norfolk Naval Shipyard

SHIP: USS John F. Kennedy, CV-67

PLATE LOCATION:
- General - Starboard side, 20 ft. forward of stern, above waterline
- Frame Number -
- Location vs. Waterline - Approximately 10 ft. above waterline

PLATE SIZE:
- "a" dimension = 4 ft. (between transverse frames)
- "b" dimension = 16" grid pattern (about 4 ft. between longitudinals)
- "t" design = not available
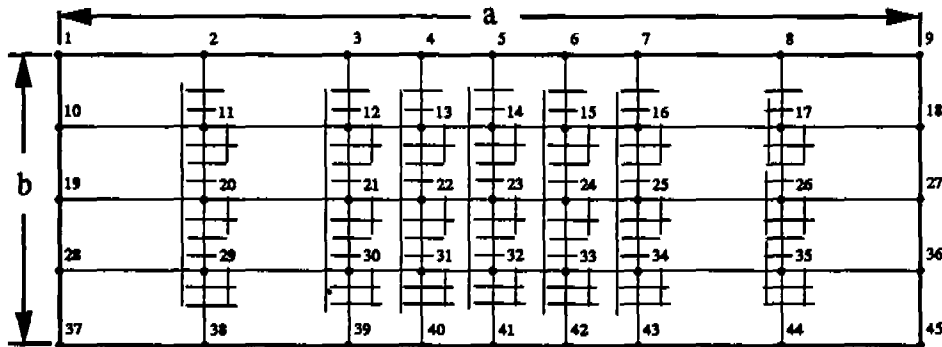
Scale: 1 Grid = 1"

Depth measurements were taken by placing a straightedge across the plate as a baseline and measuring in to the deflected surface. Accuracy is ±1/16".

LOCATION	DEPTH READING	THICKNESS	LOCATION	DEPTH READING	THICKNESS
1	2/32	0.602	24	2-2/32	0.646
2	18/32	0.575	25	1-18/32	0.602
3	25/32	0.583	26	22/32	0.598
4	27/32	0.587	27	0	0.598
5	27/32	0.598	28	8/32	0.575
6	24/32	0.594	29	1-1/32	0.575
7	18/32	0.594	30	1-29/32	0.591
8	27/32	0.598	31	2-12/32	0.606
9	0	0.606	32	2-18/32	0.626
10	8/32	0.579	33	2-8/32	0.602
11	1-5/32	0.579	34	1-28/32	0.618
12	1-13/32	0.591	35	28/32	0.602
13	1-20/32	0.571	36	1/32	0.598
14	1-20/32	0.575	37	7/32	0.569
15	1-12/32	0.591	38	30/32	0.575
16	1-2/32	0.594	39	1-20/32	0.583
17	14/32	0.610	40	1-30/32	0.567
18	0	0.602	41	2-2/32	0.602
19	10/32	0.594	42	1-29/32	0.602
20	1-8/32	0.587	43	1-24/32	0.602
21	2-2/32	0.583	44	28/32	0.602
22	2-22/32	0.567	45	3/32	0.591
23	3-15/32	-			

MEASUREMENT #7 (continued)

In-Plane View of Deformation

NOTE: Horizontal grid scale is 1 grid = 1 inch
Depth grid scale used is 1 grid = 0.5 inches

Section through points 1-9
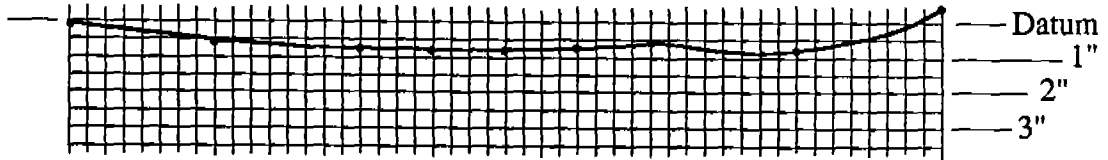
Section through points 10-18
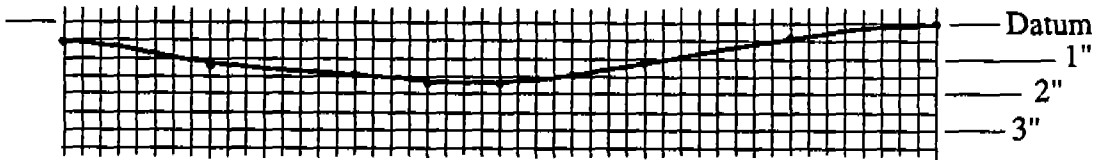
Section through points 19-27
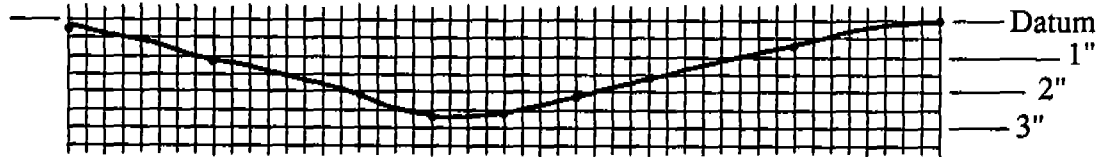
Section through points 28-36
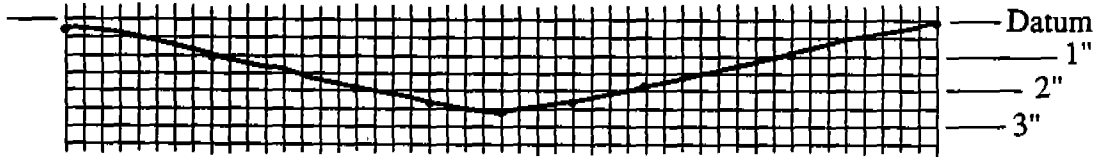
Section through points 37-45
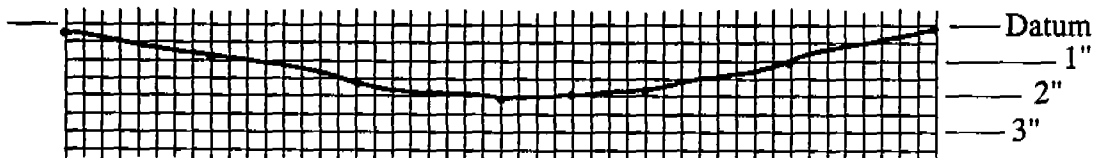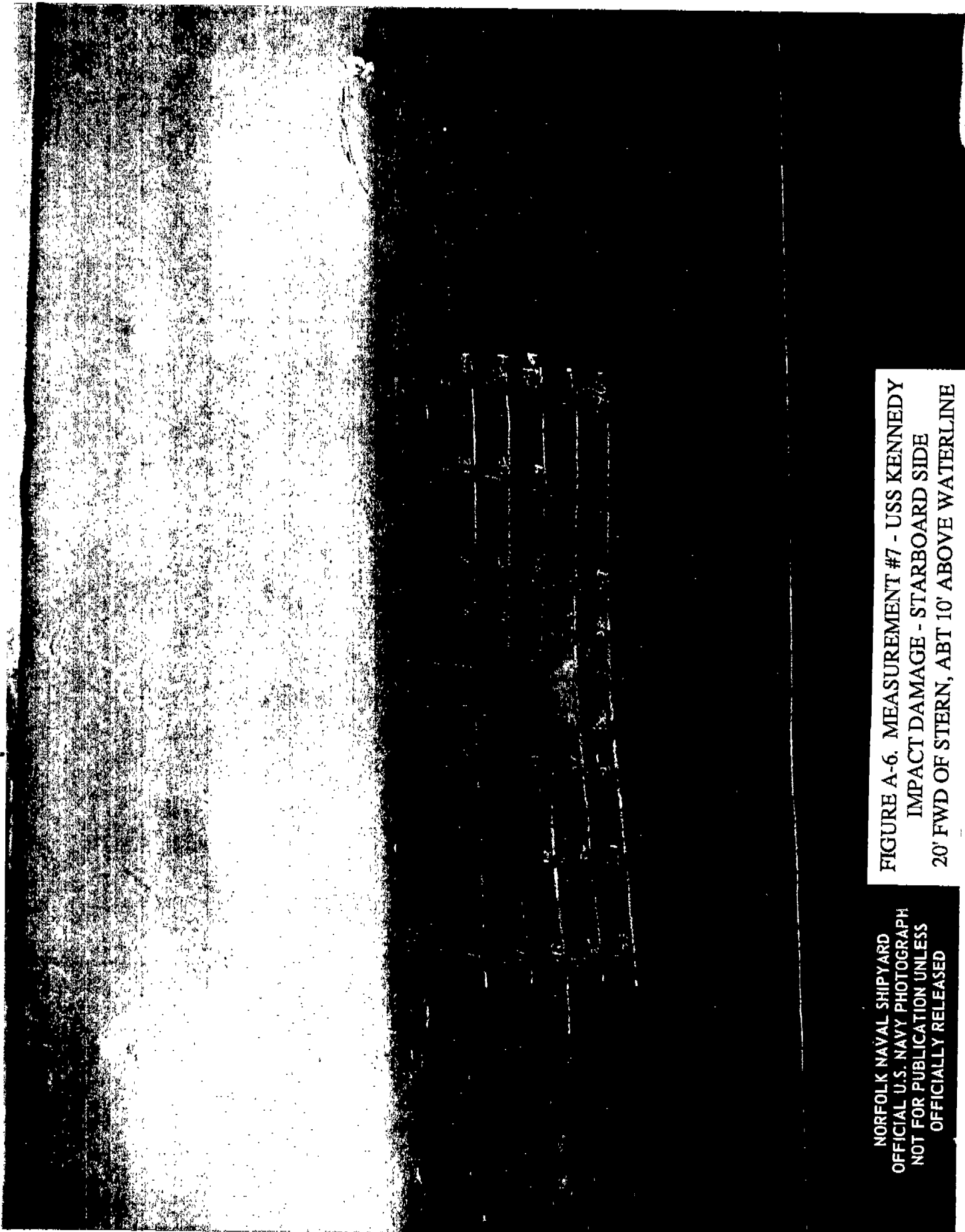
FIGURE A-6. MEASUREMENT #7 - USS KENNEDY
IMPACT DAMAGE - STARBOARD SIDE
20' FWD OF STERN, ABT 10' ABOVE WATERLINE
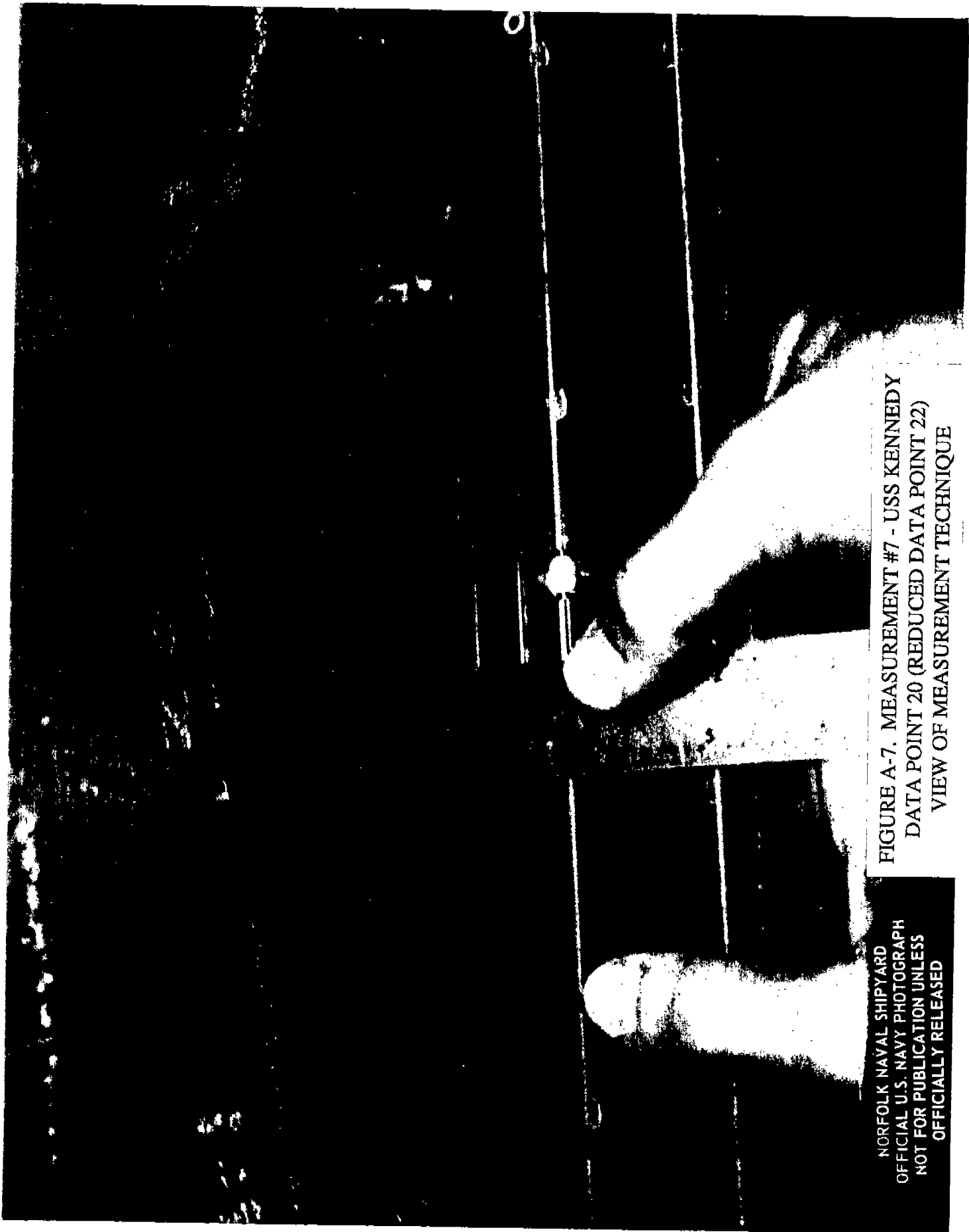
FIGURE A-7. MEASUREMENT #7 - USS KENNEDY
DATA POINT 20 (REDUCED DATA POINT 22)
VIEW OF MEASUREMENT TECHNIQUE

FIGURE A-8. MEASUREMENT #7 - USS KENNEDY
VIEW OF THICKNESS MEASUREMENT TECHNIQUE
USING ULTRASONIC GAUGE

DATE: 5-10-89

LOCATION: Norfolk Naval Shipyard

SHIP: USS John F. Kennedy, CV-67

PLATE LOCATION:
- General - Port side, aft elevator underside fairing
- Frame Number -
- Location vs. Waterline - Approximately 10 ft. above waterline

PLATE SIZE:
- "a" dimension = 24"
- "b" dimension = 16"
- "t" design = not available
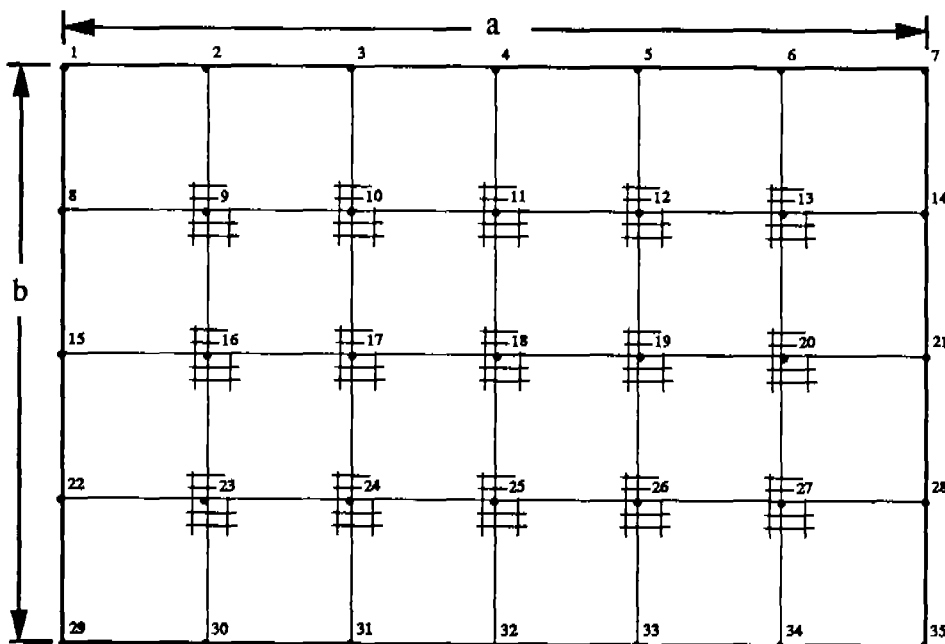
Scale: 1 Grid = 1/2"

Measurements were taken in the fore-aft direction with the dial gauge. The longitudinal frames were undeformed and the stand of the dial gauge track was bottomed to these frames.

| LOCATION	DEPTH READING	THICKNESS	LOCATION	DEPTH READING	THICKNESS
1	0.000	FR	19	1.245	0.362
2	0.357	0.398	20	0.412	0.402
3	1.079	0.358	21	0.000	FR
4	0.463	0.394	22	0.000	FR
5	0.378	0.398	23	0.301	0.390
6	0.630	0.378	24	0.461	0.350
7	0.000	FR	25	0.588	0.370
8	0.000	FR	26	0.568	0.366
9	0.297	0.386	27	0.278	0.358
10	0.749	0.386	28	0.000	FR
11	1.208	0.378	29	0.000	FR
12	0.982	0.366	30	0.331	0.382
13	0.381	0.378	31	0.423	0.354
14	0.000	FR	32	0.421	0.370
15	0.000	FR	33	0.401	0.358
16	0.194	0.382	34	0.238	0.354
17	0.516	0.362	35	0.000	FR
18	1.127	0.370			

Note: FR indicates that a frame prevented a UT thickness reading

In-Plane View of Deformation

NOTE: Horizontal grid scale is 1 grid = 1/2 inch
       Depth grid scale is 1 grid = 1/5 inch
   Greatest dent depth is 1.539" between grids 18 and 19.
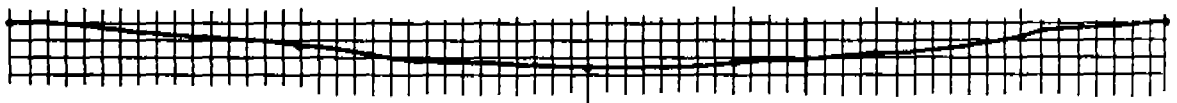
Section through points 1-7
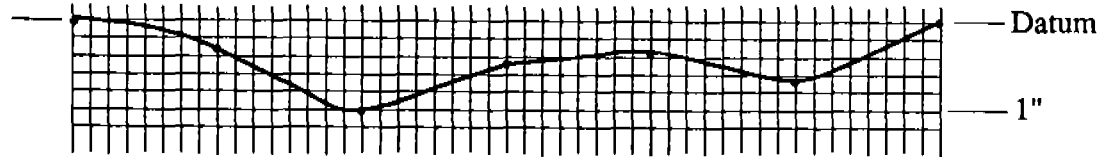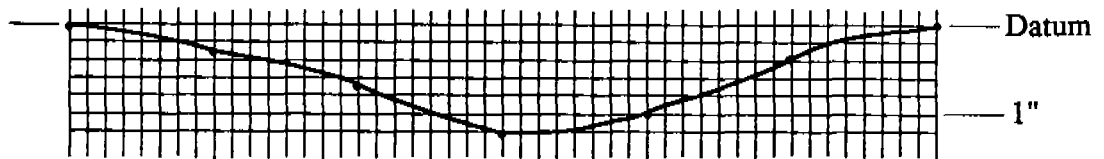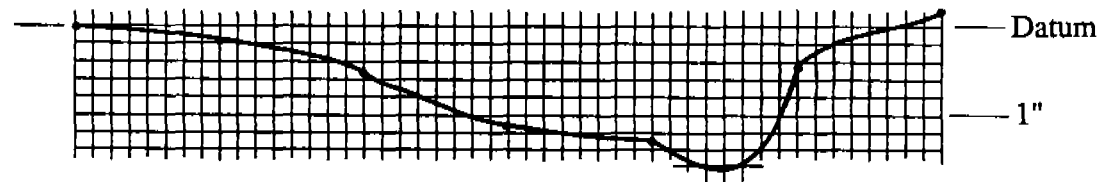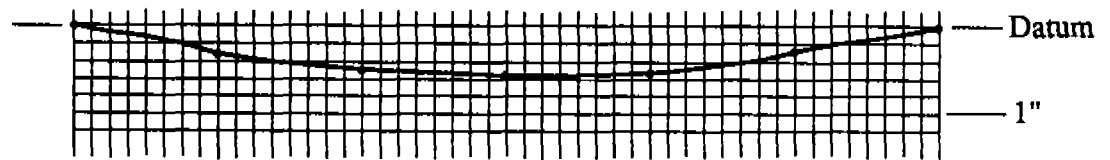
Section through points 8-14

Section through points 15-21

Section through points 22-28

Section through points 29-35
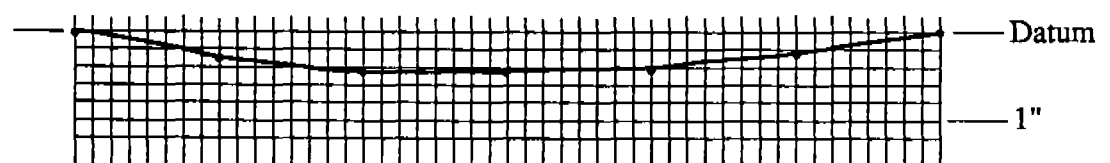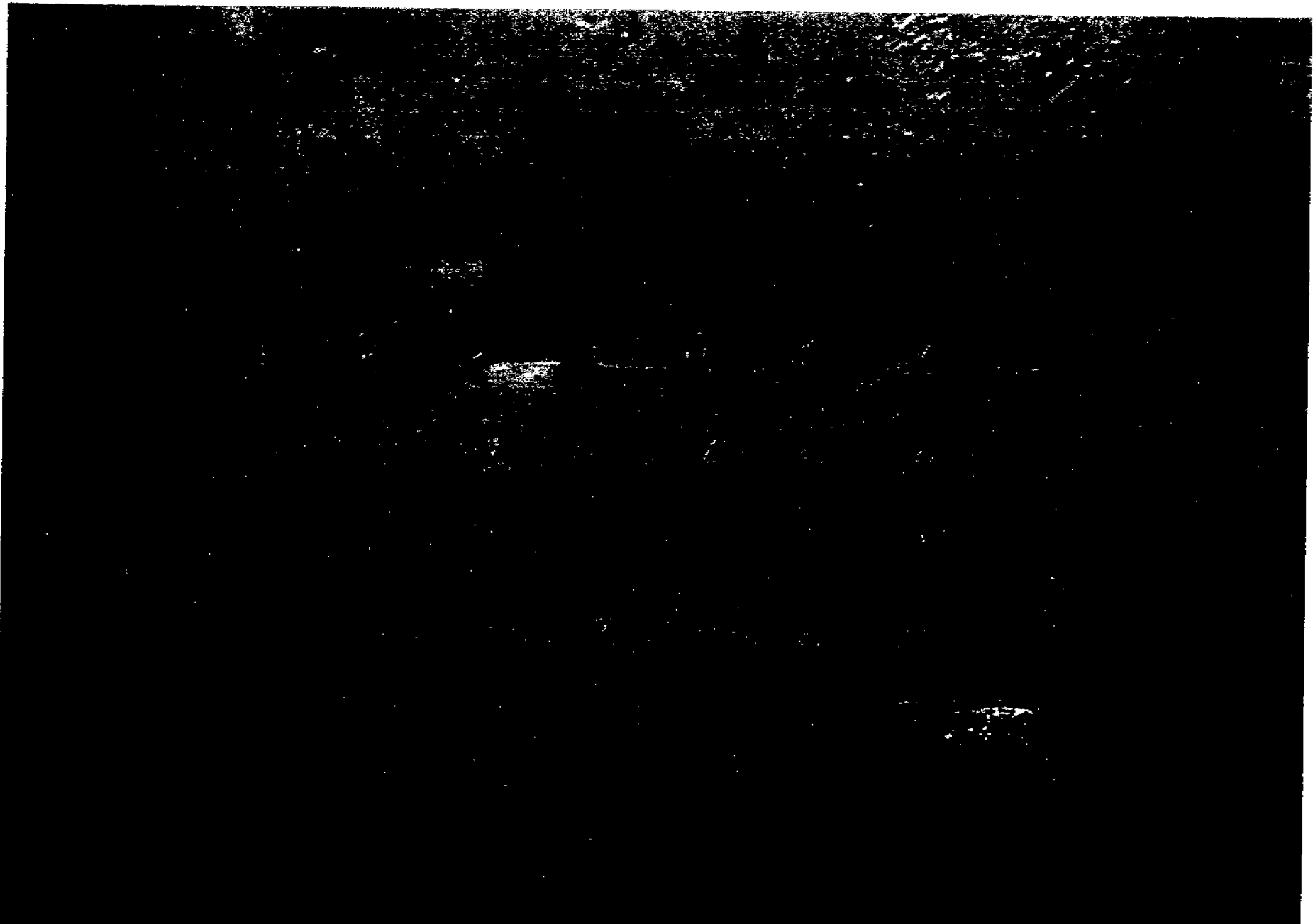
FIGURE A-9. MEASUREMENT #8 - USS KENNEDY
PORT SIDE FAIRING BELOW AFT ELEVATOR
VIEW SHOWING IMPACT DAMAGE

A-28
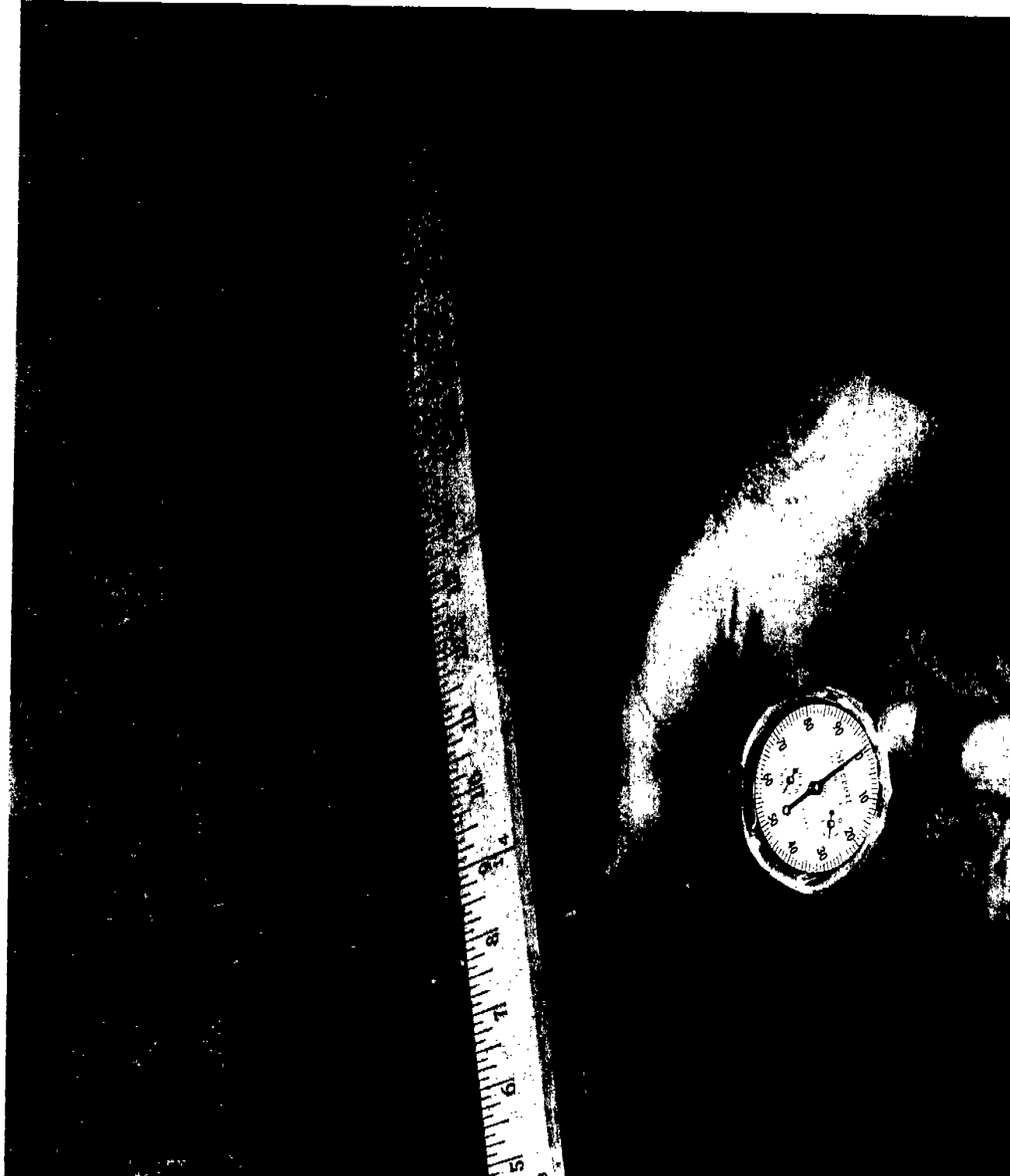
FIGURE A-10. MEASUREMENT #8 - USS KENNEDY
DATA POINT 17
VIEW OF MEASUREMENT TECHNIQUE

MEASUREMENT #9

DATE: 5-10-89

LOCATION: Norfolk Naval Shipyard

SHIP: USS Dahlgren, DDG-43

PLATE LOCATION:
- General - Port side, near frame 43, above waterline
- Type - Typical of waveslap deformation combined with an impact, bow area

PLATE SIZE:
- "a" dimension = 32"
- "b" dimension = 28" (between longitudinals)
- "t" design = 7/16"
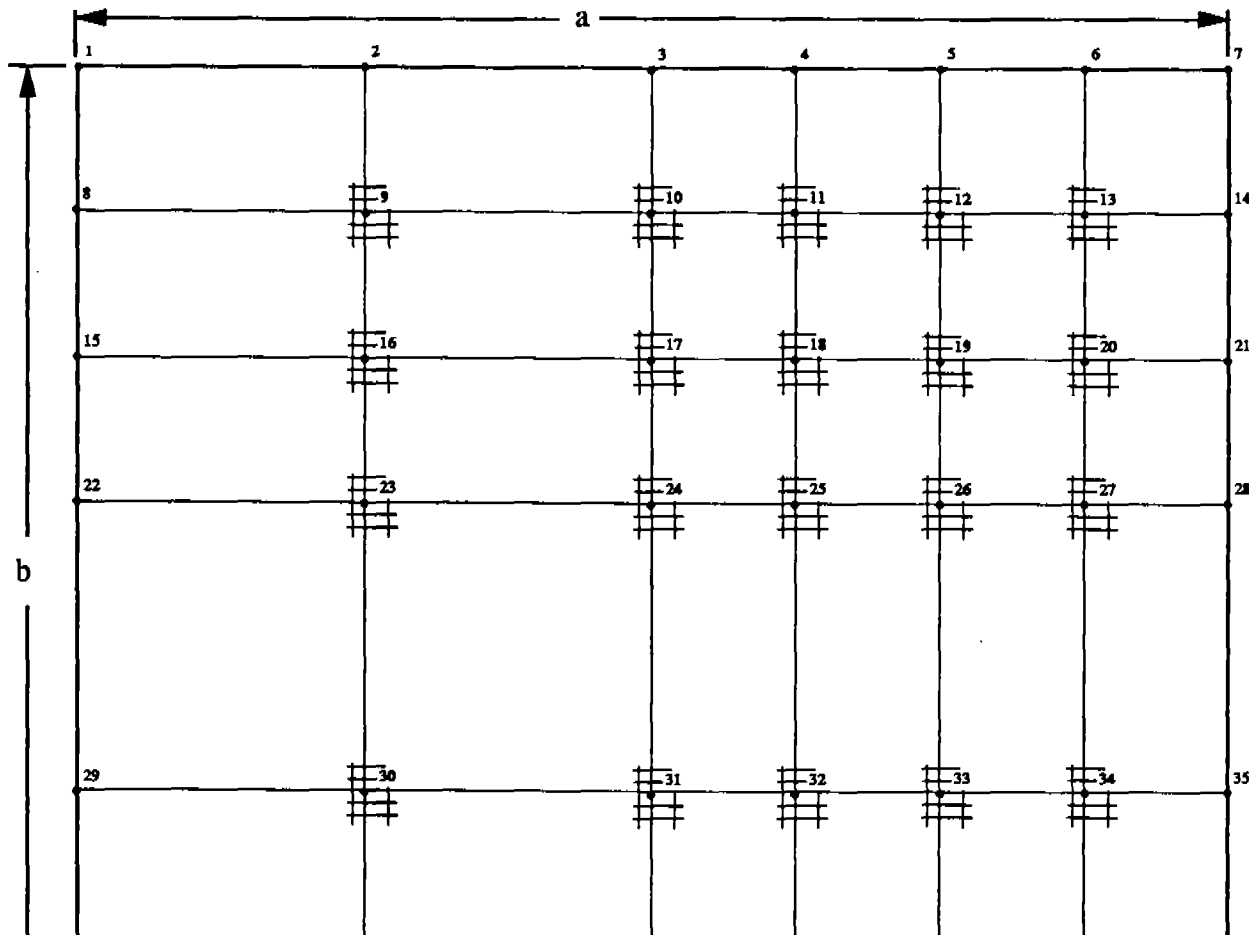
MEASUREMENT #9(continued)

LOCATION	DEPTH READING	THICKNESS	LOCATION	DEPTH READING	THICKNESS
1	0.000	FR	22	0.000	FR
2	0.000	FR	23	0.0547	0.421
3	0.000	FR	24	0.172	0.433
4	0.000	FR	25	0.215	0.437
5	0.000	FR	26	0.195	0.437
6	0.000	FR	27	0.113	0.441
7	0.000	FR	28	0.000	0.437
8	0.000	FR	29	0.000	FR
9	0.0625	0.499	30	0.0625	0.417
10	0.375	0.437	31	0.125	0.421
11	0.484	0.433	32	0.109	0.417
12	0.375	0.433	33	0.0938	0.441
13	0.203	0.411	34	0.0469	0.441
14	0.000	0.411	35	0.000	0.437
15	0.000	FR	36	0.000	FR
16	0.0313	0.445	37	0.0547	FR
17	0.281	0.445	38	0.0781	FR
18	0.328	0.445	39	0.0586	FR
19	0.25	0.437	40	0.0391	FR
20	0.109	0.449	41	0.0195	FR
21	0.000	0.413	42	0.000	FR

Note: FR indicates that a frame prevented a UT depth reading

In-Plane View of Deformation

NOTE: Horizontal grid scale is 1 grid = .5 inches
Depth grid scale is 1 grid = 0.05 inches
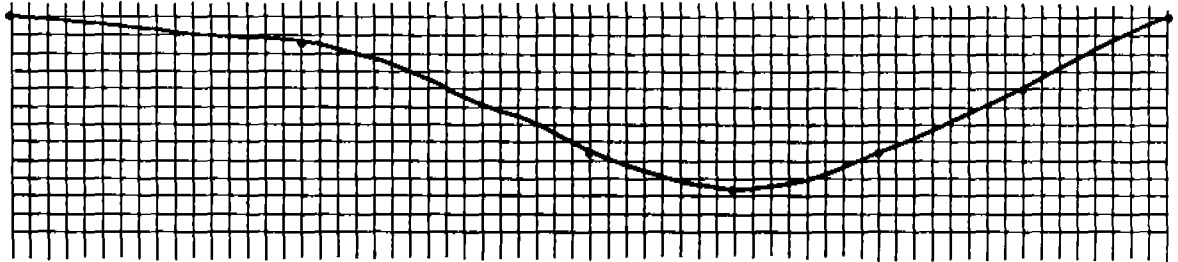
Section through points 8-14

Section through points 15-21
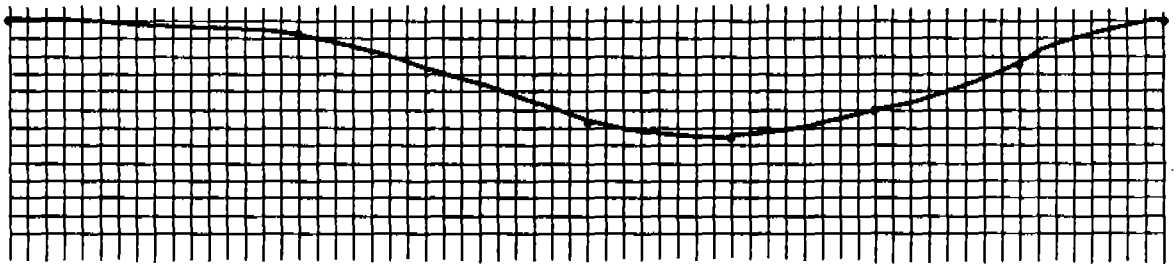
Section through points 22-28
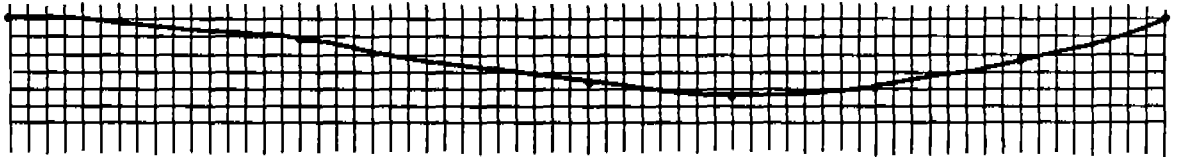
Section through points29-35

Section through points 36-42
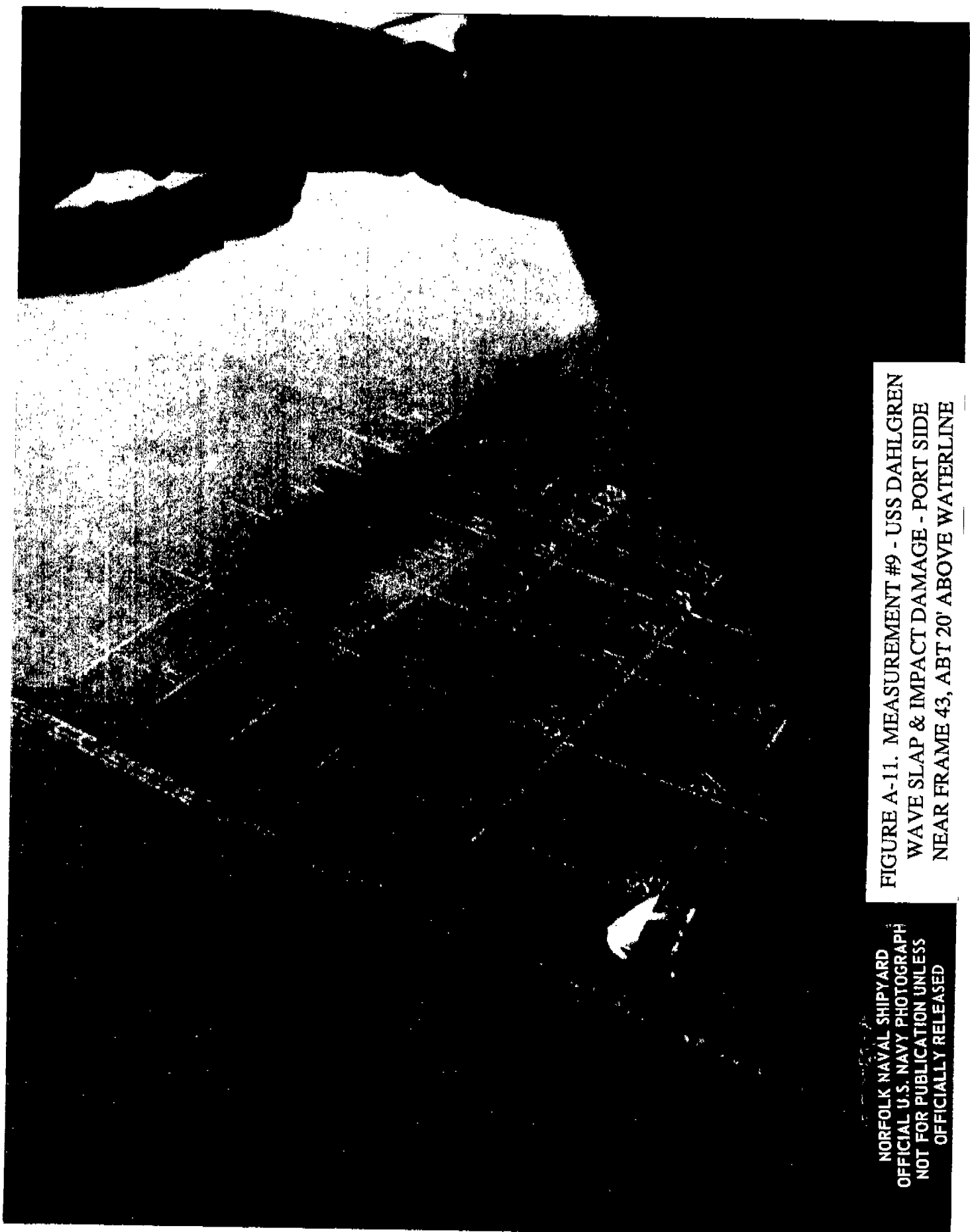
FIGURE A-11. MEASUREMENT #9 - USS DAHLGREN
WAVE SLAP & IMPACT DAMAGE - PORT SIDE
NEAR FRAME 43, ABT 20' ABOVE WATERLINE

DATE: 5-10-89

LOCATION: Norfolk Naval Shipyard

SHIP: USS Dahlgren, DDG-43

PLATE LOCATION:
- General - Port side, aft
- Type - Tug/harbor damage, at waterline

PLATE SIZE:
- "a" dimension = 42", 43" between transverse frames
- "b" dimension = 30" (between longitudinals)
- "t" design = 3/8"
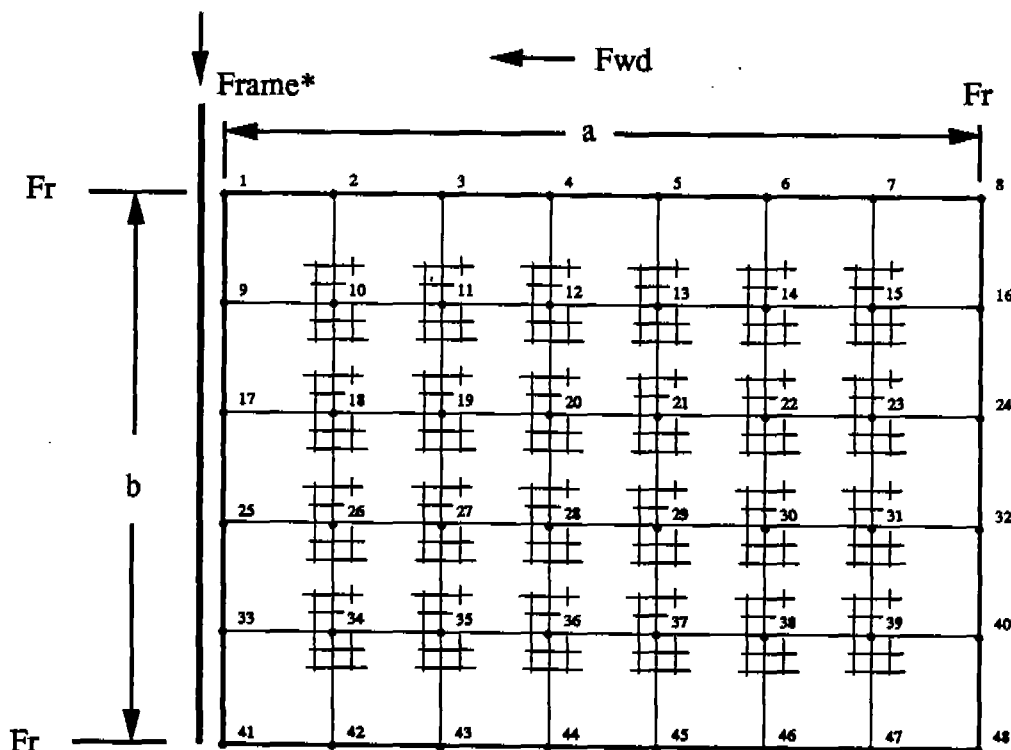
Scale 1 Grid = 1"

* It was not apparent until UT measurements were taken as to where the forward transverse frame was. It was located 1" forward from where the grid was layed out. The data does not need to be reduced since the forward most grid points (1, 9, 17, 25, 33 and 41) had zero deflection.

LOCATION	DEPTH READING	THICKNESS	LOCATION	DEPTH READING	THICKNESS
1	0.000	FR	25	0.000	0.374
2	0.000	FR	26	3/32	0.433
3	0.000	FR	27	9/32	0.457
4	0.000	FR	28	15/32	0.476
5	0.000	FR	29	20/32	0.472
6	0.000	FR	30	20/32	0.409
7	0.000	FR	31	17/32	0.421
8	0.000	FR	32	0.000	FR
9	0.000	0.429	33	0.000	0.346
10	2/32	0.449	34	2/32	0.441
11	8/32	0.445	35	2/32	0.441
12	16/32	0.429	36	3/32	0.425
13	22/32	0.461	37	5/32	0.461
14	18/32	0.469	38	7/32	0.465
15	11/32	0.457	39	5/32	0.406
16	0.00	FR	40	0.000	FR
17	0.00	0.433	41	0.000	FR
18	5/32	0.465	42	0.000	FR
19	15/32	0.445	43	0.000	FR
20	26/32	0.469	44	0.000	FR
21	1-3/32	0.484	45	0.000	FR
22	28/32	0.476	46	0.000	FR
23	18/32	0.472	47	0.000	FR
24	0.000	FR	48	0.000	FR

Note: FR indicates that a frame at that location prevented a UT thickness measurement.

In-Plane View of Deformation

NOTE: Horizontal grid scale is 1 grid = 1 inch
Depth grid scale is 1 grid = 0.25 inch

Section through points 1-8

NO DEFORMATION

Section through points 9-16 ◄─── Fwd
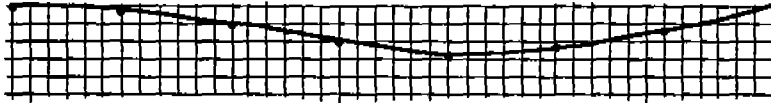
Section through points 17-24

Section through points 25-32

Section through points 33-40
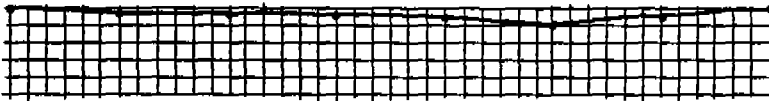
Section through points 41-48

NO DEFORMATION

A-36

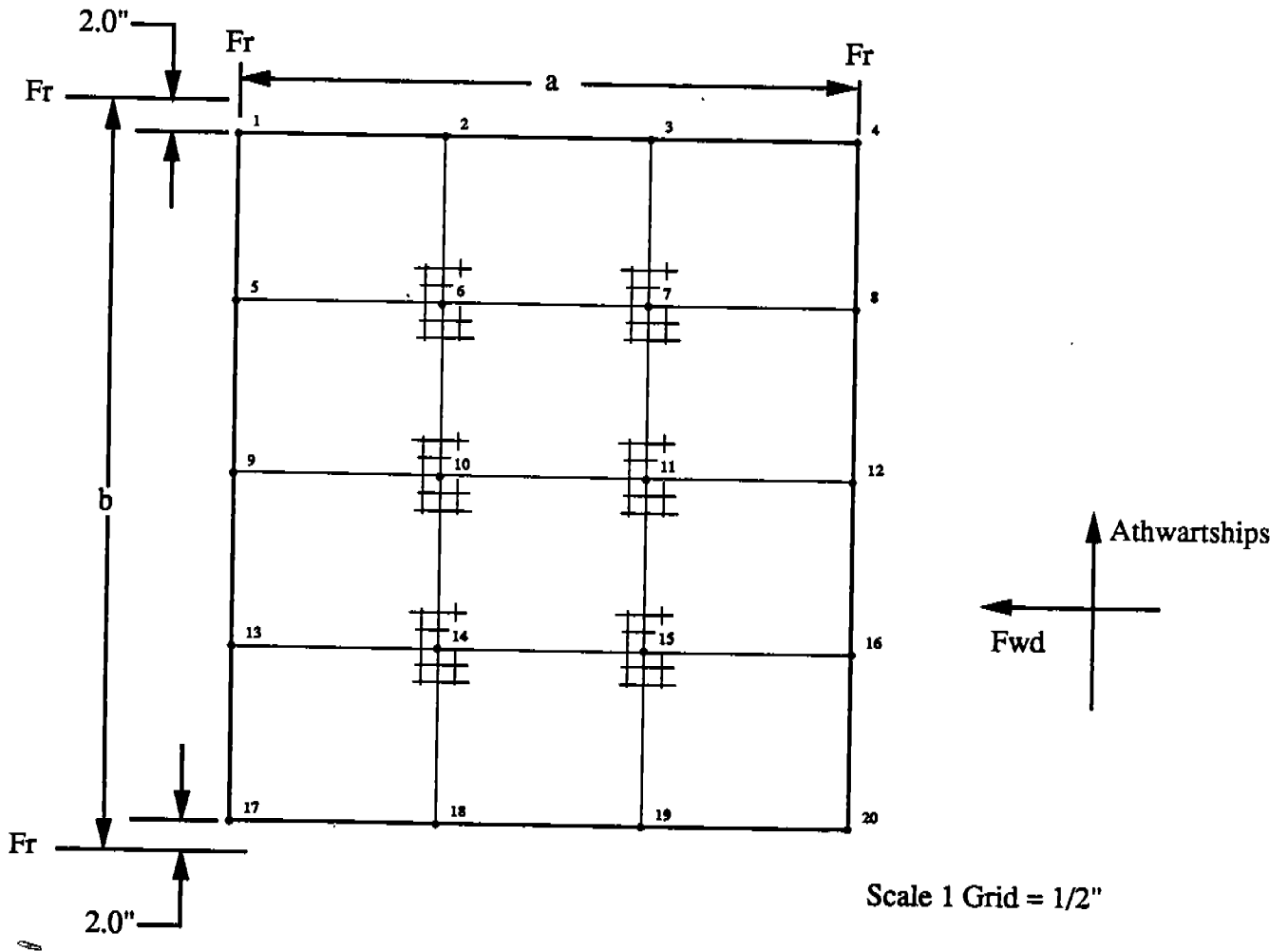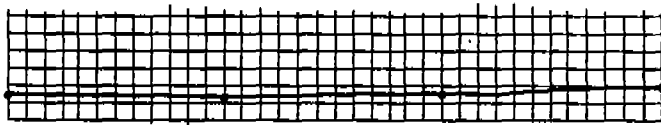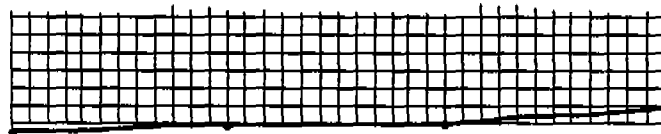DATE: 5-11-89

LOCATION: Lambert's Point Dock, Norfolk, Va.

SHIP: USNS Denebola, T-AKR-289

PLATE LOCATION:
- General - Deck #2, storage areas, starboard side
- Frame Number - Near frame 228

PLATE SIZE:
- "a" dimension = 18" between floor frames
- "b" dimension = 24" between floor frames
- "t" design = not available

Scale 1 Grid = 1/2"

Depths as Measured

LOCATION	DEPTH READING	LOCATION	DEPTH READING
1	0.170	11	0.220
2	0.170	12	0.221
3	0.170	13	0.208
4	0.171	14	0.212
5	0.216	15	0.201
6	0.217	16	0.191
7	0.213	17	0.157
8	0.200	18	0.167
9	0.224	19	0.183
10	0.221	20	0.159

Reduced Data.

LOCATION	DEPTH READING	THICKNESS	LOCATION	DEPTH READING	THICKNESS
1	0.010	0.870	11	0.060	0.890
2	0.010	0.886	12	0.051	0.866
3	0.010	0.870	13	0.048	0.890
4	0.011	0.882	14	0.052	0.882
5	0.046	0.866	15	0.041	0.878
6	0.047	0.882	16	0.031	0.886
7	0.043	0.878	17	+0.003	0.878
8	0.040	0.878	18	0.007	0.882
9	0.064	0.890	19	0.023	0.890
10	0.061	0.886	20	+0.001	0.890

NOTE: A "+" indicates the deflection was upward at this location.

In-Plane View of Deformation

NOTE: Horizontal grid scale is 1 grid = 1/2 inch.
    Vertical grid scale is 1 grid = 0.01 inch.

Section through points 1-4
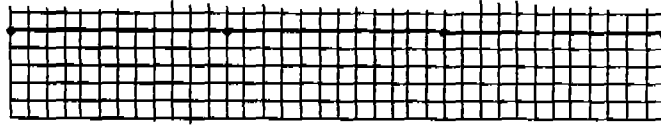
Section through points 5-8

Section through points 9-12

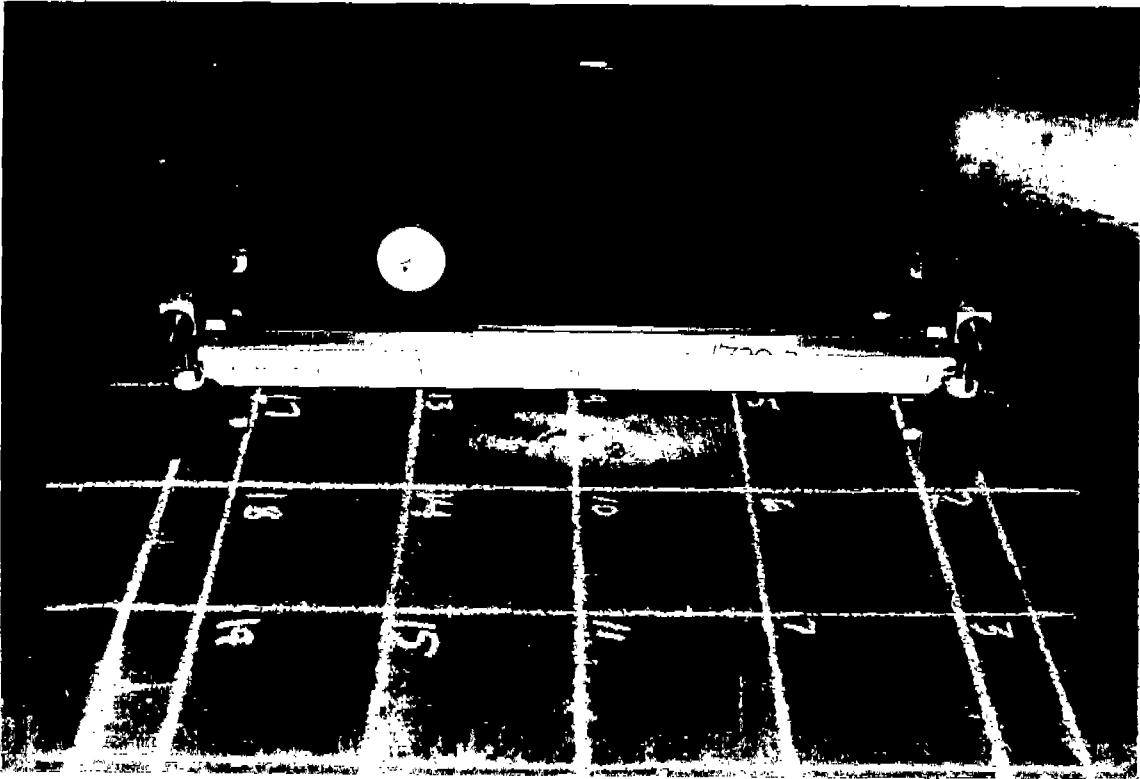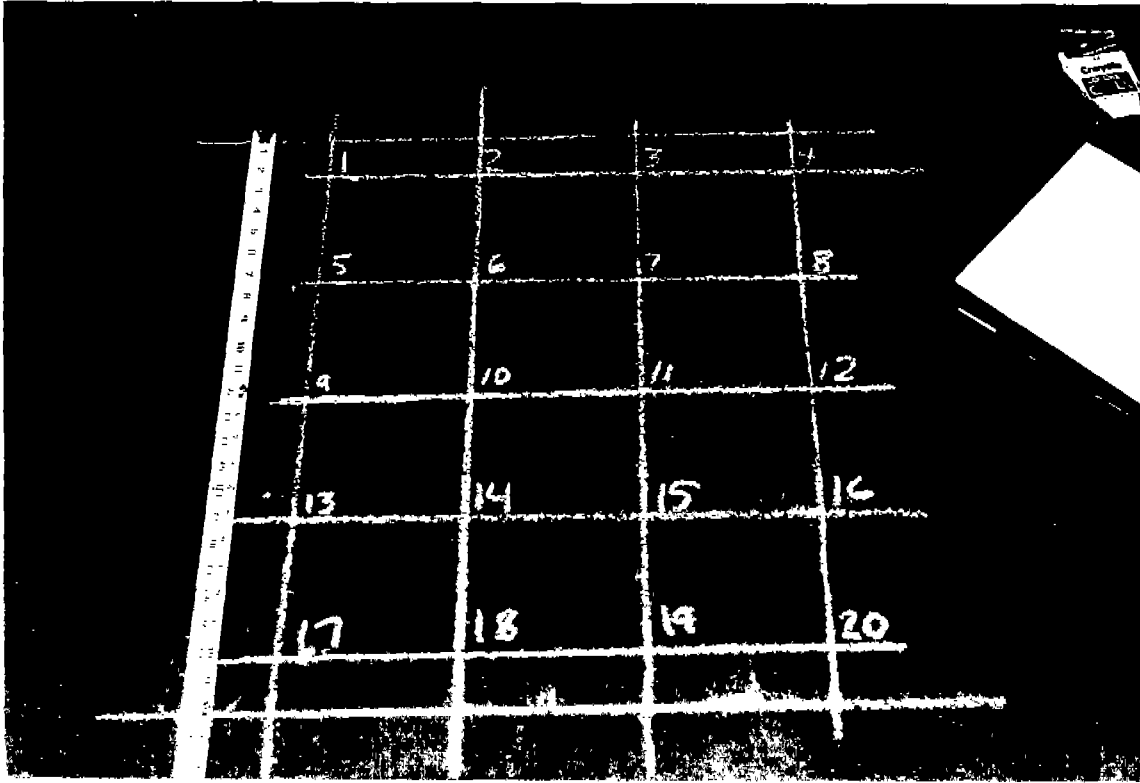Section through points 13-16

Section through points 17-20

FIGURE A-12. MEASUREMENT #11 - USNS DENEBOLA
VEHICLE CARGO DECK #2, FRAME 228, STARBOARD
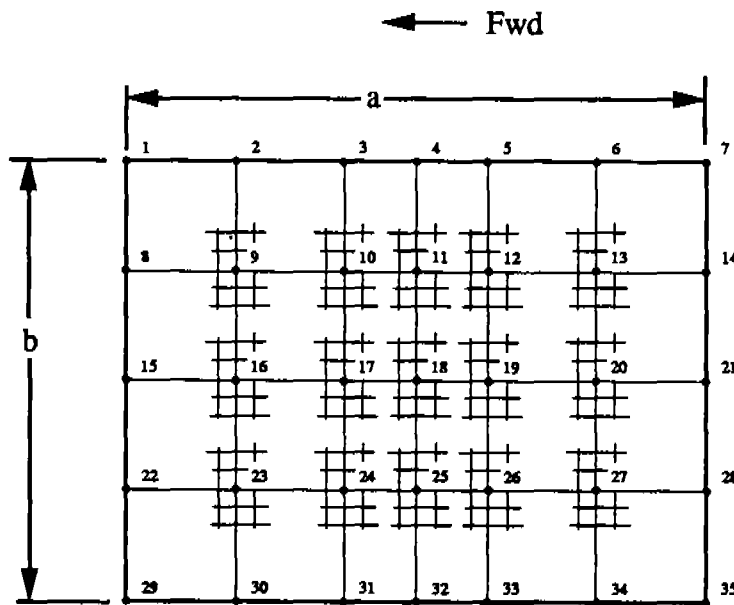
DATE: 5-11-89

LOCATION: NORSHIPCO, Norfolk, Va.

SHIP: USNS Vega, T-AK-286

PLATE LOCATION:
- General - Port side, waterline proximity
- Frame Number - Near frame 149

PLATE SIZE:
- "a" dimension = 32" (between transverse frames)
- "b" dimension = 30" (between longitudinals)
- "t" design = not available

Scale 1 Grid = 1"

LOCATION	DEPTH READING	THICKNESS	LOCATION	DEPTH READING	THICKNESS
1	8/32	FR	19	2-10/32	0.705
2	30/32	0.724	20	1-5/32	0.685
3	1-12/32	0.709	21	0	FR
4	1-15/32	0.728	22	7/32	FR
5	1-10/32	0.728	23	1-20/32	0.713
6	21/32	0.705	24	2-11/32	0.717
7	0	FR	25	2-11/32	0.701
8	18/32	FR	26	2-1/32	0.724
9	1-24/32	0.709	27	1	0.728
10	2-14/32	0.681	28	0	FR
11	2-16/32	0.693	29	0	FR
12	2-7/32	0.685	30	1-5/32	Bad Paint
13	1-5/32	0.709	31	1-21/32	0.689
14	0	FR	32	1-20/32	0.709
15	0	FR	33	1-14/32	Bad Paint
16	1-21/32	0.681	34	23/32	Bad Paint
17	2-18/32	0.669	35	0	Bad Paint
18	2-19/32	0.705			

Note: FR indicates that a frame at that location prevented a UT thickness reading.
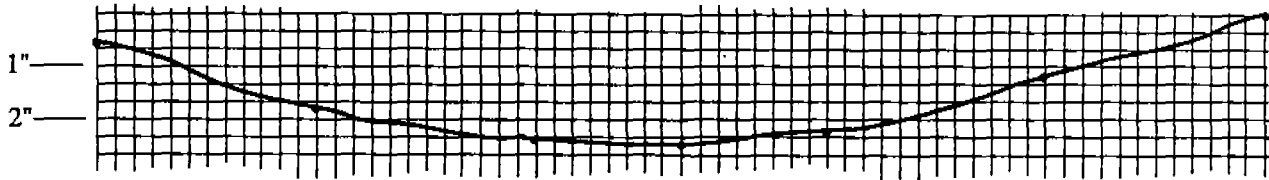
In-Plane View of Deformation

NOTE: Width grid scale is 1 grid = 1/2 inch
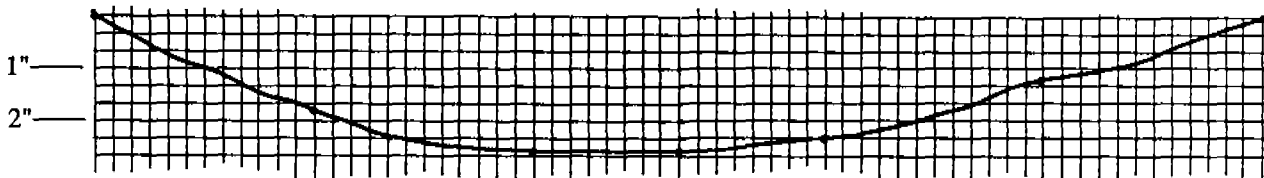   Depth grid scale is 1 grid = 1/3 inch

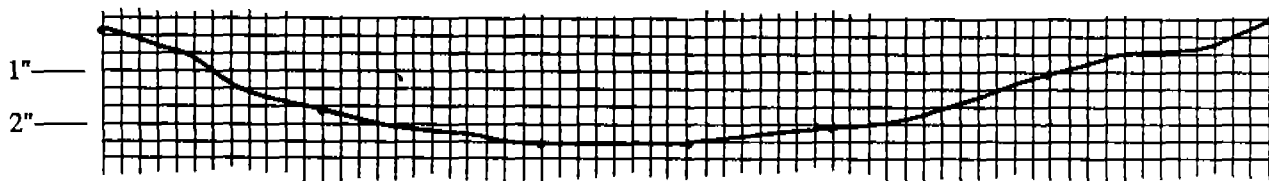Section through points 1-7
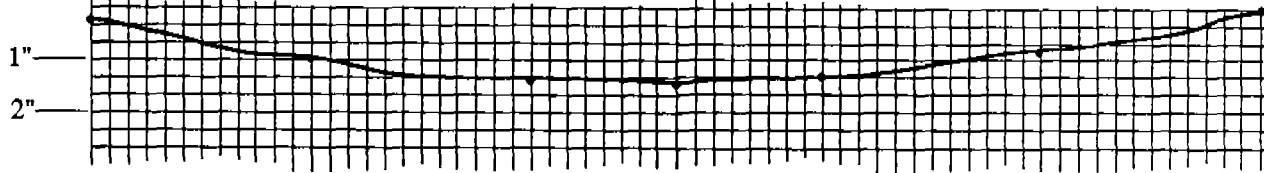
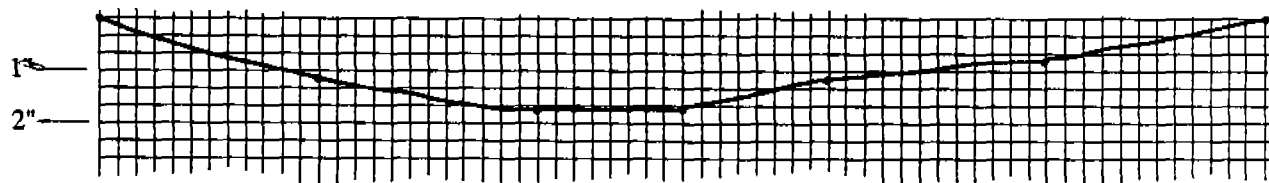Section through points 8-14

Section through points 15-21

Section through points 22-28

Section through points 29-35
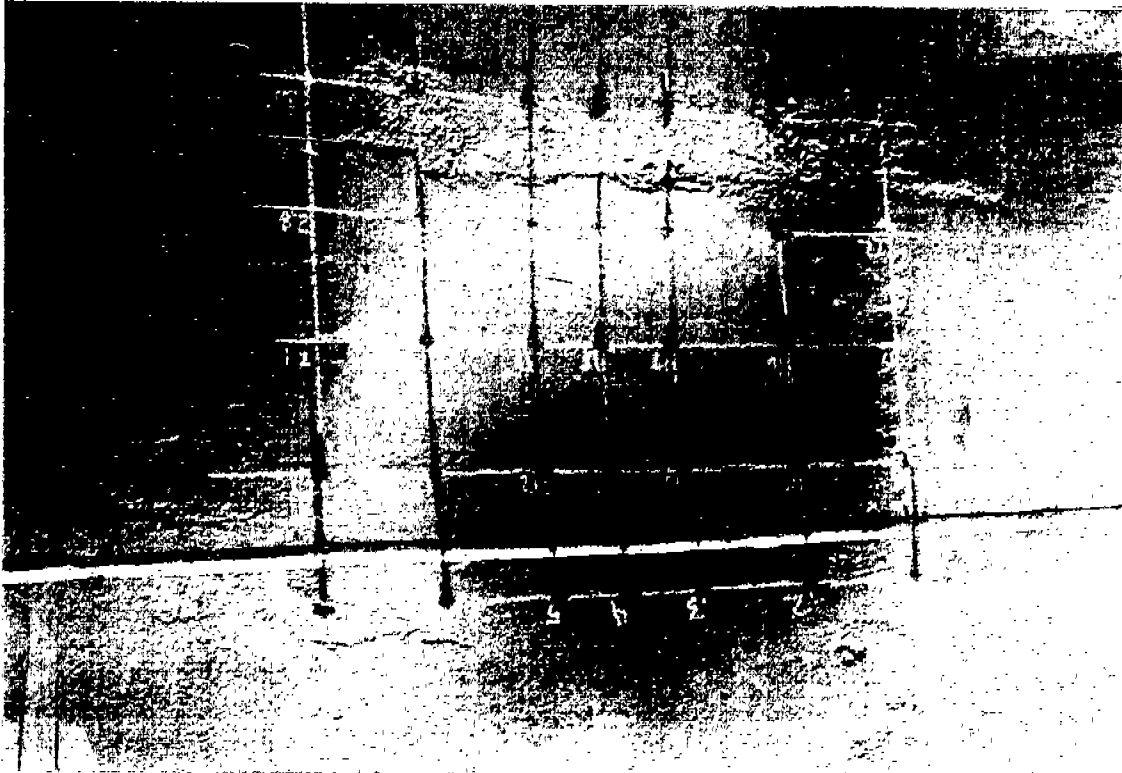
FIGURE A-13. MEASUREMENT #12 - USNS VEGA
PORT SIDE, FRAME 149, AT WATERLINE

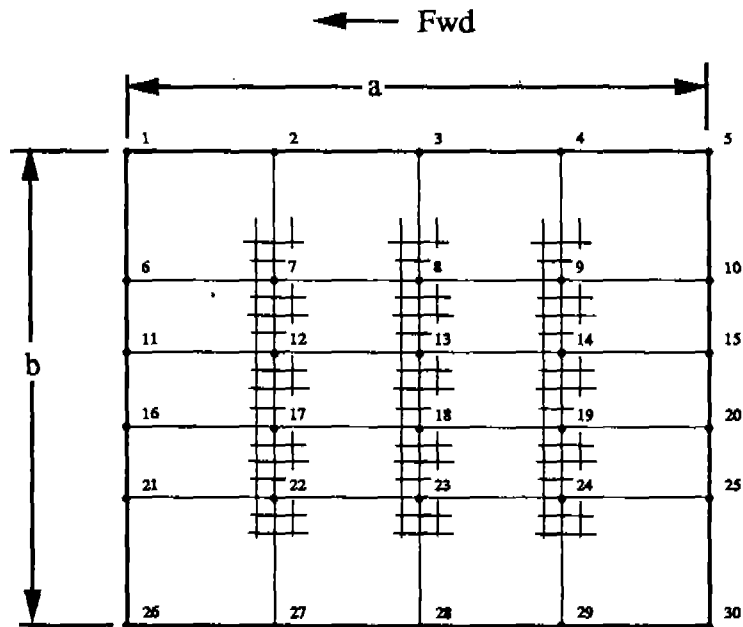DATE: 5-11-89

LOCATION: NORSHIPCO, Norfolk, Va.

SHIP: USNS Vega, T-AK-286

PLATE LOCATION:
- General - Port side, below waterline, crease impact
- Frame Number - Near frame 176

PLATE SIZE:
- "a" dimension = 32" (between transverse frames)
- "b" dimension = 26" (between longitudinal frames)
- "t" design = not available

Scale 1 Grid = 1"

LOCATION	DEPTH READING	THICKNESS	LOCATION	DEPTH READING	THICKNESS
1	0	FR	16	0	FR
2	0	FR	17	11/32	0.583
3	0	FR	18	21/32	0.583
4	0	FR	19	21/32	0.591
5	0	FR	20	0	FR
6	0	FR	21	0	FR
7	8/32	0.551	22	5/32	*
8	20/32	0.555	23	13/32	*
9	5/32	*	24	12/32	*
10	0	FR	25	0	FR
11	0	FR	26	0	FR
12	19/32	0.543	27	0	FR
13	1-4/32	0.555	28	0	FR
14	14/32	0.583	29	0	FR
15	0	FR	30	0	FR

* Due to the fresh, wet paint, not all thickness measurements returned a reading.
Note: FR indicates that a frame at that location prevented a UT thickness reading.
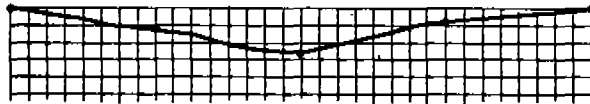
In-Plane View of Deformation

NOTE: Horizontal grid scale is 1 grid = 1 inch
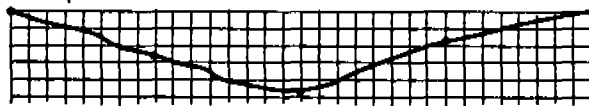Depth grid scale is 1 grid = 0.25 inch

Section through points 1-5
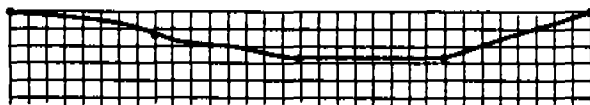
NO DEFORMATION

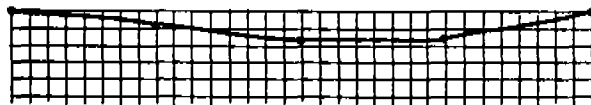Section through points 6-10

Section through points 11-15

Section through points 16-20

Section through points 21-25

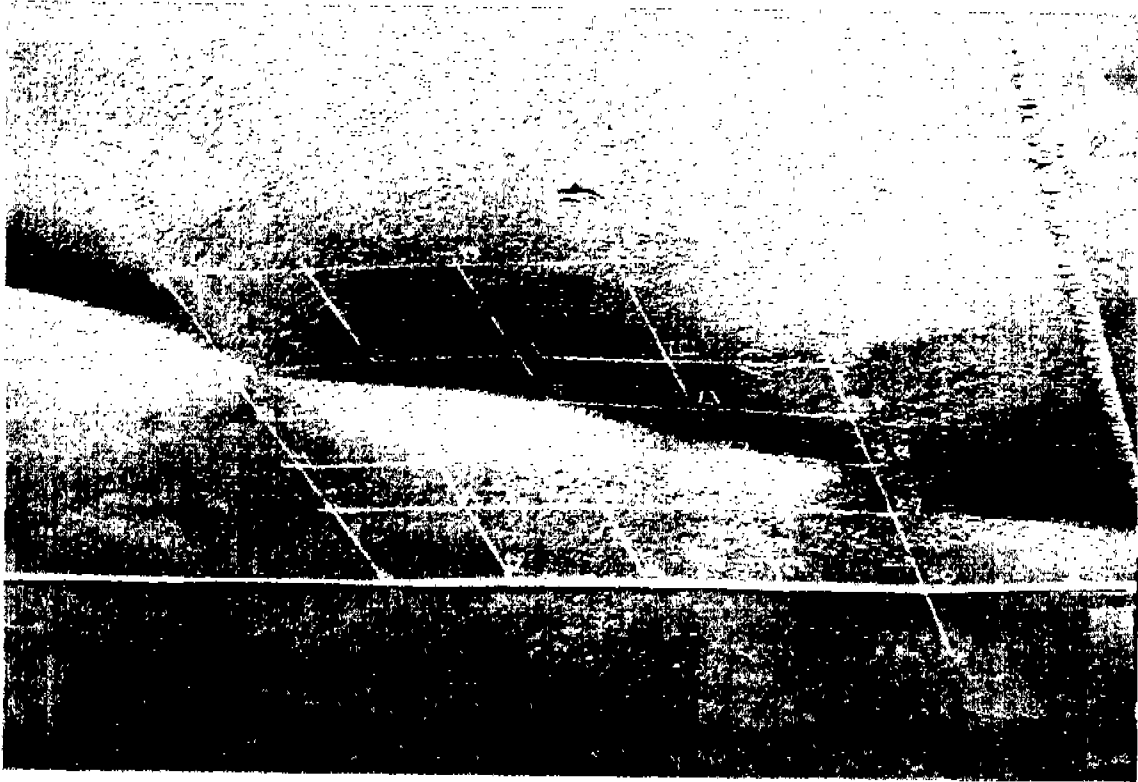Section through points 26-30

NO DEFORMATION

FIGURE A-14. MEASUREMENT #13 - USNS VEGA
IMPACT DAMAGE - PORT SIDE
UNDER BOW, BELOW WATERLINE
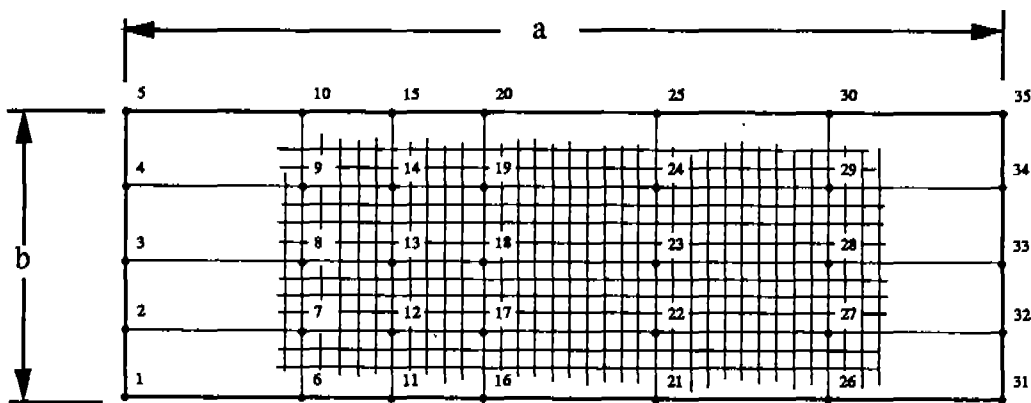
DATE: 9-11-89

LOCATION: NORSHIPCO, Norfolk, Va.

SHIP: Commercial Passenger Vessel

PLATE LOCATION:
   • General - Underside, midspan, starboard

Looking
Aft

PLATE SIZE:
   • "a" dimension = 100"
   • "b" dimension = 32"
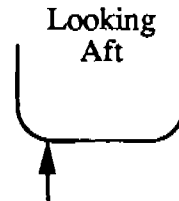
Scale 1 Grid = 2"

Measurements were taken by placing a straightedge across the plate (as a baseline) and using a machined ruler to measure the deflected surface. Accuracy is ±1/64". Thicknesses were obtained using ultra-sonic thickness gauge. Accuracy is ±0.003".

LOCATION	DEPTH READING	THICKNESS	LOCATION	DEPTH READING	THICKNESS
1	0.000	FR	19	0.734	0.961
2	0.0469	FR	20	0.000	FR
3	0.125	FR	21	0.000	FR
4	0.0625	FR	22	0.125	*
5	0.000	FR	23	0.313	*
6	0.000	FR	24	0.422	*
7	0.188	0.945	25	0.000	FR
8	0.406	0.929	26	0.000	FR
9	0.375	0.929	27	0.000	*
10	0.000	FR	28	0.141	*
11	0.000	FR	29	0.281	*
12	0.547	0.953	30	0.000	FR
13	1.000	0.929	31	0.000	FR
14	1.031	0.917	32	0.000	*
15	0.000	FR	33	0.000	*
16	0.000	FR	34	0.000	*
17	0.313	*	35	0.000	FR
18	0.641	*			

* Measurements could not be taken at these points

Note: FR indicates that a frame at that location prevented a UT thickness reading

In-Plane View of Deformation

NOTE: Horizontal grid scale is 1 grid = 2 inches
 Depth grid scale is 1 grid = 1/5 inch

Section through points 1-31

NO DEFORMATION

Section through points 2-32

Section through points 3-33

Section through points 4-34
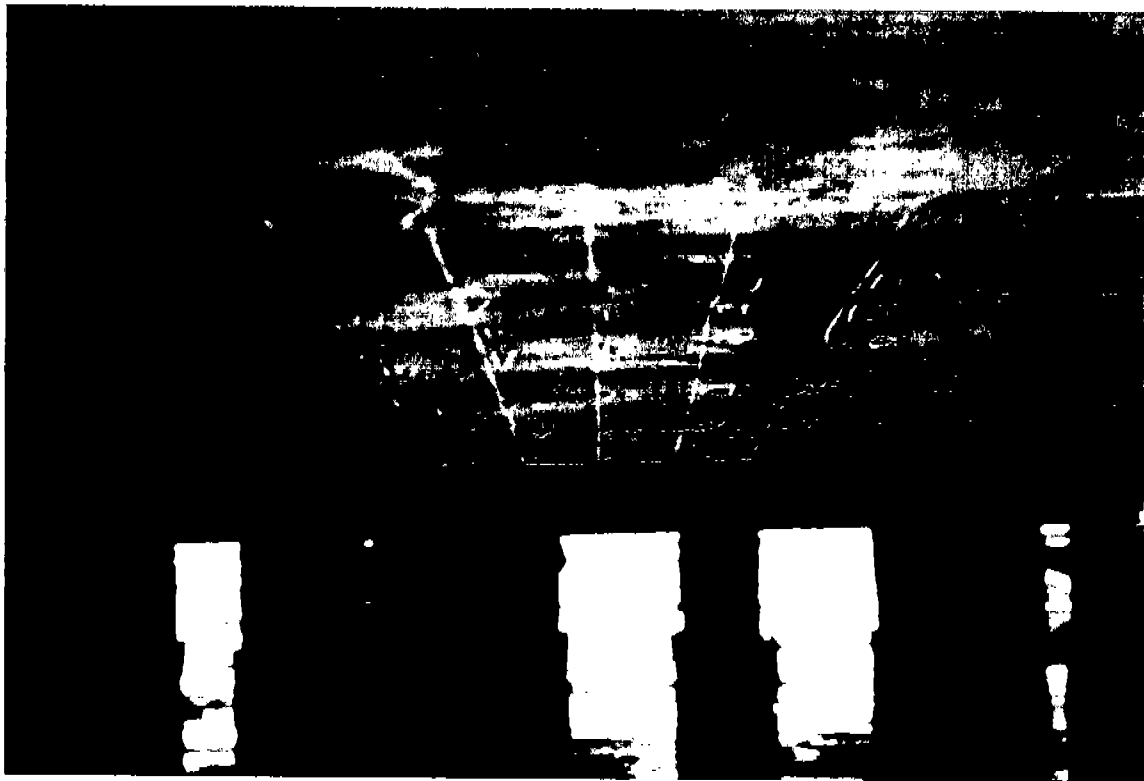

Section through points 5-35

NO DEFORMATION
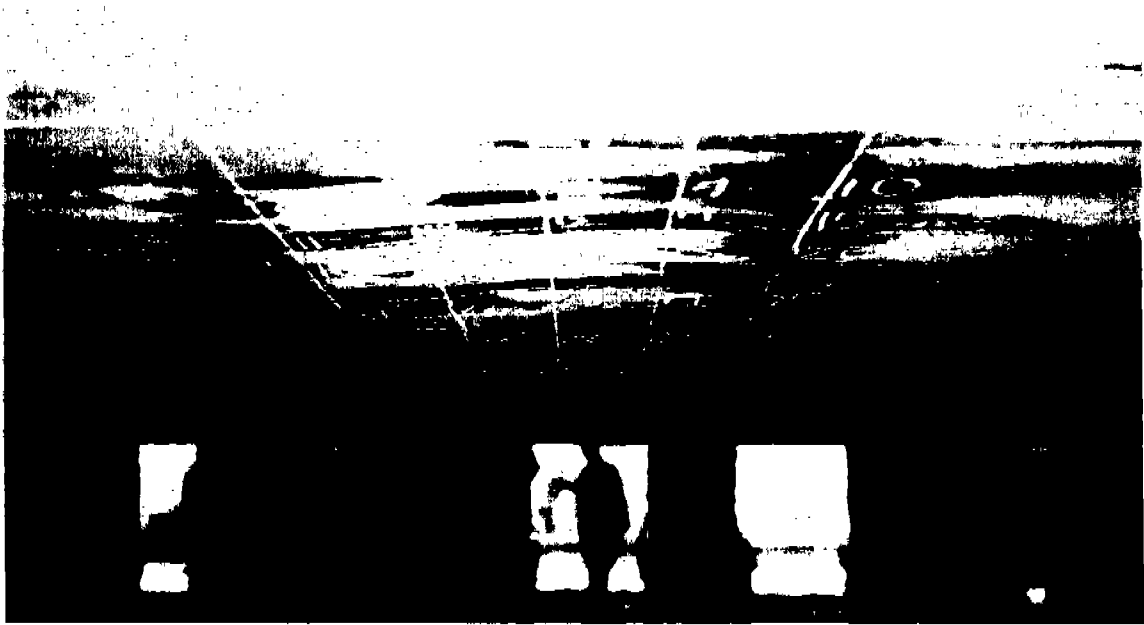
FIGURE A-15. MEASUREMENT #14 - COMMERCIAL PASSENGER SHIP
HULL GROUNDING - PORT SIDE, AMIDSHIPS
VIEWS LOOKING INBOARD SHOWING BOTTOM PLATING

DATE: 9-11-89

LOCATION: NORSHIPCO, Norfolk, Va.

SHIP: Commercial Passenger Vessel

PLATE LOCATION:
  • General - Starboard side, midbody, waterline

PLATE SIZE:
  • "a" dimension = 36"
  • "b" dimension = 16"
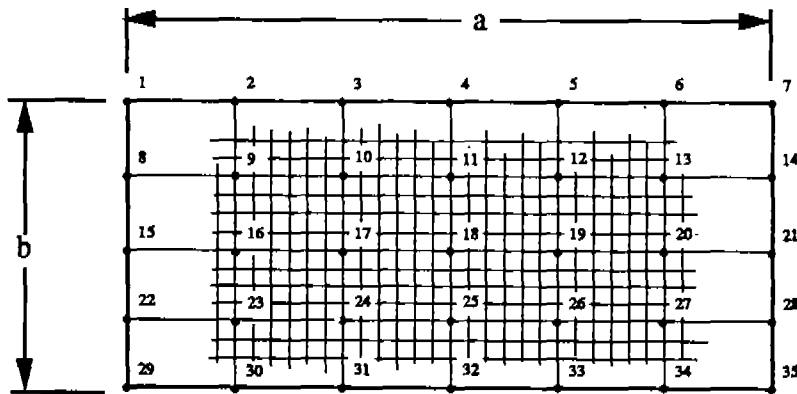
Scale: 1 Grid = 1"

Measurements were taken using the straightedge method.
Accuracy is ±1/64".

LOCATION	DEPTH READING	THICKNESS	LOCATION	DEPTH READING	THICKNESS
1	0.000		19	1.938	
2	0.000		20	0.344	
3	0.000		21	0.000	
4	0.000		22	0.000	
5	0.000		23	1.063	
6	0.000		24	1.750	
7	0.000		25	1.625	
8	0.000		26	1.094	
9	1.031		27	0.406	
10	1.547		28	0.000	
11	1.219		29	0.000	
12	0.578		30	0.938	
13	0.172		31	1.641	
14	0.000		32	1.750	
15	0.000		33	1.188	
16	1.156		34	0.578	
17	1.797		35	0.000	
18	1.422				

Note: Thickness measurements were unobtainable due to thick paint and roughness.

In-Plane View of Deformation

NOTE: Horizontal grid scale is 1 grid = 1 inch
Depth grid scale is 1 grid = 1/5 inch

Section through points 1-7

NO DEFORMATION

Section through points 8-14

Section through points 15-21
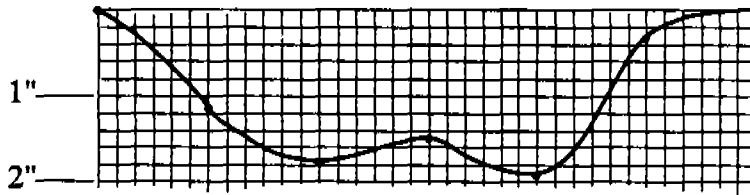
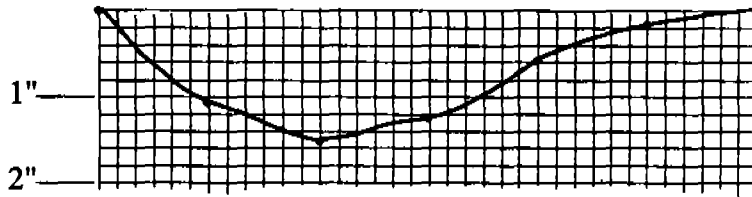Section through points 22-28
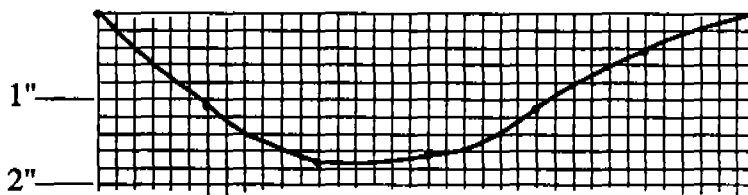
Section through points 29-35
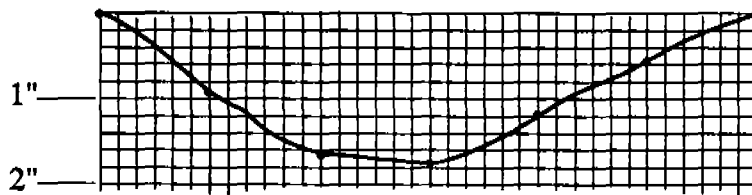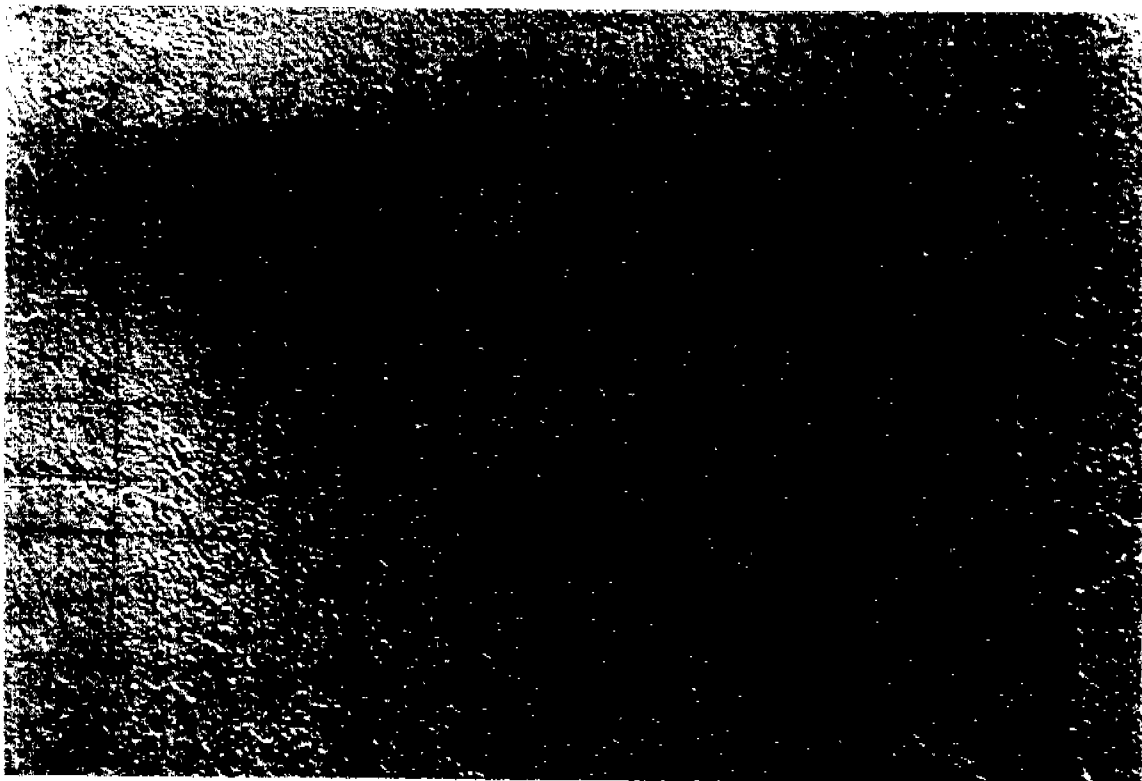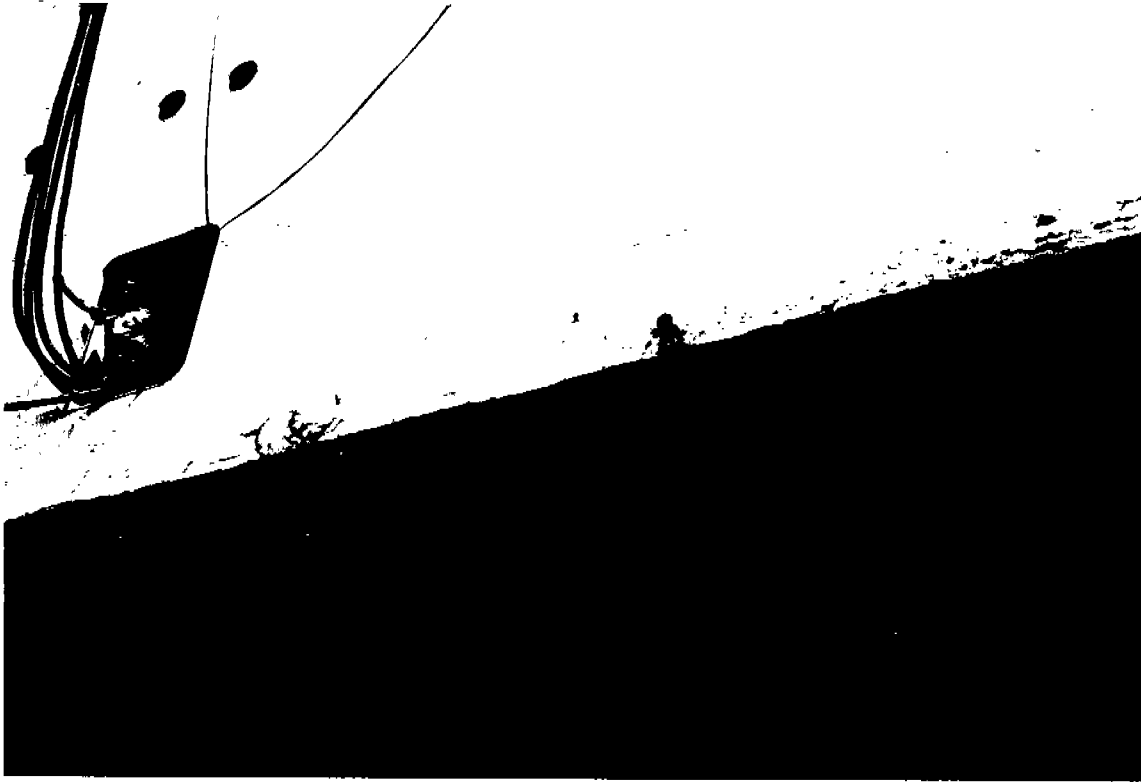
FIGURE A-16. MEASUREMENT #15 - COMMERCIAL PASSENGER SHIP
PORT SIDE, AMIDSHIPS, AT WATERLINE

DATE: 9-11-89

LOCATION: NORSHIPCO, Norfolk, Va.

SHIP: Commercial Passenger Vessel

PLATE LOCATION:
  • General - Bow, port side, 6 ft. above waterline

PLATE SIZE:
  • "a" dimension = 26"
  • "b" dimension = 24"
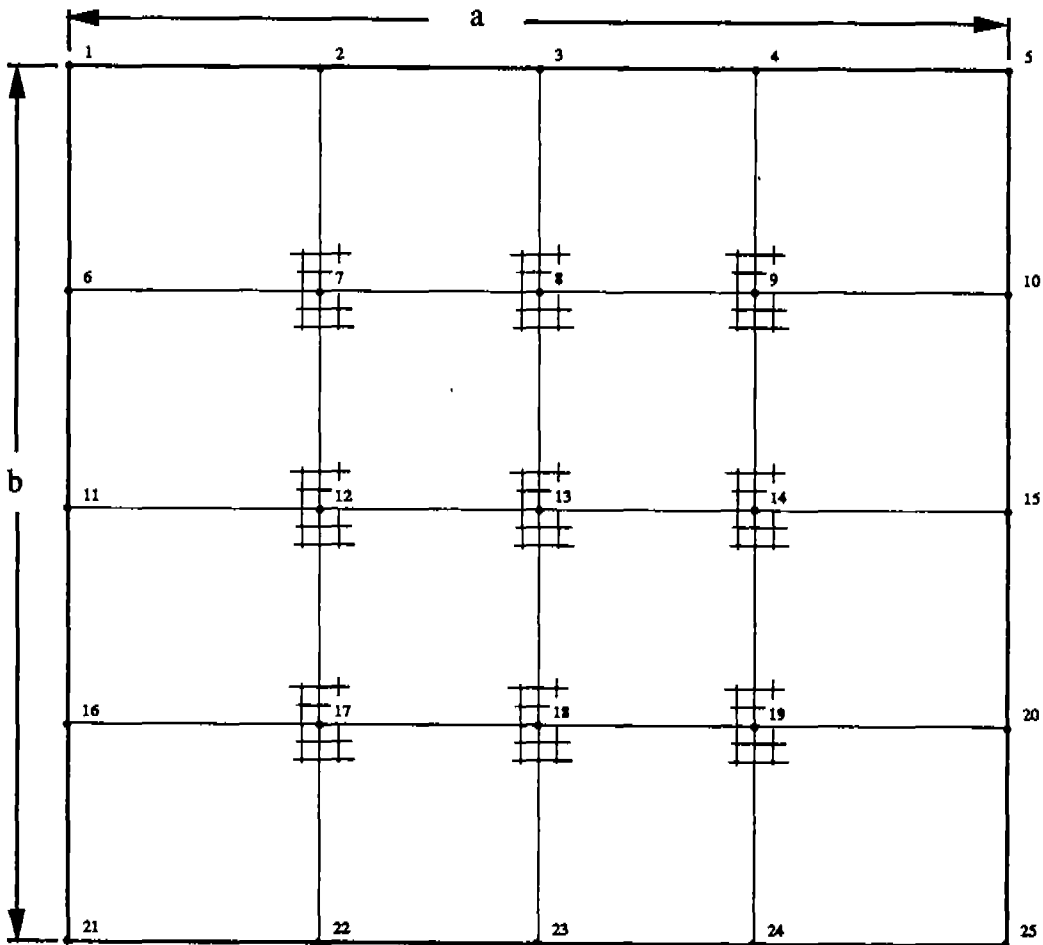
Scale: 1 Grid = 1/2"

Measurements were taken using straightedge method.
Accuracy is ±1/64". Thicknesses were obtained using
ultrasonic thickness gauge. Accuracy is ±0.003".

LOCATION	DEPTH READING	THICKNESS	LOCATION	DEPTH READING	THICKNESS
1	0.000	FR	13	1.016	0.630
2	0.000	FR	14	0.828	0.638
3	0.000	FR	15	0.000	FR
4	0.000	FR	16	0.000	FR
5	0.000	FR	17	0.391	0.657
6	0.000	FR	18	0.594	0.646
7	0.313	0.622	19	0.500	0.638
8	0.453	0.657	20	0.000	FR
9	0.313	0.630	21, 25	0.000	FR
10	0.000	FR	22	0.188	0.622
11	0.000	FR	23	0266	0.630
12	0.594	0.634	24	0.172	0.618

Note: FR indicates that a frame at this location prevented a UT thickness measurement

In-Plane View of Deformation

NOTE: Horizontal grid scale is 1 grid = 2 inches
Depth grid scale is 1 grid = 1/5 inch

Section through points 1-5

NO DEFORMATION

Section through points 6-10

1"——

Section through points 11-15

1"——

Section through points 16-20

1"——

Section through points 21-25

1"——
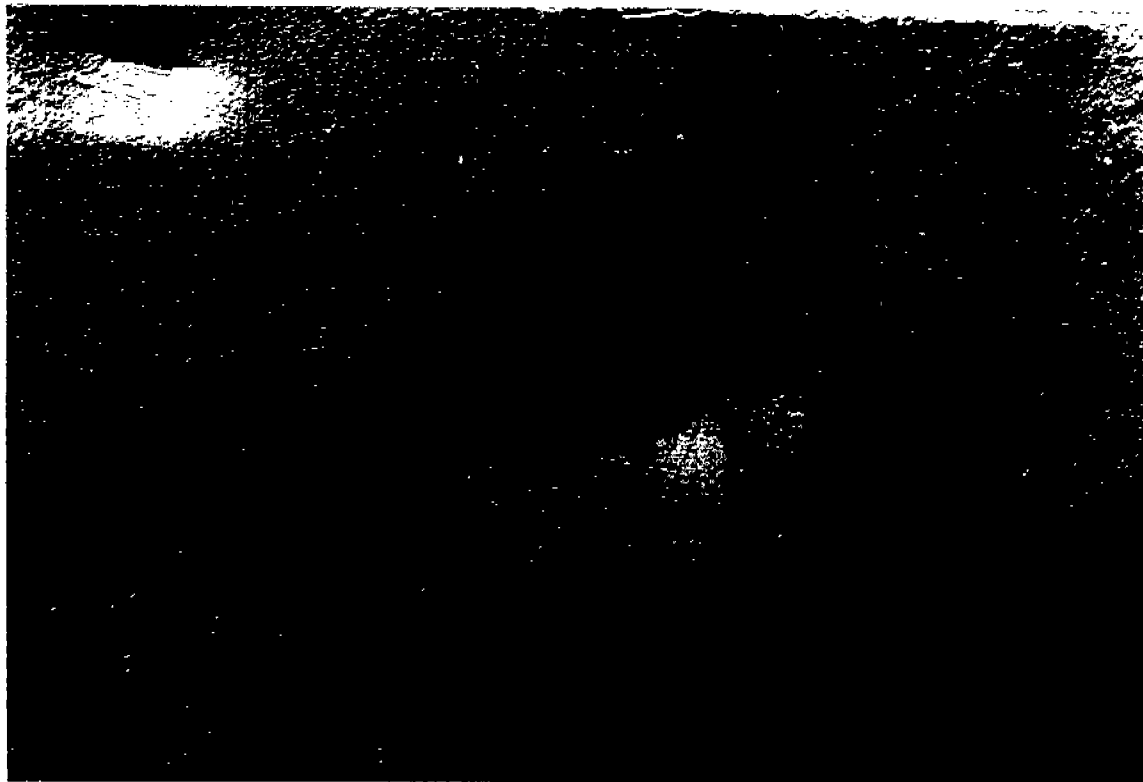
FIGURE A-17. MEASUREMENT #16 - COMMERCIAL PASSENGER SHIP
STARBOARD SIDE, AFT, AT WATERLINE

DATE: 9-12-89

LOCATION: Norfolk Naval Shipyard

SHIP: USS King, DDG-41

PLATE LOCATION:
  • General - Starboard side, bow, waterline

PLATE SIZE:
  • "a" dimension = 30"
  • "b" dimension = 24"
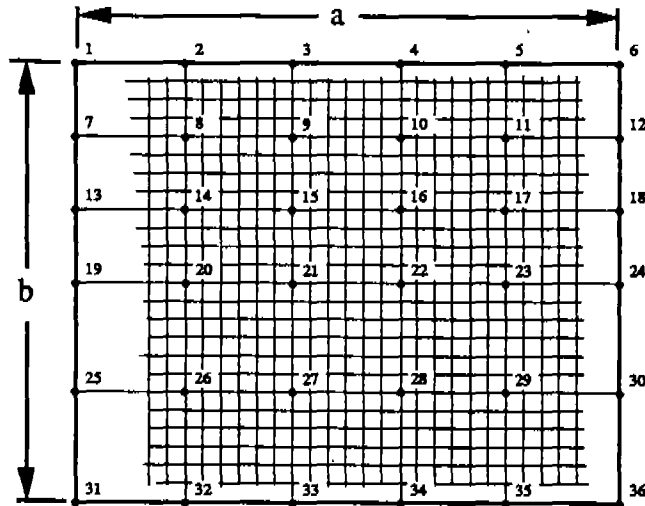
Scale: 1 Grid = 1"

Measurements were taken using straightedge method.
Accuracy is ±1/64". Thicknesses were obtained using
ultrasonic thickness gauge. Accuracy is ±0.003".

LOCATION	DEPTH READING	THICKNESS	LOCATION	DEPTH READING	THICKNESS
1	0.109	FR	19	0.000	FR
2	0.141	FR	20	0.188	0.445
3	0.250	FR	21	0.406	0.457
4	0.391	FR	22	0.828	0.425
5	0.281	FR	23	0.531	0.425
6	0.000	FR	24	0.000	FR
7	0.000	FR	25	0.000	FR
8	0.109	0.402	26	0.172	0.433
9	0.266	0.413	27	0.266	0.425
10	0.641	0.417	28	0.391	0.433
11	0.469	0.406	29	0.281	0.421
12	0.000	FR	30	0.000	FR
13	0.000	FR	31	0.000	0.492*
14	0.141	0.425	32	0.094	0.469
15	0.391	0.441	33	0.125	0.461
16	1.016	0.413	34	0.156	0.461
17	0.750	0.429	35	0.156	0.469
18	0.000	FR	36	0.000	0.465*

*Should be unreadable
NOTE: Frame under points 1-6 is bent (damaged)

MEASUREMENT #17 (continued)

In-Plane View of Deformation

NOTE: Horizontal grid scale is 1 grid = 1 inch
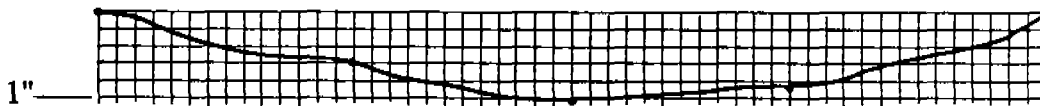Depth grid scale is 1 grid = 1/5 inch

Section through points 1-6
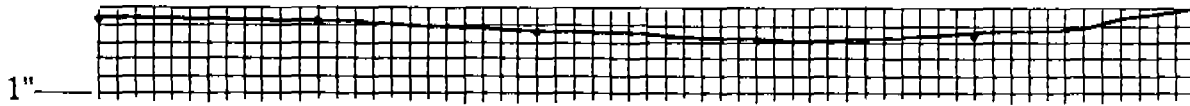
Section through points 7-12

Section through points 13-18

Section through points 19-24

Section through points 25-30

Section through points 31-36

A-63
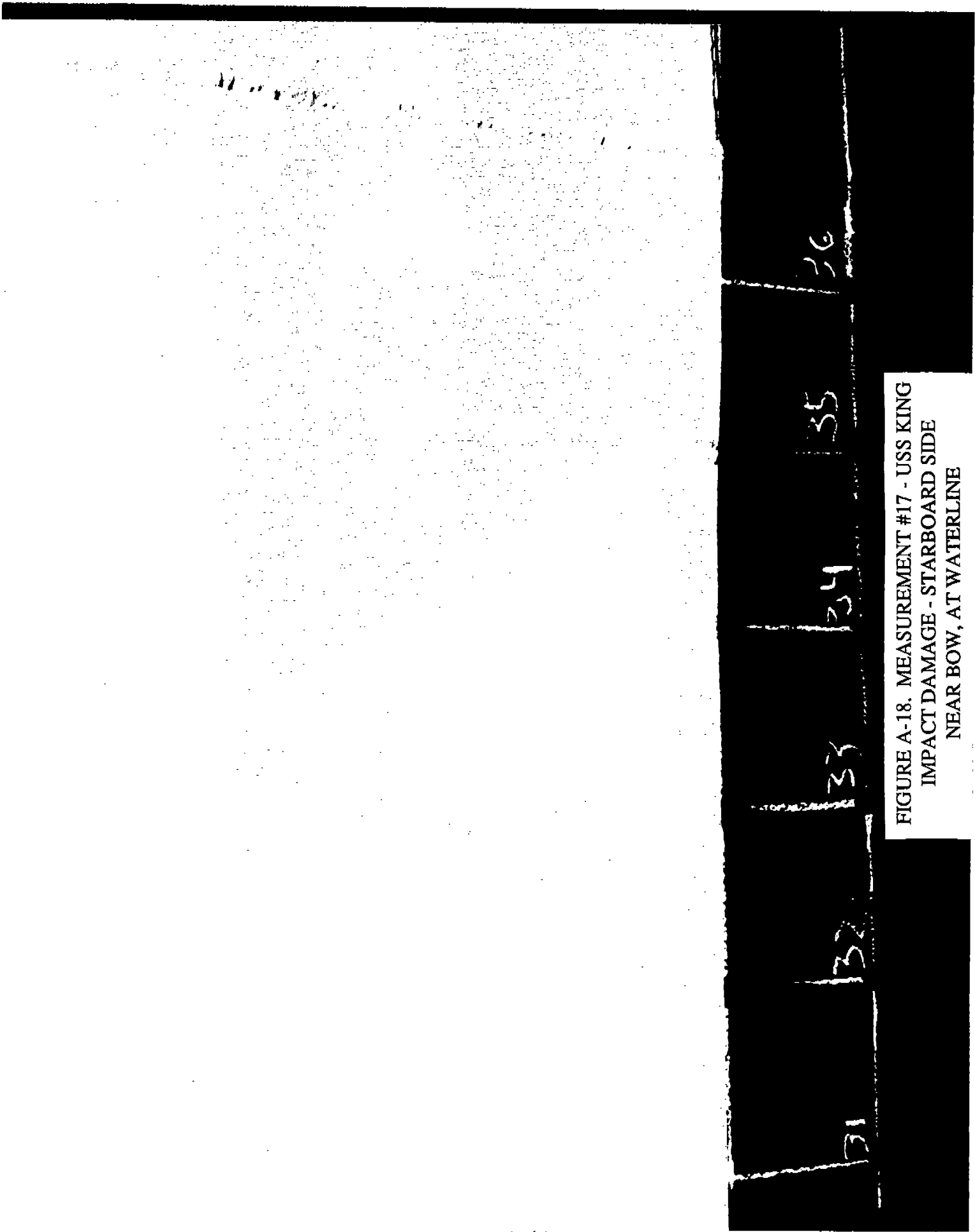
FIGURE A-18. MEASUREMENT #17 - USS KING
IMPACT DAMAGE - STARBOARD SIDE
NEAR BOW, AT WATERLINE

DATE: 9-12-89

LOCATION: Norfolk Naval Shipyard

SHIP: USS King, DDG-41

PLATE LOCATION:
  • General - Port, waterline, bow

PLATE SIZE:
  • "a" dimension = 60"
  • "b" dimension = 38"
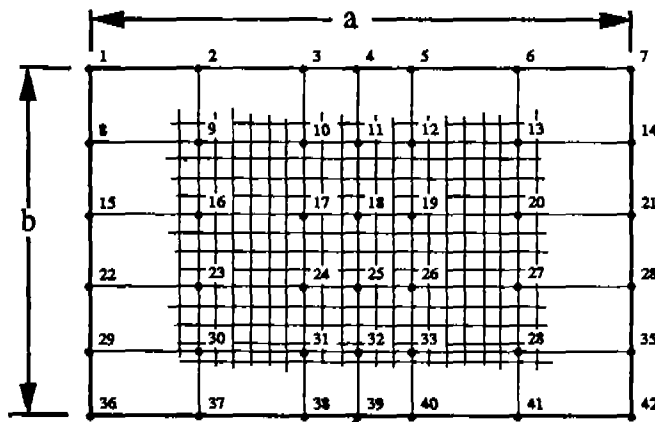
Scale 1 Grid = 2"

Middle frame is bent ——

Measurements were taken using straightedge method.
Accuracy is ±1/64". Thicknesses were obtained using
ultrasonic thickness gauge. Accuracy is ±0.003".

LOCATION	DEPTH READING	THICKNESS	LOCATION	DEPTH READING	THICKNESS
1	0.000	FR	22	0.000	FR
2	0.000	FR	23	0.375	0.453
3	0.000	FR	24	0.422	0.449
4	0.000	FR	25	0.281	FR
5	0.000	FR	26	0.422	0.457
6	0.000	FR	27	0.250	0.465
7	0.000	FR	28	0.000	FR
8	0.000	FR	29	0.000	FR
9	0.125	0.457	30	0.188	0.461
10	0.266	0.441	31	0.141	0.465
11	0.188	FR	32	0.000	FR
12	0.406	0.433	33	0.125	0.461
13	0.297	0.445	34	0.109	0.472
14	0.000	FR	35	0.000	FR
15	0.000	FR	36	0.000	FR
16	0.266	0.445	37	0.000	FR
17	0.828	0.437	38	0.000	FR
18	1.141	FR	39	0.000	FR
19	1.188	0.437	40	0.000	FR
20	0.594	0.445	41	0.000	FR
21	0.000	FR	42	0.000	FR

NOTE: Middle frame (points 11, 18, 25, 32) is bent

In-Plane View of Deformation

NOTE: Horizontal grid scale is 1 grid = 1 inch
      Depth grid scale is 1 grid = 1/5 inch

Section through points 1-6

NO DEFORMATION

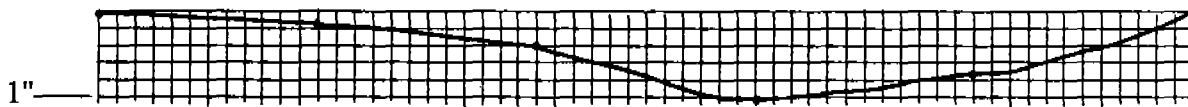Section through points 8-14
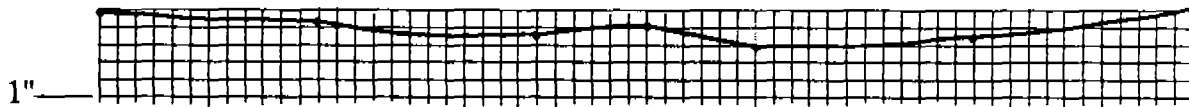
Section through points 15-21

Section through points 22-28

Section through points 29-35

Section through points 36-42

NO DEFORMATION
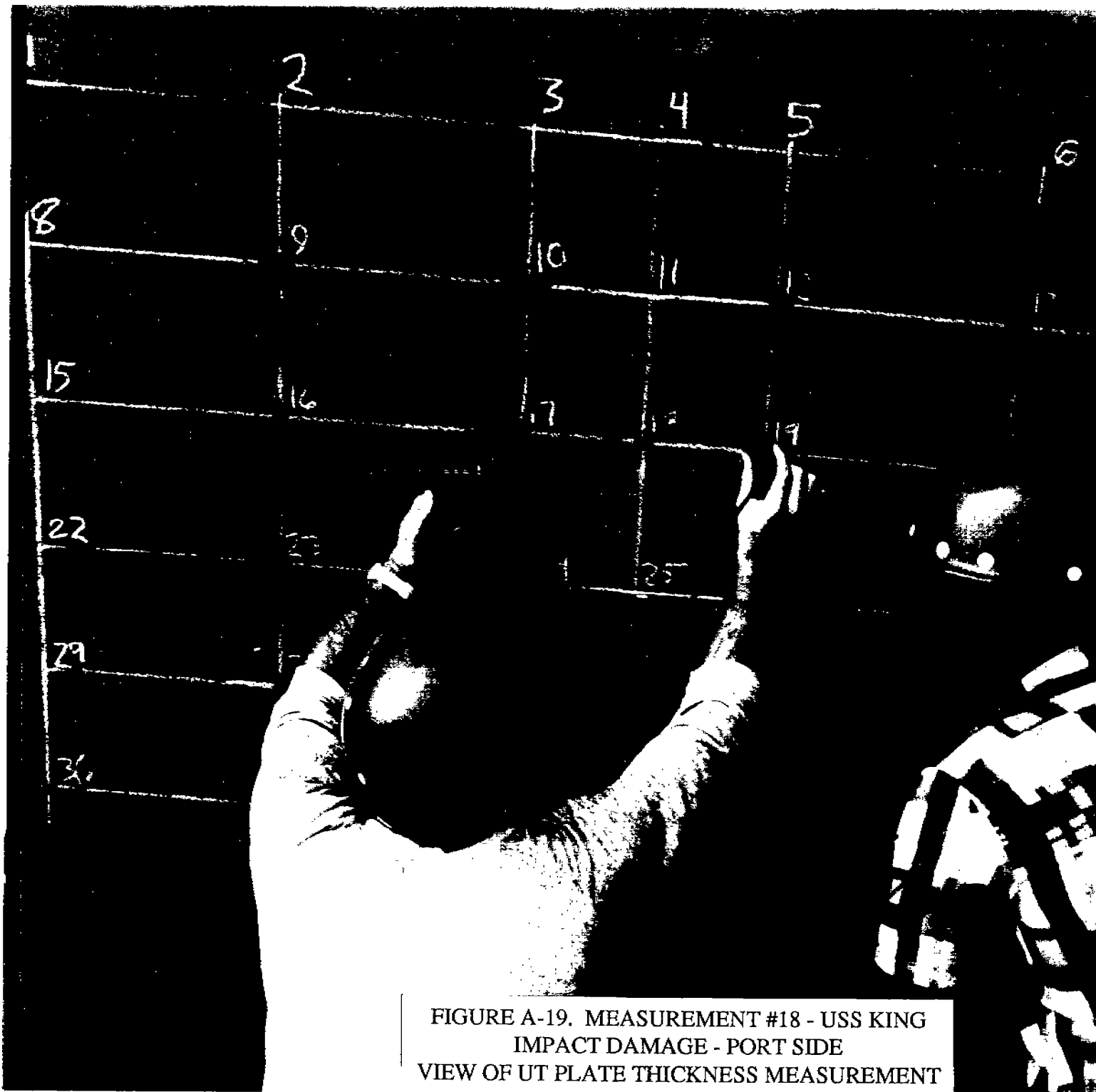
FIGURE A-19. MEASUREMENT #18 - USS KING
IMPACT DAMAGE - PORT SIDE
VIEW OF UT PLATE THICKNESS MEASUREMENT

DATE: 9-12-89

LOCATION: Norfolk Naval Shipyard

SHIP: USS Conyngham, DDG-17

PLATE LOCATION:
- General - Starboard bow, 1 ft. above waterline

PLATE SIZE:
- "a" dimension = 48"
- "b" dimension = 18"
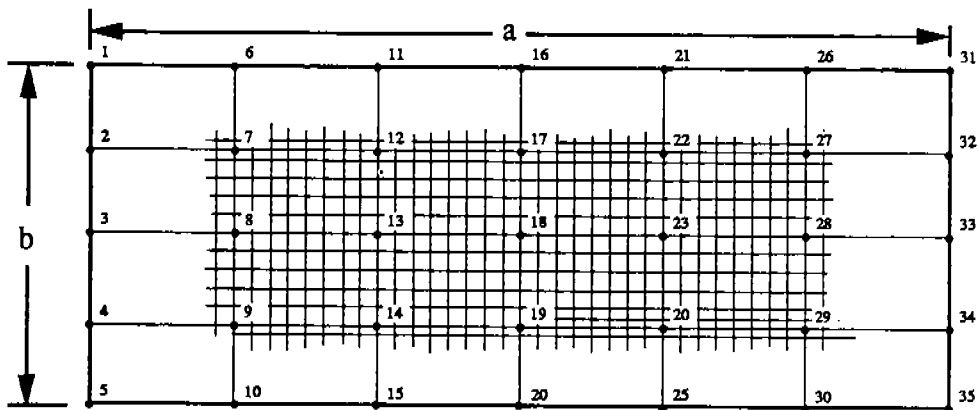
Scale: 1 Grid = 1"

Measurements were taken using straightedge method.
Accuracy is ±1/64". Thicknesses were obtained using
ultrasonic thickness gauge. Accuracy is ±0.003".

LOCATION	DEPTH READING	THICKNESS	LOCATION	DEPTH READING	THICKNESS
1	0.000	FR	19	0.100	0.429
2	0.091	FR	20	0.000	FR
3	0.124	FR	21	0.000	FR
4	0.085	FR	22	0.273	0.402
5	0.000	FR	23	0.408	0.413
6	0.000	FR	24	0.193	0.413
7	0.501	0.386	25	0.000	FR
8	0.622	0.406	26	0.000	FR
9	0.269	0.398	27	0.240	0.406
10	0.000	FR	28	0.317	0.421
11	0.000	FR	29	0.169	0.409
12	0.308	0.396	30	0.000	FR
13	0.393	0.406	31	0.000	FR
14	0.187	0.409	32	0.000	FR
15	0.000	FR	33	0.000	FR
16	0.000	FR	34	0.000	FR
17	0.232	0.374	35	0.000	FR
18	0.261	0.421			

NOTE: FR indicates that a frame at that location prevented a UT thickness reading.

In-Plane View of Deformation

NOTE: Horizontal grid scale is 1 grid = 1 inch
　　　 Depth grid scale is 1 grid = 0.1 inch

Section through points 1-31
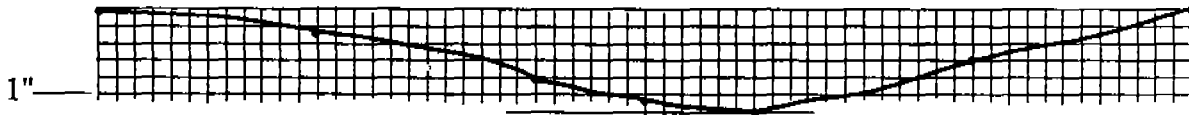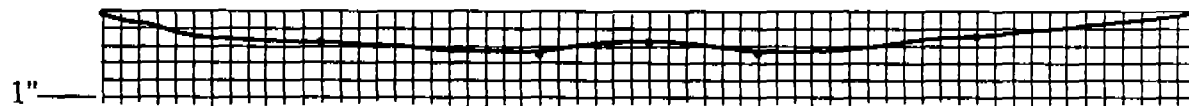
NO DEFORMATION

Section through points 2-32

.5" ——

Section through points 3-33

.5" ——

Section through points 4-34

.5" ——

Section through points 5-35

NO DEFORMATION

A-71

FIGURE A-20. MEASUREMENT #19 - USS CONYNGHAM
WAVE SLAP/IMPACT DAMAGE
STARBOARD SIDE, BOW, AT WATERLINE

DATE: 9-12-89

LOCATION: Norfolk Naval Shipyard

SHIP: USS Hayler, DD-997

PLATE LOCATION:
- General - Port, mid-hull, 1 ft. above waterline

PLATE SIZE:
- "a" dimension = 48"
- "b" dimension = 18"

Next frame
4' over

Scale: 1 Grid = 1"
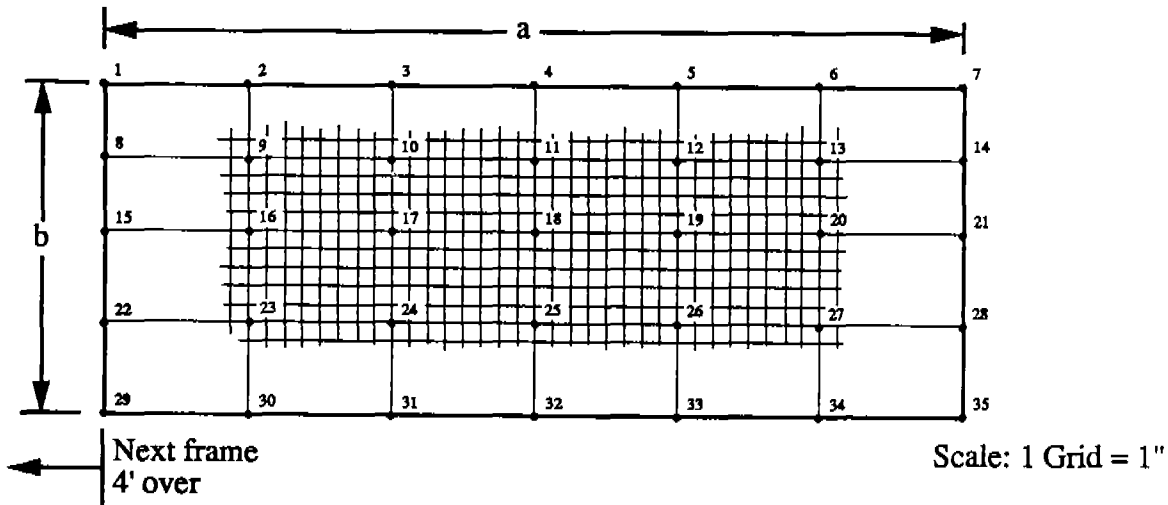
NOTE: 8' frame spacing at mid-hull only 1/2 of panel used since dent was on one half only. Longitudinal stiffeners 18" apart at mid-hull.
Measurements were taken using straightedge method. Accuracy is ±1/64". Thicknesses were obtained using ultrasonic thickness gauge. Accuracy is ±0.003".

LOCATION	DEPTH READING	THICKNESS	LOCATION	DEPTH READING	THICKNESS
1	0.000	FR	19	0.156	0.476
2	0.031	FR	20	0.063	0.492
3	0.219	FR	21	0.000	FR
4	0.156	FR	22	0.000	0.516
5	0.094	FR	23	0.063	0.488
6	0.000	FR	24	0.141	0.472
7	0.000	FR	25	0.125	0.496
8	0.000	*	26	0.063	0.492
9	0.203	0.476	27	0.031	0.457
10	0.969	0.409	28	0.000	FR
11	0.563	0.437	29	0.000	FR
12	0.188	0.437	30	0.000	FR
13	0.031	*	31	0.000	FR
14	0.000	FR	32	0.000	FR
15	0.000	*	33	0.000	FR
16	0.156	0.488	34	0.000	FR
17	0.469	0.465	35	0.000	FR
18	0.375	0.492			

Note: FR indicates that a frame at that location prevented a UT thickness reading
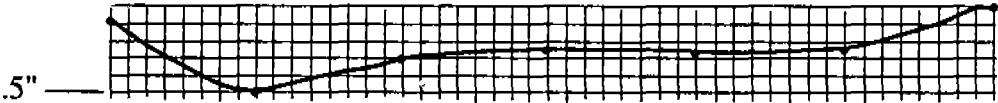* - Thickness measurements could not be obtained

In-Plane View of Deformation

NOTE: Horizontal grid scale is 1 grid = 1 inch
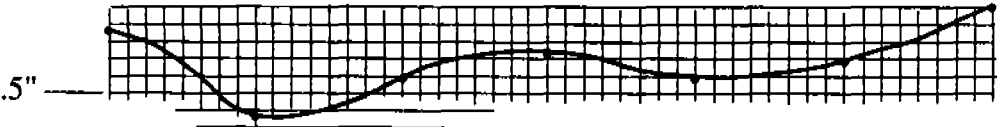   Depth grid scale is 1 grid = 0.125 inch

Section through points 1-7
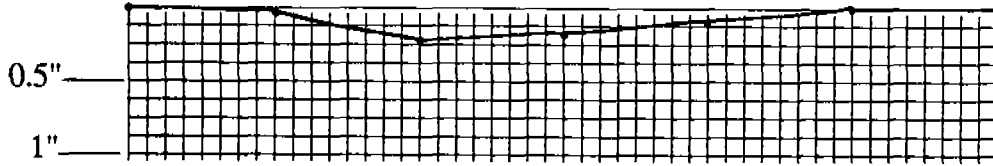
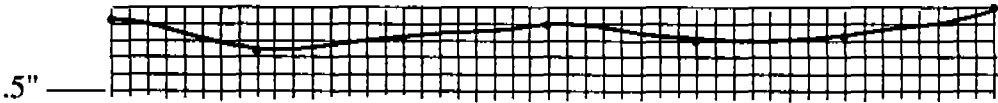Section through points 8-14

Section through points 15-21

Section through points 22-28

Section through points 29-35

NO DEFORMATION
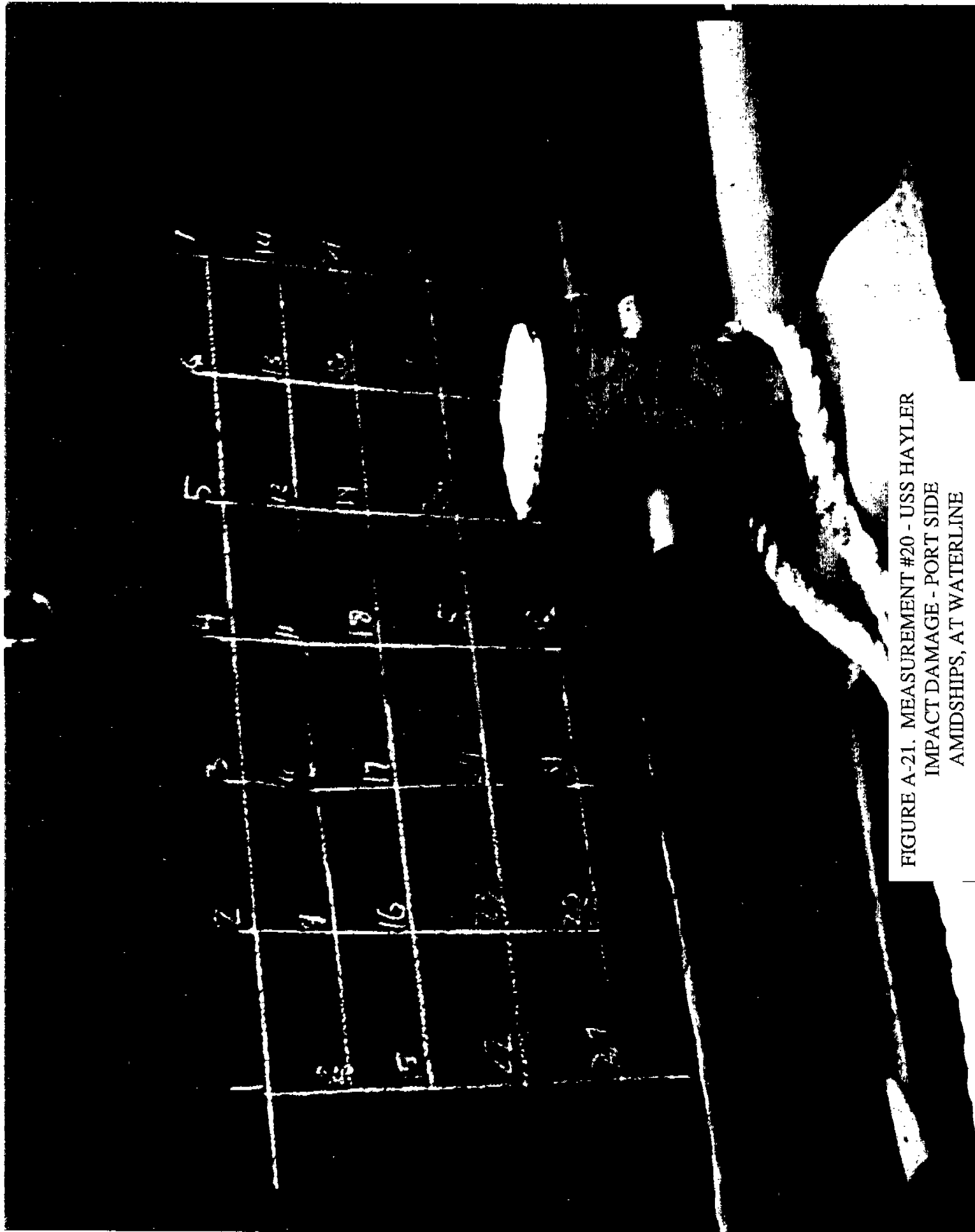
FIGURE A-21. MEASUREMENT #20 - USS HAYLER
IMPACT DAMAGE - PORT SIDE
AMIDSHIPS, AT WATERLINE

MEASUREMENT #21

DATE: 9-13-89

LOCATION: Norfolk Naval Shipyard

SHIP: USS Conyngham, DDG-17

PLATE LOCATION:
- General - Starboard , aft
- Specific - Frame 193

PLATE SIZE:
- "a" dimension = 52"
- "b" dimension = 29"
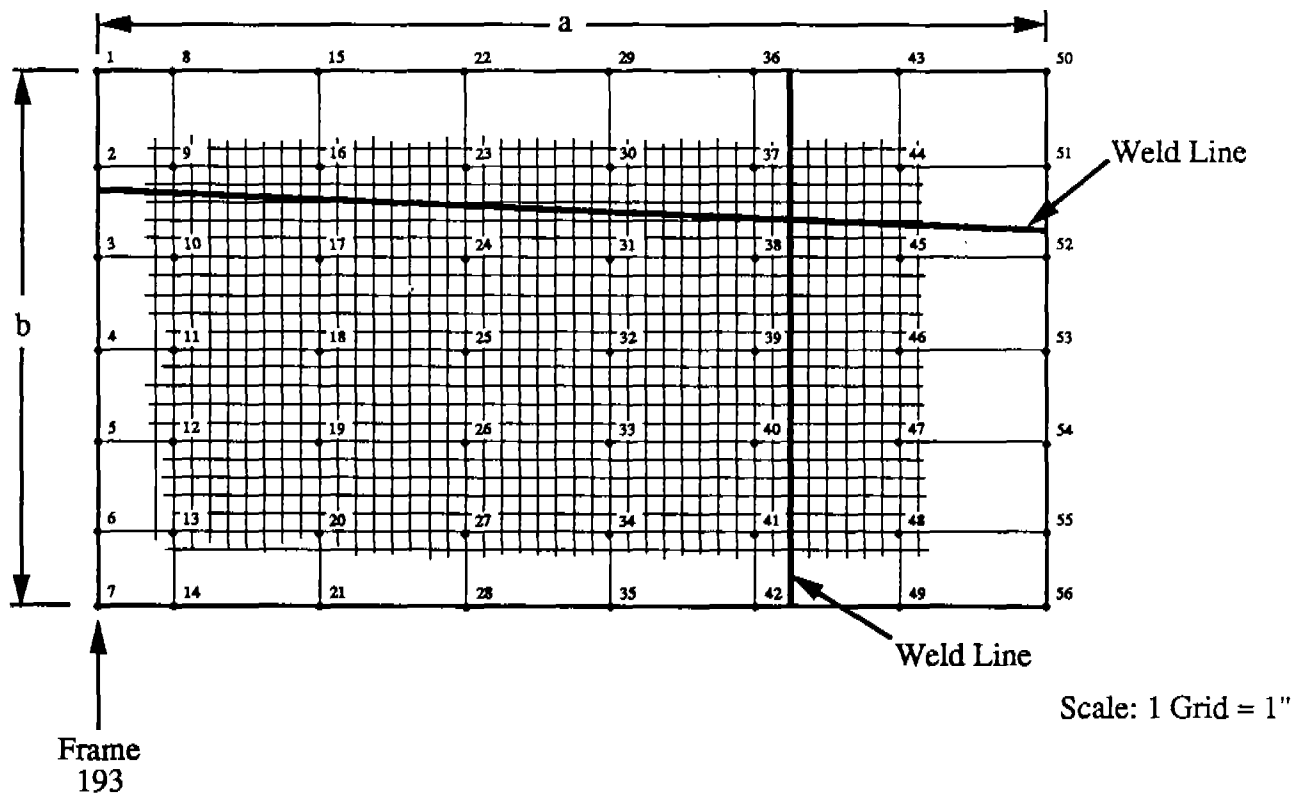
Scale: 1 Grid = 1"

Frame
193

Depth measurements were taken using straightedge method.
Accuracy is ±1/64". Thicknesses were obtained using
ultrasonic thickness gauge. Accuracy is ±0.003".

LOCATION	DEPTH READING	THICKNESS	LOCATION	DEPTH READING	THICKNESS
1	0.000	FR	20	0.234	0.484
2	0.344	FR	21	0.000	FR
3	0.656	FR	22	0.000	FR
4	1.016	FR	23	0.422	0.445
5	1.031	FR	24	0.875	0.500
6	0.438	FR	25	0.984	0.508
7	0.000	FR	26	0.625	0.488
8	0.000	FR	27	0.203	0.480
9	0.344	0.425	28	0.000	FR
10	0.638	0.524	29	0.000	FR
11	1.031	0.500	30	0.266	0.472
12	0.922	0.492	31	0.578	0.504
13	0.375	0.488	32	0.703	0.496
14	0.000	FR	33	0.453	0.504
15	0.000	FR	34	0.156	0.492
16	0.375	0.457	35	0.000	FR
17	0.781	0.500	36	0.000	FR
18	1.000	0.488	37	0.172	0.445
19	0.625	0.496	38	0.391	*

* - No reading available due to weld crossing

LOCATION	DEPTH READING	THICKNESS
39	0.516	0.516
40	0.453	0.512
41	0.172 ·	0.496
42	0.000	FR
43	0.000	FR
44	0.072	0.508
45	0.375	0.421
46	0.563	0.409
47	0.281	0.406
48	0.000	0.398
49	0.000	FR
50	0.000	FR
51	0.000	FR
52	0.000	FR
53	0.000	FR
54	0.000	FR
55	0.000	FR
56	0.000	FR

NOTE: All four plates that are welded together appear to have different thicknesses.
FR indicates that a frame prevented a UT thickness measurement

In-Plane View of Deformation

NOTE: Horizontal grid scale is 1 grid = 1 inch
Depth grid scale is 1 grid = 1/5 inch

Section through points 2-51

1"

Section through points 3-52

1"
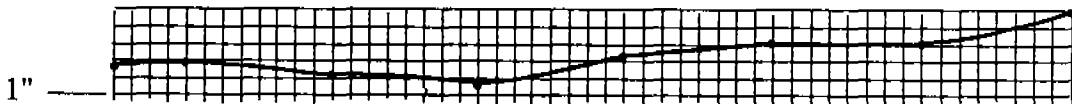
Section through points 4-53

1"

Section through points 5-54

1"

Section through points 6-55

1"
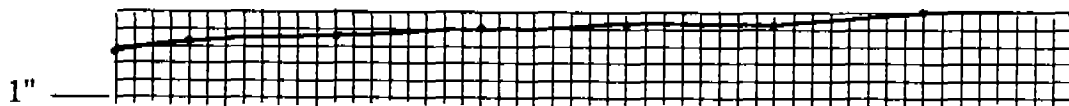
FIGURE A-22. MEASUREMENT #21 - USS CONYNGHAM
IMPACT DAMAGE - STARBOARD SIDE
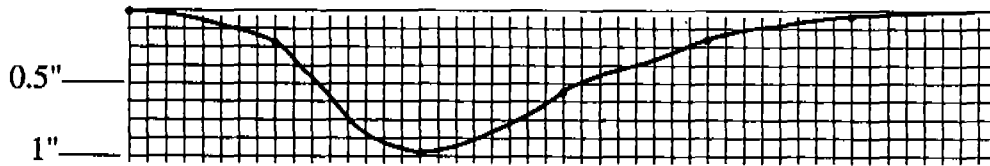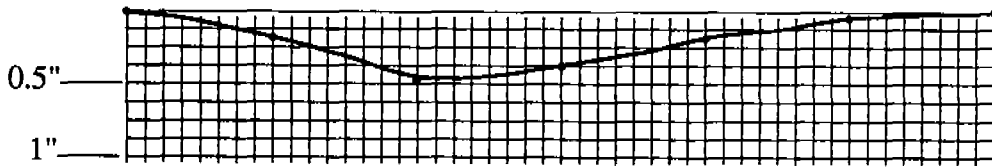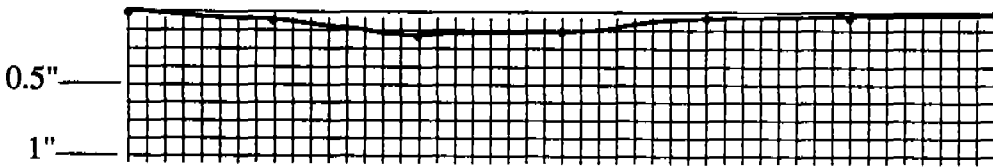AFT, AT WATERLINE

DATE: 9-13-89

LOCATION: Norfolk Naval Shipyard

SHIP: USS Hayler, DD-997

PLATE LOCATION:
   • General - Starboard , bow, 1 ft. above waterline

PLATE SIZE:
   • "a" dimension = 30"
   • "b" dimension = 24"

Depth measurements were taken using straightedge
method. Accuracy is ±1/64". Thicknesses were
obtained using ultrasonic thickness gauge. Accuracy
is ±0.003".

LOCATION	DEPTH READING	THICKNESS	LOCATION	DEPTH READING	THICKNESS
1	0.047	FR	22	1.688	0.417
2	0.072	FR	23	0.875	0.413
3	0.109	FR	24	0.000	FR
4	0.125	FR	25	0.000	FR
5	0.188	FR	26	0.297	0.409
6	0.156	FR	27	1.328	0.449
7	0.000	FR	28	2.109	0.433
8	0.281	0.488	29	0.906	0.461
9	0.422	0.516	30	0.000	FR
10	0.391	0.508	31	0.000	FR
11	0.219	*	32	0.297	FR
12	0.000	FR	33	1.141	FR
13	0.000	FR	34	1.797	FR
14	0.422	0.441	35	0.813	FR
15	0.891	0.413	36	0.000	FR
16	1.000	0.417	37	0.000	FR
17	0.578	0.441	38	0.328	0.406
18	0.000	FR	39	0.813	0.403
19	0.000	FR	40	1.031	0.429
20	0.313	0.402	41	0.625	0.421
21	1.281	0.402	42	0.000	FR

* - Eyelet in way

In-Plane View of Deformation

NOTE: Horizontal grid scale is 1 grid = 2 inch
      Depth grid scale is 1 grid = 0.25 inch

Section through points 1-6

1"

Section through points 7-12

1"

Section through points 13-18

1"

Section through points 19-24

1"

2"

Section through points 25-30

1"

2"

Section through points 31-36

1"

2"
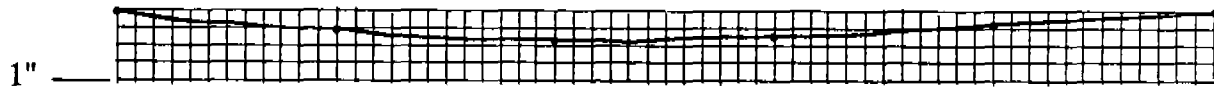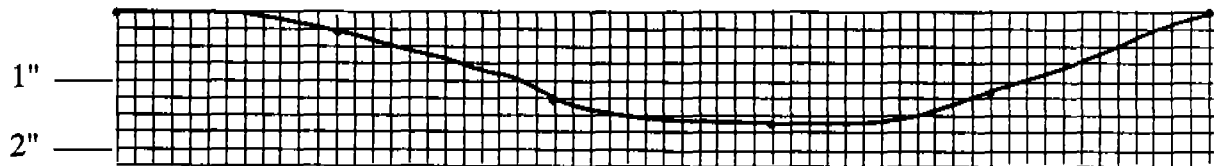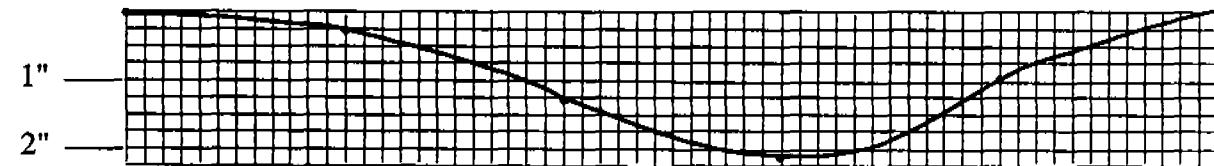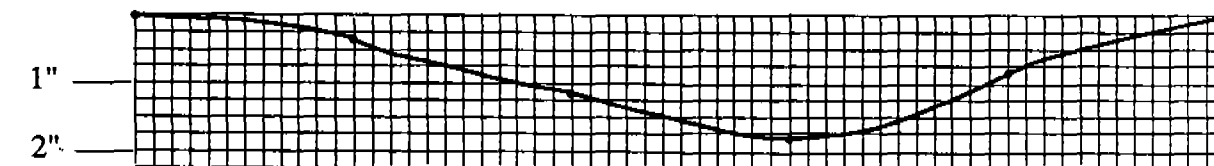
Section through points 37-42

1"
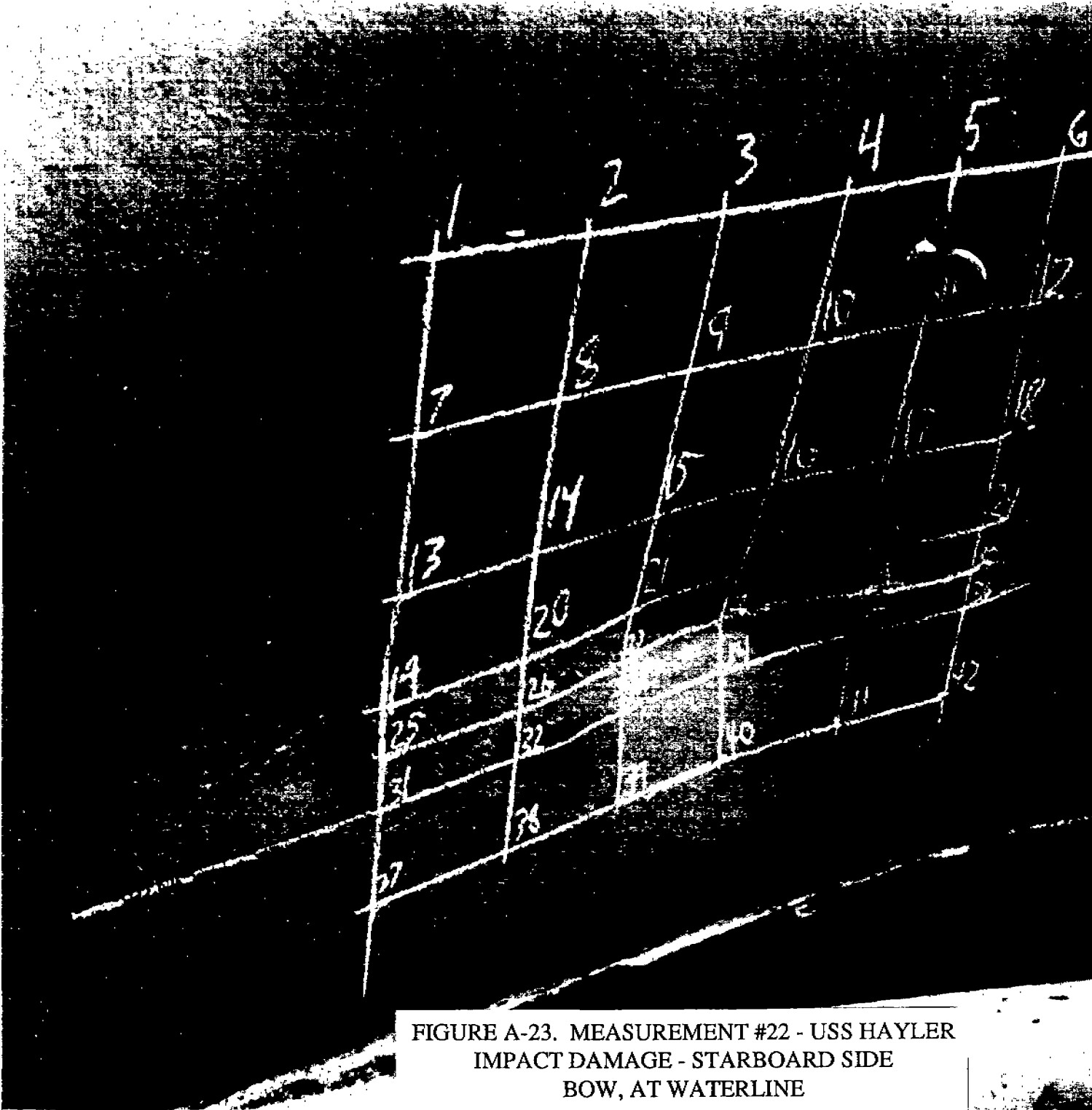
FIGURE A-23. MEASUREMENT #22 - USS HAYLER
IMPACT DAMAGE - STARBOARD SIDE
BOW, AT WATERLINE

DATE: 9-13-89

LOCATION: Norfolk Naval Shipyard

SHIP: USS Roosevelt, CVN-71

PLATE LOCATION:
- General - Starboard , elevator sponson, underside
- Deformation caused by wave slap

PLATE SIZE:
- "a" dimension = 24"
- "b" dimension = 39"
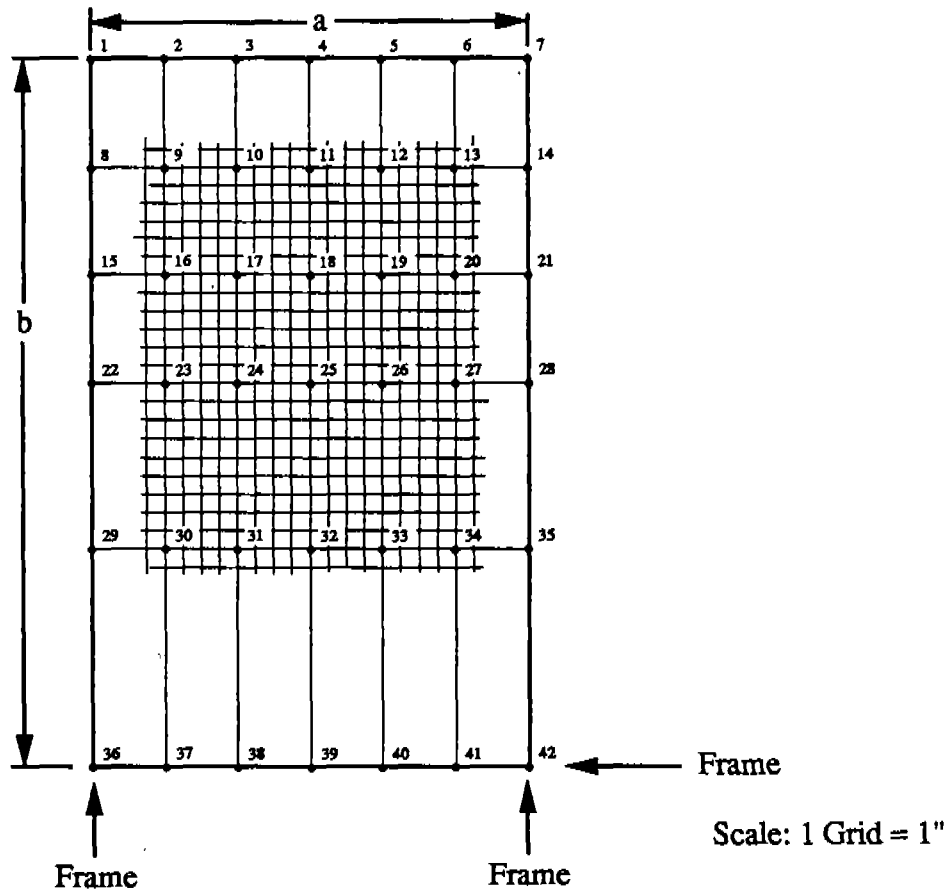
Depth measurements were taken using straightedge method. Accuracy is ±1/64". Thicknesses were obtained using ultrasonic thickness gauge. Accuracy is ±0.003".

LOCATION	DEPTH READING	THICKNESS	LOCATION	DEPTH READING	THICKNESS
1	0.000	FR	22	0.000	FR
2	0.109	0.354	23	0.072	0.331
3	0.188	0.339	24	0.156	0.323
4	0.219	0.335	25	0.172	0.331
5	0.172	0.339	26	0.141	0.331
6	0.125	0.343	27	0.047	0.323
7	0.000	FR	28	0.000	FR
8	0.000	FR	29	0.000	FR
9	0.109	0.335	30	0.031	0.327
10	0.203	0.331	31	0.094	0.315
11	0.219	0.331	32	0.109	0.323
12	0.172	0.299	33	0.094	0.315
13	0.094	0.346	34	0.047	0.315
14	0.000	FR	35	0.000	FR
15	0.000	FR	36	0.000	FR
16	0.063	0.335	37	0.000	FR
17	0.156	0.335	38	0.000	FR
18	0.188	0.327	39	0.000	FR
19	0.141	0.319	40	0.000	FR
20	0.072	0.323	41	0.000	FR
21	0.000	FR	42	0.000	FR

NOTE: FR indicates that a frame at that location prevented UT thickness measurements.

In-Plane View of Deformation

NOTE: Horizontal grid scale is 1 grid = 1 inch
        Depth grid scale is 1 grid = 0.05 inches

Section through points 1-7

0.25"——

Section through points 8-14

0.25"——

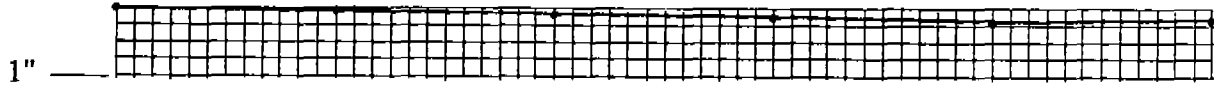Section through points 15-21

0.25"——

Section through points 22-28

0.25"——

Section through points 29-35

0.25"——
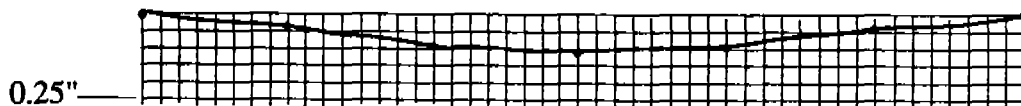
FIGURE A-24. MEASUREMENT #23 - USS ROOSEVELT
WAVE SLAP DAMAGE - STARBOARD SIDE
UNDERSIDE OF ELEVATOR SPONSON

FIGURE A-25. MEASUREMENT #23 - USS ROOSEVELT
VIEW SHOWING SPONSON PLATE MEASURED

A-89

APPENDIX B
Critical Strain Energy Density (SED$_c$) Model

Background

A review was made of the paper entitled "The Influence of Weld Metal Properties, Weld Geometry and Applied Load on Weld System Performance," by Peter Matic and Mitchell I. Jolles [19]. The paper reports the results of the computational prediction of the performance of the weld metal heat affected zone (HAZ) and parent material for an HY-100 steel weldment. The prediction includes the use of finite element stress analyses in determining the stress distribution in the weld, HAZ, and parent metal, the experimentally determined stress-strain behaviors including fracture point for each material zone, and the failure or fracture criteria based on the strain energy density concept for each material zone (there are four subzones in HAZ).

The finite element stress analyses for the system uses a rather extensive detailed elastic-plastic analyses available on ABAQUS code. The localized areas of interest, i.e. weld, HAZ, and adjacent parent material, have very fine 2D plane strain elements so that the stress field in these areas can be described in great detail. The degree of difficulty in determining the stress field in an element depends upon the complexity of the geometry. If a single material is used in conjunction with a simple geome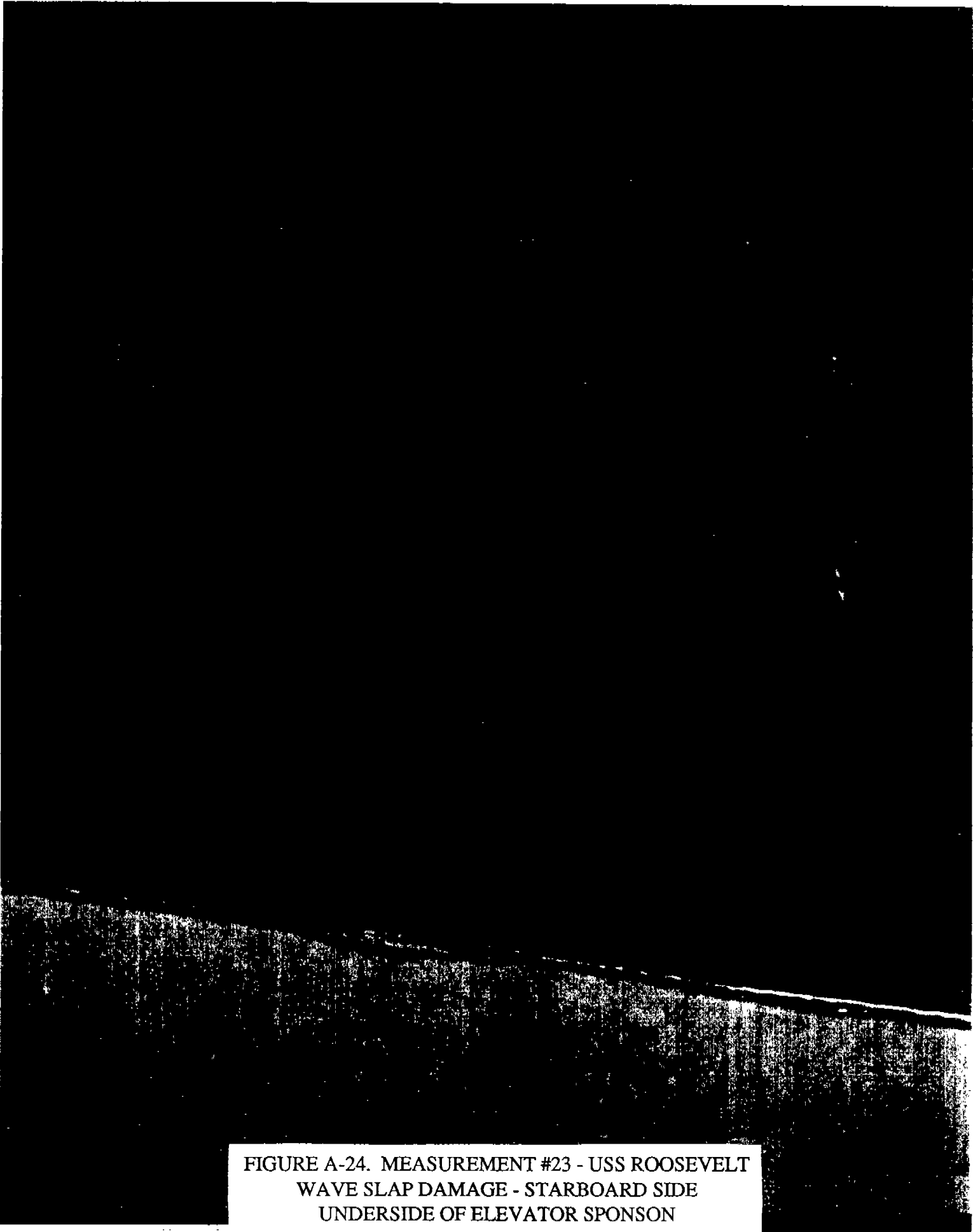try, the stress field may be expressed by closed form solutions derived from strength of material considerations and/or the theory of elasticity. As the material characteristics and geometric configuration becomes more complicated, the use of detailed finite element analyses becomes inevitable. Since a complete stress distribution is needed in conjunction with the strain energy density function to assess the fracture of constituent materials, the finite element analysis can be time consuming, and in many cases, costly.

The strain energy density function concept for predicting the fracture of materials was proposed by Sih [20]. The strain energy per unit mass in a material is expressed as:

$$W = \int_0^{\varepsilon_{11}} \frac{\sigma_{11}\, \delta\varepsilon_{11}}{\rho} + \int_0^{\varepsilon_{22}} \frac{\sigma_{22}\, \delta\varepsilon_{22}}{\rho} + \int_0^{\varepsilon_{33}} \frac{\sigma_{33}\, \delta\varepsilon_{33}}{\rho}$$
$$+ \int_0^{\varepsilon_{12}} \frac{\sigma_{12}\, \delta\varepsilon_{12}}{\rho} + \int_0^{\varepsilon_{23}} \frac{\sigma_{23}\, \delta\varepsilon_{23}}{\rho} + \int_0^{\varepsilon_{31}} \frac{\sigma_{31}\, \delta\varepsilon_{31}}{\rho} \qquad \text{(B-1)}$$

Where σ_{ij} and ε_{ij} (i, j = 1, 2, 3) are the six stress and strain fields, and ρ is the density of the material. The function W then represents the strain energy per unit mass of material. For most engineering material, the density is, however, more or less invariant. Therefore, one can use SED = W$_v$ to represent the strain energy per unit volume, or Strain Energy Density, without losing any accuracy.

The fracture characteristics are based upon the uniaxial stress-strain curves including fracture for each of the materials of interest. It is assumed that the nonlinear (or plastic) behavior of the material under combined stress field can be predicted from the uniaxial stress-strain curve using

Prandl-Ruess or effective stress-strain relations. Based on this, it is possible to obtain a critical value of SED, called SED_c, for each material at which the material is supposed to fracture. For a system with many elements such as that described by finite element analysis, the SED value of each element can be numerically determined under a given external load or internal thermomechanical load. The maximum load carrying capability of a system can then be predicted by calculating the SED values as a function of applied load until a load level is reached such that the corresponding SED value of an element attains the SED_c value of the material.

In other words:

$$\left(\frac{SED}{SED_c}\right)_N = 1 \qquad N = N_c \quad (N_c \text{ is the element } N_o)$$

$$\left(\frac{SED}{SED_c}\right)_N < 1 \qquad \text{for all } N \text{ not equal to } N_c$$

The strain energy density approach assumes all material media to be homogeneous. The stress concentration due to any defects or imperfections in the materials can be calculated by the use of finite element models. For example, a void in the material will be realized by the modeling and the stress singularity at the vicinity of the void can be predicted accurately by a finite element model or a closed form expression. However, this approach has little to do with the microstructure or crystalinity of the material and therefore the physical meaning of fracture may be lost in the mathematical exercises.

In addition, for a structural configuration where local defects such as cracks, flaws, or voids are presented, a much more detailed stress calculation must be performed before a fracture assessment can be done. This can be time consuming and costly. For this situation, the more traditional fracture mechanics approach seems more suitable for fracture prediction.

The advantage of the fracture toughness and J-integral approaches is that only the far field stress field is required for fracture prediction. This eliminates the need to obtain the stress field at the vicinity of the imperfection, and is therefore less costly and more time efficient. However, for a structure with several dissimilar materials and no apparent localized imperfection, the strain energy density function may be more appropriate despite the fact that lengthy stress calculation need to be performed.

Sih has proposed the use of strain energy density in predicting crack growth in two and three dimensional media. There are three hypotheses used in his proposal:

1. The direction of crack propagation at any point along the crack border is toward the region with the minimum value of the strain energy density factor, S, as compared with other regions on the same spherical surface surrounding the point.
2. Crack extension occurs when the strain energy density factor in the region determined by hypothesis 1, S = S(min). reaches a critical value, say S_{cr}.
3. The length, r_o, of the initial crack extension is assumed to be proportional to S(min) such that $S(min)/r_o$ remains constant along the crack front.

The strain energy density factor S is defined as:

$$\frac{dW}{dV} = \frac{S}{r} \qquad \text{(B-2)}$$

and

$$S = a_{11}(K_1{}^2) + 2a_{12}(K_1 K_2) + a_{22}(K_2{}^2) + a_{33}(K_3{}^2) \qquad \text{(B-3)}$$

It can be seen that Sih still uses the stress intensity factors in determining the stress distributions at the crack tip. The only difference in the crack extension criteria between his theory and the "conventional" theory is that Sih proposes that crack propagation occurs when the strain energy density factor reaches a critical value, while the latter proposes that crack propagation starts when the stress intensity factor at the crack tip reaches a critical value. It is to be noted that for either a homogeneous medium or one with a crack, the same strain energy density concept is used (FUNCTION for a homogeneous medium and FACTOR for a medium with crack). The stress fields have to be determined by either a finite element analysis or through other closed form expressions (such as the crack tip stress distributions).

Application of SED_c Model To Ship Steel

The strain energy density criterion is related to the area under the stress strain curve. To evaluate the effect of prestrain, the area of the curve representing the percent cold work must be subtracted from the total area. The integration of the true stress -true strain curve was used to estimate the residual toughness after 15% prior plastic strain. As will be shown, this amount of cold work represents about 5% of the total area under the curve for Sample A2 steel and 11% for the Sample B2 steel. The calculations are as follows:

$$\sigma = \sigma_0\, \varepsilon^n \qquad\qquad 0 \le \varepsilon \le \varepsilon_{uts}$$

$$\text{and}$$

$$\sigma = \sigma_0{}' + m\varepsilon \qquad\qquad \varepsilon_{uts} \le \varepsilon \le \varepsilon_c$$

therefore,

$$SED_c = \int_0^{\varepsilon_c} \sigma\, d\varepsilon = \sigma_0 \int_0^{\varepsilon_{uts}} \varepsilon^n\, d\varepsilon + \int_{\varepsilon_{uts}}^{\varepsilon_c} (\sigma_0{}' + m\varepsilon)\, d\varepsilon \qquad \text{(B-4)}$$

$$SED_c = \frac{\sigma_0\, \varepsilon_{uts}{}^{n+1}}{n+1} + \sigma_0{}' (\varepsilon_c - \varepsilon_{uts}) + \frac{m\, (\varepsilon_c{}^2 - \varepsilon_{uts}{}^2)}{2}$$

$$\text{where } \varepsilon_c = \varepsilon_f = \ln\left(\frac{1}{1 - RA}\right) \qquad \text{(B-5)}$$

where RA = Reduction in Area from the ASTM E8 tensile test [21]. The criterion for failure is the condition where any element in the finite element network attains a critical strain energy density value (SEDc).

For a uniform, homogeneous steel plate loaded in bending, the effect of prior plastic strain can be estimated as:

$$SED_{15\%} = \frac{\sigma_0\, \varepsilon_{15\%}^{n+1}}{n+1} \qquad\qquad (B\text{-}6)$$

where $\varepsilon_{15\%}$ = true strain corresponding to a deformation of 15%. The remaining strain energy density (residual toughness), as a percentage of the original strain energy density, would then be expressed as:

$$SEDc_R(\%) = \frac{SED_c - SED_{15\%}}{SED_c} \qquad\qquad (B\text{-}7)$$

This estimate would also apply to a more complex geometry. For different weld metal zones, a similar calculation would have to be made for each zone.

From the results of the tensile tests on the two plates of ABS-B ship steel, an estimate was made of the critical strain energy density, SED_c, on the basis of the area under the uniaxial stress-strain curve.

For the Sample A plate, the area representing 14% deformation was subtracted from the total area under the stress-strain curve to account for the effects of a 14% prestrain. The maximum prestrain was limited to 14% for Sample A since the test data showed that the strain at ultimate was 15%. A maximum prestrain of 15% was assumed for the Sample B plate. The results of the SED_c analysis are as follows:

Sample A:

$$\sigma_0 = 119467 \text{ psi} \qquad m = 76804$$

$$n = 0.167 \qquad \varepsilon_c = 1.378$$

$$\sigma_o' = 75064 \text{ psi} \qquad \varepsilon_{uts} = 0.139$$

$$SED_c = \frac{119467 \, (0.139)^{1.167}}{1.167} + 75064 \, (1.378 - 0.139)$$

$$+ \frac{76804 \, (1.378^2 - 0.139^2)}{2}$$

$$SED_c = 175,414 \, \frac{\text{in-lbs}}{\text{in}^3}$$

For $\varepsilon_{14\%} = 0.131$

$$SED_{14} = \frac{119467 \, (0.131)^{1.167}}{1.167}$$

$$SED_{14} = 9,551 \, \frac{\text{in-lbs}}{\text{in}^3}$$

$$SED_{cR} = \frac{175414 - 9551}{175414} = 0.946$$

Residual Toughness

SED_{cR} = 0.946 for Sample A

Sample B:

$\sigma_0 = 138835$ psi $m = 77092$

$n = 0.203$ $\varepsilon_c = 0.891$

$\sigma_o' = 83481$ psi $\varepsilon_{uts} = 0.162$

$$SED_c = \frac{138835\ (0.162)^{1.203}}{1.203} + 83481\ (0.891 - 0.162)$$

$$+ \frac{77092\ (0.891^2 - 0.162^2)}{2}$$

$$SED_c = 103,368\ \frac{in\text{-}lbs}{in^3}$$

For $\varepsilon_{15\%} = 0.140$

$$SED_{15} = \frac{138835\ (0.140)^{1.203}}{1.203}$$

$$SED_{15} = 10,840\ \frac{in\text{-}lbs}{in^3}$$

$$SED_{cR} = \frac{103368 - 10840}{103368} = 0.895$$

Residual Toughness

$SED_{cR} = 0.895$ for Sample B

These results indicate that steel sample A2 displays higher residual toughness than steel sample B2 after prior plastic strain. In addition, a comparison between the critical strain energy density of the two steel samples of as-received ABS ship steel shows that the critical strain energy density (SED_C) for Sample B2 was only about 59% of the critical strain energy density for Sample A2. In other words, there was a considerable variation in critical strain energy density for the two samples of ABS ship steel.

APPENDIX C

Strain Energy Density Fracture Mechanics (SED$_{FM}$) Model

Background

Tensile testing is by far the most routine, inexpensive mechanical test method, short of impact testing, and is currently used by a large number of test laboratories. Ductility ratio based on %RA is a commonly used toughness parameter, but it has limited applicability. Only stress intensity parameters in conjunction with NDE techniques can be used quantitatively to calculate maximum operating service that will confidently assure life in a specified environment. Estimating a stress intensity parameter from a tensile test has many obvious advantages and many models are available for estimating K_{Ic} from tensile data but they are generally empirical and therefore restricted in use to a particular material or strength level. The model that was found to be most adaptable to handling a variety of materials over a wide range of strength is that proposed by Bockrath and Glasco [22].

The difference between the proposed model and conventional J-integral analysis is (1) the estimation of the size of a damage zone at the tip of a crack, and (2) the use of the strain energy density from UTS to the fracture strength to calculate the total energy at the crack tip. This zone is characterized by localized plastic deformation that includes micro-void coalescence (MVC) and is therefore not necessarily a constant volume process.

Referring to Figure C.1, the damage zone is nested inside the zone of uniform plastic yielding, where the metal is stressed above its yield point but below UTS. In this region, plastic deformation is fairly well understood. The metals volume and Poisson's ratio is constant.

Its flow behavior is accurately described by an exponential function with a constant strain hardening coefficient, and the octahedral shear stress accurately translates uniaxial deformation into bi-axial and tri-axial deformation. This makes the metal's behavior in this zone amenable to analysis.

The inner zone, the damage zone, corresponds to the region of the stress strain curve where necking occurs. This region is not accurately described by plasticity models. Void growth can cause a variable density and Poisson's ratio. The strain hardening coefficient is not constant and the octahedral shear stress does not accurately describe deformation.

The two plastic zones correspond to different locations on the true-stress true-strain curves as shown in Figure C.2, where the different strain energy densities are illustrated relative to their location on the engineering and true-stress true-strain curve. Examining the true stress-true strain curve of Figure C.2 shows that typically the majority of the plastic strain energy density is under the stress-strain curve after necking occurs or UTS.

Therefore, two analytically different plastic zones exist; (1) uniform plastic deformation zone and the (2) DZ or damage zone. The plastic strain energy absorbed at the crack tip is then the sum of the two zones.

The plastic energy absorbed in the uniform zone, U_u, during crack growth is evaluated by determining the local strain energy density absorbed in an elemental volume and integrating around the crack tip where the stress is between yield stress and ultimate stress.
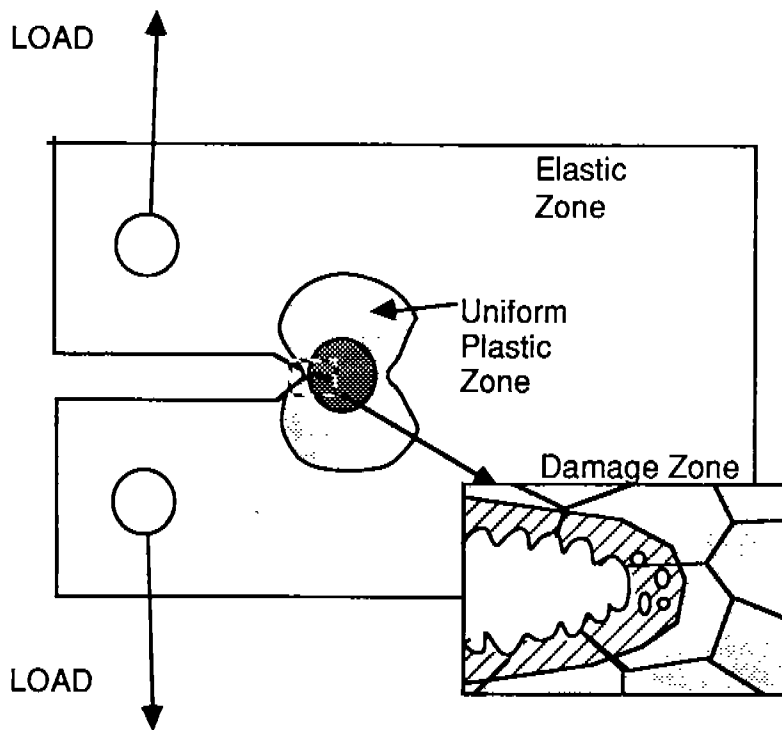
C-1

Figure. C.1 Characterization of the Stress-Strain Field in Front of a Crack Showing the
Elastic, Uniform Plastic, and Damage Zone as Related to True-Stress-Strain
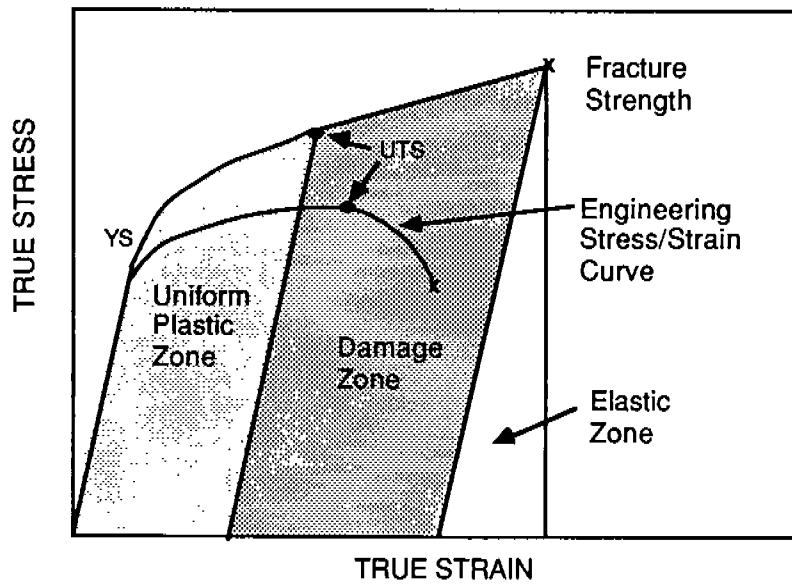Curve in Figure C.2

Figure C.2. Typical True Stress-Strain Curve Showing the Strain Energy Density Under the
Curve, and the Zones Relating to the Strain Field in Front of a Crack Tip as
Shown in Figure C.1

The plastic energy absorbed in the damage zone, U_f, during crack growth has been empirically related to the strain energy density from ultimate stress to fracture. Unstable crack growth occurs when the total plastic energy absorbed in the two zones is less than the elastic energy released during crack growth, U_e.

$$U_e = (\pi \sigma^2 c)/E \geq (U_f + U_u) \qquad (C\text{-}1)$$

Solving for half crack length

$$c = E (U_f + U_u) / \pi \sigma^2 \qquad (C\text{-}2)$$

Application Of SEDFM Model To Ship Steel

Since only tensile data for the as-received material was available, in order to estimate the effects of prestrain on the fracture properties the effects of prestrain on the tensile properties had to be estimated. Three key properties would change when the material is plastically deformed, the yield stress, the strain at ultimate, and the RA. The reasoning behind this is that if a sample of the as-received material were to be strained to some value (say 10%) and the load released, when the load was reapplied, the sample would deform elastically until the stress reached the maximum stress previously applied. The stress-strain curve would then approximately follow the same curve as the as-received material from there to fracture. Since nothing was done to the sample that is not normally done during a tensile test, the UTS and FS would remain the same. However, the "new", strained material would display a larger yield stress, and the strain between yield and ultimate would be reduced. In addition, since the sample was plastically deformed, its cross section was reduced, so the RA of the "new" material would also be reduced to some extent.

In order to estimate the new yield strengths for materials deformed by 5%, 10% and 15%, an exponential curve was fit between the yield and the ultimate for the as-received material, and the stress for the desired strains was calculated. The effect of the elastic component is on the order of 0.2%, which is small when compared to the desired strains, and was ignored for computational simplicity.

The strain at ultimate for the three conditions was estimated by subtracting the prestrain directly from the strain at ultimate measured for the as-received material. The "original" area used to calculate the RA for the strained material is determined by the amount the material was strained. The relationship between the "new" RA, the prestrain, and the RA of the as received material is:

$$RA_{new} = 1 - (1 + \varepsilon)(1 - RA) \qquad (C\text{-}3)$$

where RA_{new} is the calculated reduction in area for the prestrained material, ε is the amount of prestrain and RA is the reduction in area of the as-received material.

Since the strain at ultimate for S/N A2 in the as-received condition was 15%, the maximum prestrain used for calculation was 14%.

Tables C.1a and C.1b list the tensile data measured for the two steel specimens evaluated. Tables C.2a and C.2b list the estimated values for yield strength, strain at ultimate, and reduction in area for samples with 5%, 10% and 14% prestrain for Sample A2, and 5%, 10% and 15% prestrain for Sample B2. The data relating percent prestrain to fracture stress is plotted in Figures 5.5a and 5.6a for the Sample A2 material and in Figures 5.5b and 5.6b for the Sample B2 material. Tables 5.3a and 5.3b list the estimates for K_{Ic} and the Damage Tolerance Index (DTI = K_{Ic}/YS) for the two steel samples for the various amounts of prestrain. Also listed in these tables is the

minimum thickness for plane strain $\{B_{Ic} = 2.5\,(DTI)^2\}$ in accordance with ASTM E399 and the maximum thickness for 100% ductile shear ($B_c = 0.4\,B_{Ic}$).

Table C.1a. Tensile Properties Steel A

Yield Strength (ksi)	61.4
Ultimate Strength (ksi)	74.9
Fracture Strength (ksi)	44.2
Strain at Ultimate (%)	15.0
Reduction in Area (%)	74.8

Table C.1b. Tensile Properties Steel B

Yield Strength (ksi)	58.6
Ultimate Strength (ksi)	81.9
Fracture Strength (ksi)	62.5
Strain at Ultimate (%)	17.6
Reduction in Area (%)	59.0

Table C.2a. Estimated Effect of Prestrain on Tensile Properties for Sample A

Prestrain (%)	0.00	5.00	10.00	14.00
Yield Strength (ksi)	61.40	71.20	73.5	74.60
Strain at Ultimate (%)	0.15	0.10	0.05	0.01
Reduction in Area (%)	74.80	73.50	72.30	71.30

Table C.2b. Estimated Effect of Prestrain on Tensile Properties for Sample B

Prestrain (%)	0.00	5.00	10.00	15.00
Yield Strength (ksi)	58.60	74.50	78.50	80.90
Strain at Ultimate (%)	.176	0.126	0.076	0.026
Reduction in Area (%)	59.00	56.90	54.90	52.80

REFERENCES

1. "Japanese Shipbuilding Quality Standard (Hull Part). " Society of Naval Architects of Japan, Tokyo, Japan, 1982.

2. "Rules for Building and Classing Steel Vessels. "American Bureau of Shipping, Paramus, New Jersey, 1988.

3. Kmiecik, M., "A Review of Fabrication Distortion Tolerances for Ship Plating in the Light of the Compressive Strength of the Plates. " Lloyd's Register Technical Association, Paper No. 6 Session 1986-87.

4. "Rules for the Construction and Classification of Steel Ships. " Det Norske Veritas Oslo, Norway, II Sec. 8, 1977.

5. Basar, N. S. and Stanley, R. F., "Survey of Structural Tolerances in the United States Commercial Shipping Industry. "Ship Structure Committee Report SSC-273, 1978.

6. "Record." American Bureau of Shipping Baltimore, Maryland: Port City Press, 1988.

7. Capt. Richard Sharpe, RN, Janes Fighting Ships 1989-90. Surrey, UK, 92nd ed., 1989.

8. Popov, E.P., Mechanics of Materials, 2nd ed., Englewood Cliffs, N.J.: Prentice-Hall, Inc., 1976.

9. COSMOS/M Finite Element Program, Version 1.6, June 1990. Developed by Structural Research and Analysis Corporation, Santa Monica, California.

10. MSC/NASTRAN Finite Element Program, Version 65. Developed by MacNeal - Schwendler Corporation, Los Angeles, California.

11. "ADINA - A Finite Element Program for Automatic Dynamic Incremental Nonlinear Analysis", Report ARD 87-1, December, 1987. Developed by ADINA R&D, Inc. Watertown, MA.

12. "Test Method for Plane-Strain Fracture Toughness of Metallic Materials," ASTM E399.

13. "Standard Test Method for J_{Ic}, a Measure of Fracture Toughness," ASTM E813-88.

14. "Methods for Crack Opening Displacement (COD) Testing," The British Standards Institution, BS 5762:1979.

15. "Standard Practice for R-Curve Determination," ASTM E561-86.

16. "Guidance on Some Methods for the Derivation of Acceptance Levels for Defects in Fusion Welded Joints," British Standards Institution PD6493, 1980.

17. Naval Sea Systems Command Contract N00024-86-C-4219, TI No. 5C4551, "Underwater Dry Habitat Welding and Testing - Phase 2 Certification of Structural Performance of Weldments," Reports 4551/1 of 30 September 1988.

18. MIL-S-22698B AMEND 1 of 2 November 1982, "Steel Plate and Shapes, Weldable Ordinary Strength and Higher Strength: Hull Structural".

19. Matic, P., and Jolles, M.I., "The Influence of Weld Metal Properties, Weld Geometry, and Applied Load on Weld System Performance," *Naval Engineering Journal*, March 1988.

20. Sih, G.C., "The Strain Energy Density Fracture Concept and Criterion," *Journal of the Aeronautical Society of India*, Vol 37, No. 1, 1985

21. "Standard Methods of Tension Testing of Metallic Materials," ASTM E8-89.

22. Bockrath, G.E., Glassco, J.B., " A Method of Calculating R-Curves from Uniaxial Tensile Stress-Strain Curves," Presented at ASTM E-24 meeting, Louisville, Kentucky, March 18, 1980.

BIBLIOGRAPHY

1. Irwin, G.R., de Wit, Roland, "A Summary of Fracture Mechanics Concepts," the American Society for Testing and Materials, 1983, pp. 56-65.

2. Liu, H.W., "On the Fundamental Basis of Fracture Mechanics," *Engineering Fracture Mechanics*, Vol. 17, No. 5, 1983, pp. 425-438.

3. Clarke, G.A., Andrews, W.R., Begley, J.A., Donald, J.K., Embley, G.T., Landes, J.D., McCabe, D.E., Underwood, J.H., " A Procedure for the Determination of Ductile Fracture Toughness Values Using J-Integral Techniques," *Journal of Testing and Evaluation*, JTEVA, Volume 7, No. 1, January 1979, pp.49-56.

4. Cobanogl, M.M., Kardos, G., "Comparison of Methods for Fracture Toughness Determination in Steels," *Journal of Testing and Evaluation*, JTEVA, Volume 9, No. 2, March 1981, pp. 104-110.

5. "Establishing Toughness Requirements for Low- and Intermediate-Strength Steels in Weapons Systems," NRC Reports, 1981.

6. Ritchie, R.O., "Why Ductile Mechanics?" *Journal of Engineering Materials and Technology*, Volume 105, January 1983, pp. 1-7.

7. Raymond, L., "Critical Strain Energy Density as a Fracture Mechanics Criterion," Naval Sea Systems Command, Department of the Navy, SBIR Proposal Topic Number N87-73.

8. Raymond, L., "Estimate of Fracture Toughness of Toughness Steels (HY-Grade) on the Upper Shelf," January 1980.

9. "Standard Test Method for J_{Ic}, a Measure of Fracture Toughness," ASTM E813-88.

10. "Rapid Inexpensive Tests for Determining Fracture Toughness," NMAB/NRC, National Academy of Sciences, 1976, pp.45-49.

11. Harrison, J.D., "The State-of-the-Art in Crack Tip Opening Displacement (CTOD) Testing and Analysis," *Metal Construction*, Sept, Oct, Nov, 1980.

12. "Methods for Crack Opening Displacement (COD) Testing," The British Standards Institution, BS 5762:1979.

13. Bockrath, G.E., Glassco, J.B., " A Method of Calculating R-Curves from Uniaxial Tensile Stress-Strain Curves," Presented at ASTM E-24 meeting, Louisville, Kentucky, March 18, 1980.

14. Kamath, M.S., " The R-Curve Approach to Fracture," The Welding Institute Research Bulletin, June, 1977, pp.145-150.

15. "Standard Practice for R-Curve Determination," ASTM E561-86.

16. Matic, P., and Jolles, M.I., "The Influence of Weld Metal Properties, Weld Geometry, and Applied Load on Weld System Performance," *Naval Engineering Journal*, March 1988.

17. Sih, G.C., Some Basic Problems in Fracture Mechanics and New Concepts," *Engineering Fracture Mechanics*, Vol 5, 1973, pp. 365-377.

18. Sih, G.C., "Fracture Mechanics Applied to Engineering Problems -Strain Energy Density Fracture Criterion," *Engineering Fracture Mechanics*, Vol 6, 1974, pp. 361-386.

19. Sih, G.C., "The Strain Energy Density Fracture Concept and Criterion," *Journal of the Aeronautical Society of India*, Vol 37, No. 1, 1985

20. Sih, G.C., "Introductory Chapter: A Three Dimensional Strain Energy Density Factor Theory of Crack Propagation,"

21. Raymond, L., Crumly, W.R., "Theory of Ductile Fracture Applied to Predicting the Burst Pressure of Vessels Made from High Toughness Steel," Engineering Research Center (ERC) Report, ERC #78-433, CSULB, Long Beach, California, November 1978.

22. Raymond, L., Crumly, W.R., "A Strain Energy Density Model to Quantify Slow Strain Rate, Smooth Bar, Stress Corrosion Tensile Tests in Terms of K_{IH}," Presented at the Int'l Conf. on Interaction of Steels with Hydrogen in Petroleum Ind. Pressure Vessel Service, Sponsored by MPC/API, Paris, France, 28-30 March 1989.

23. "Standard Methods of Tension Testing of Metallic Materials ," ASTM E8-89.

24. "Standard Test Method for Tensile Strain-Hardening Exponents (n-values) of Metallic Sheet Material," ASTM E646-78.

25. "Rapid Inexpensive Tests for Determining Fracture Toughness," Appendix G: Other Ductility Tests, NMAB-328, National Academy of Sciences, Washington, D.C., 1976, pp.190-205.

26. Bockrath, G.E., Glassco, J.B., " A Theory of Ductile Fracture," MDC G2895, April 1974, McDonnell Douglas Astronautics Company, Long Beach, CA.

<u>COMMITTEE ON MARINE STRUCTURES</u>

Commission on Engineering and Technical Systems

National Academy of Sciences - National Research Council

The COMMITTEE ON MARINE STRUCTURES has technical cognizance over
the interagency Ship Structure Committee's research program.

Stanley G. Stiansen (Chairman), Riverhead, NY
Mark Y. Berman, Amoco Production Company, Tulsa, OK
Peter A. Gale, Webb Institute of Naval Architecture, Glen Cove, NY
Rolf D. Glasfeld, General Dynamics Corporation, Groton, CT
William H. Hartt, Florida Atlantic University, Boca Raton, FL
Paul H. Wirsching, University of Arizona, Tucson, AZ
Alexander B. Stavovy, National Research Council, Washington, DC
Michael K. Parmelee, Ship Structure Committee, Washington, DC

<u>LOADS WORK GROUP</u>

Paul H. Wirsching (Chairman), University of Arizona, Tucson, AZ
Subrata K. Chakrabarti, Chicago Bridge and Iron Company, Plainfield, IL
Keith D. Hjelmstad, University of Illinois, Urbana, IL
Hsien Yun Jan, Martech Incorporated, Neshanic Station, NJ
Jack Y. K. Lou, Texas A & M University, College Station, TX
Naresh Maniar, M. Rosenblatt & Son, Incorporated, New York, NY
Solomon C. S. Yim, Oregon State University, Corvallis, OR

<u>MATERIALS WORK GROUP</u>

William H. Hartt (Chairman), Florida Atlantic University, Boca Raton, FL
Fereshteh Ebrahimi, University of Florida, Gainesville, FL
Santiago Ibarra, Jr., Amoco Corporation, Naperville, IL
Paul A. Lagace, Massachusetts Institute of Technology, Cambridge, MA
John Landes, University of Tennessee, Knoxville, TN
Mamdouh M. Salama, Conoco Incorporated, Ponca City, OK
James M. Sawhill, Jr., Newport News Shipbuilding, Newport News, VA

SHIP STRUCTURE COMMITTEE PUBLICATIONS

SSC-348   Corrosion Experience Data Requirements by Karl A. Stambaugh and John C. Knecht   1988

SSC-349   Development of a Generalized Onboard Response Monitoring System (Phase I) by F. W. DeBord, Jr. and B. Hennessy 1987

SSC-350   Ship Vibration Design Guide by Edward F. Noonan   1989

SSC-351   An Introduction to Structural Reliability Theory by Alaa E. Mansour   1990

SSC-352   Marine Structural Steel Toughness Data Bank by J. G. Kaufman and M. Prager   1990

SSC-353   Analysis of Wave Characteristics in Extreme Seas by William H. Buckley   1989

SSC-354   Structural Redundancy for Discrete and Continuous Systems by P. K. Das and J. F. Garside   1990

SSC-355   Relation of Inspection Findings to Fatigue Reliability by M. Shinozuka   1989

SSC-356   Fatigue Performance Under Multiaxial Load by Karl A. Stambaugh, Paul R. Van Mater, Jr., and William H. Munse 1990

SSC-357   Carbon Equivalence and Weldability of Microalloyed Steels by C. D. Lundin, T. P. S. Gill, C. Y. P. Qiao, Y. Wang, and K. K. Kang   1990

SSC-358   Structural Behavior After Fatigue by Brian N. Leis   1987

SSC-359   Hydrodynamic Hull Damping (Phase I) by V. Ankudinov 1987

SSC-360   Use of Fiber Reinforced Plastic in Marine Structures by Eric Greene   1990

SSC-361   Hull Strapping of Ships by Nedret S. Basar and Roderick B. Hulla   1990

SSC-362   Shipboard Wave Height Sensor by R. Atwater   1990

SSC-363   Uncertainties in Stress Analysis on Marine Structures by E. Nikolaidis and P. Kaplan   1991

None   Ship Structure Committee Publications - A Special Bibliography   1983